A Formulation for the Static Permittivity of Water and Steam at Temperatures from 238 K to 873 K at Pressures up to 1200 MPa, Including Derivatives and Debye–Hückel Coefficients

Cite as: Journal of Physical and Chemical Reference Data **26**, 1125 (1997); https://doi.org/10.1063/1.555997
Submitted: 12 February 1997 . Published Online: 15 October 2009

D. P. Fernández, A. R. H. Goodwin, Eric W. Lemmon, J. M. H. Levelt Sengers, and R. C. Williams

A Formulation for the Static Permittivity of Water and Steam at Temperatures from 238 K to 873 K at Pressures up to 1200 MPa, Including Derivatives and Debye–Hückel Coefficients

D. P. Fernández[a)]

Physical and Chemical Properties Division, National Institute of Standards and Technology, Gaithersburg, Maryland 20899 and Departamento Química de Reactores, Comisión Nacional de Energía Atomica, Avenue del Libertador 8250, 1429 Buenos Aires, Argentina

A. R. H. Goodwin and E. W. Lemmon[b)]

Center for Applied Thermodynamics Studies, University of Idaho, Moscow, Idaho 83844-1011

J. M. H. Levelt Sengers

Physical and Chemical Properties Division, National Institute of Standards and Technology, Gaithersburg, Maryland 20899

R. C. Williams

Center for Applied Thermodynamics Studies, University of Idaho, Moscow, Idaho 83844-1011

Received February 12, 1997; revised manuscript received March 17, 1997

A new formulation is presented of the static relative permittivity or dielectric constant of water and steam, including supercooled and supercritical states. The range is from 238 K to 873 K, at pressures up to 1200 MPa. The formulation is based on the ITS-90 temperature scale. It correlates a selected set of data from a recently published collection of all experimental data. The set includes new data in the liquid water and the steam regions that have not been part of earlier correlations. The physical basis for the formulation is the so-called g-factor in the form proposed by Harris and Alder. An empirical 12-parameter form for the g-factor as a function of the independent variables temperature and density is used. For the conversion of experimental pressures to densities, the newest formulation of the equation of state of water on the ITS-90, prepared by Wagner and Pruss, has been used. All experimental data are compared with the formulation. The reliability of the new formulation is assessed in all subregions. Comparisons with previous formulations are presented. Auxiliary dielectric-constant formulations as functions of temperature are included for the saturated vapor and liquid states. The pressure and temperature derivatives of the dielectric constant and the Debye–Hückel limiting-law slopes are calculated, their reliability is estimated, and they are compared with experimentally derived values and with previous correlations. All equations are given in this paper, along with short tables. An implementation of this formulation for the dielectric constant is available on disk [A. H. Harvey, A. P. Peskin, and S. A. Klein, NIST/ASME Steam Properties, NIST Standard Reference Database 10, Version 2.1, Standard Reference Data Program, NIST, Gaithersburg, MD (1997)]. [S0047-2689(97)00104-9]

Key words: data correlation; Debye–Hückel coefficients; g-factor; ITS-90; static dielectric constant; static relative permittivity; steam; supercritical steam; supercooled water; water.

Contents

[a)] Present address: Facultad de Ciencias Exactas y Naturales, Universidad de Buenos Aires, Ciudad Universitaria, Pabellon 2, 1428 Buenos Aires, Argentina.

[b)] Present address: Physical and Chemical Properties Division, National Institute of Standards and Technology, Boulder, CO 80303.

List of Tables

List of Figures

List of Symbols

Roman

a	radius of cavity
A_ϕ	D.H. osmotic coefficient
A_V	D.H. coefficient for volume
A_H	D.H. coefficient for enthalpy

A_K	D.H. coefficient for compressibility
A_C	D.H. coefficient for heat capacity
D.H.	Debye–Hückel (coefficient)
$\boldsymbol{e}$	unit vector
e	charge of proton
E	electric field
E_c	cavity field
E_o	external field
E_1	instantaneous local field
E_i	internal field or averaged local field
L_i	Lagrange-interpolation coefficients
$\boldsymbol{M}$	total dipole moment
n	number density
N_A	Avogadro's number
N_c	number of molecules inside a spherical cavity
N_k	coefficients in expression for g-factor
P	dipolar density
$\boldsymbol{P}$	polarization per unit volume
p	pressure
p_o^*	0.101 325 MPa
$p(X_i)$	weight factor for molecule i
q	exponent for glass transition anomaly
T	absolute temperature, ITS-90
T_c	critical temperature
U	intermolecular energy
V_{el}	electrostatic energy
V_o	non-electrostatic energy
X_i	positional and orientational coordinates of molecule i

Greek

α_c	critical exponent
α	molecular polarizability
ϵ	static dielectric constant or relative permittivity
ϵ_o	permittivity of vacuum
ϵ_∞	infinite-frequency dielectric constant
θ	reduced temperature difference with the critical temperature
μ	dipole moment for isolated molecule
μ_d	effective dipole moment
ν	refractive index
ρ	amount-of-substance density
ρ_c	critical density

1. Introduction

1.1. Importance

The dielectric properties of water in its fluid phases determine its solvent behavior in natural and industrial settings, and its essential role in living organisms. One aspect of the dielectric properties is the static (zero-frequency limit) relative permittivity or dielectric constant. This property determines the strength of electrostatic interactions of ionic solutes in water, and therefore plays a major role in aqueous physical chemistry. In particular, the static dielectric constant and its pressure and temperature derivatives determine the infinite-dilution limiting slopes of thermodynamic properties of electrolytes in water according to the theory of Debye and Hückel,[1] and also play a key role in the Born model[2] of solvation of aqueous electrolyte solutions. These values of the dielectric constant and its derivatives can be derived in a consistent way from a formulation of the static dielectric constant of liquid water as a function of pressure and temperature.

The temperature and pressure range of interest to geologists and geochemists far exceeds that of liquid water below its boiling point. Pressurized high-temperature water, including supercritical water, is encountered in the deep earth and ocean. Furthermore, efficient generation of electricity by means of steam requires reduction of shutdowns due to malfunctioning. Knowledge of the fate and action of water impurities is of vital importance to the performance of boilers, heat exchangers, and turbines. There is also a recent vigorous interest in supercritical water as a reaction medium. In this regime of strongly diverging compressibility, pressure is not a useful independent variable, and formulations are conveniently done in terms of density and temperature as independent variables.

1.2. Complexity

In what follows, the symbol ϵ will denote the static relative permittivity or dielectric constant, made dimensionless by expressing it in units of ϵ_o, the vacuum permittivity.

The static dielectric constant ϵ of water [Figs. 1(A), 1(B)] has a complicated behavior not found in most other fluids.

In nonpolar fluids, $\epsilon-1$ is roughly proportional to density, with a prefactor depending on the molecular polarizability. In polar fluids, the breaking of the correlations between the dipoles as the temperature increases gives rise to a negative temperature dependence of the dielectric constant at fixed density.

This simple behavior is visible in water only in the dilute steam phase. The actual behavior is dominated by the huge increase of the dielectric constant in the region where water is hydrogen-bonded. The experimental values of ϵ range from close to 1 in steam to over 100 in pressurized and supercooled water.

The large rise of the dielectric constant in the range of liquid and supercooled water has, so far, defied quantitative theoretical description in terms of intermolecular forces, notwithstanding valiant and sustained effort during the best part of the present century. Computer simulations are beginning to make inroads, but the results for the dielectric constant appear to be highly sensitive to details of the intramolecular and intermolecular potential, while any given potential can usually give acceptable results only in limited ranges of temperature and density. The high-temperature range is somewhat easier to describe, given the fact that hydrogen bonding is much weaker. Promising results have been recently obtained by computer simulation.

From the point of view of constructing an accurate correlation, availability of theoretical guidance is desirable for several reasons: it might suggest the form of a correlating

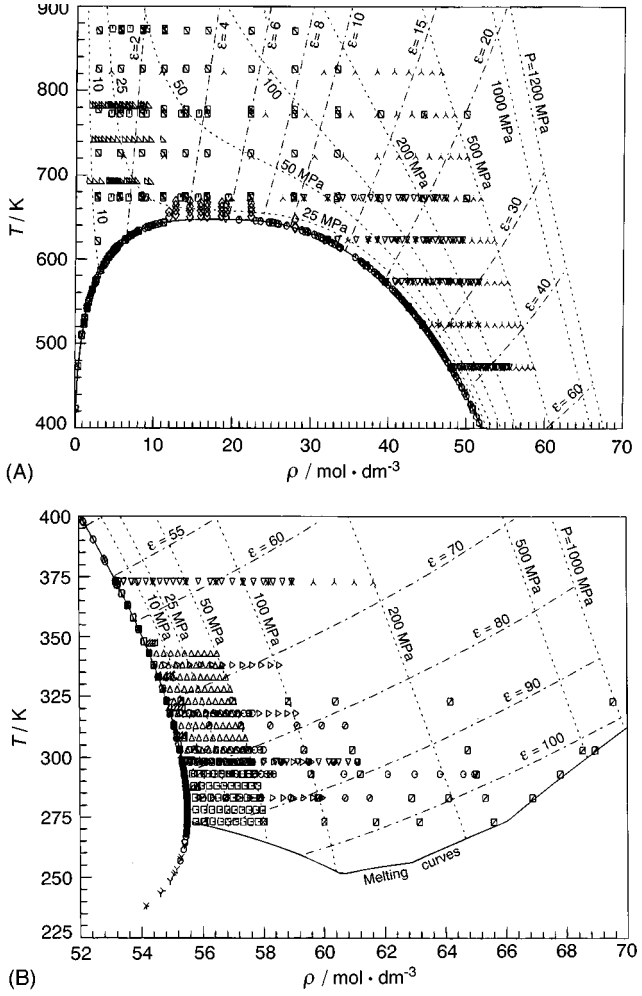

FIG. 1. (A) The evaluated experimental data for the dielectric constant ϵ of water and steam (Ref. 3) above 400 K, in their dependence on density and temperature. Isobars (- - - -) and iso-ϵ curves (– · – · –) are indicated. Symbols: Table 6. (B) As Fig. 1(A), but for the liquid region below 400 K. Symbols: Table 6.

equation, could fill in data gaps, enable a choice between discrepant data, and govern extrapolation. In Sec. 2, the theory of the dielectric constant of a system of dipolar and polarizable molecules is summarized, including the useful models resulting from this theory, and high-temperature computer simulation and analytical results are discussed and referenced.

1.3. Previous Correlations

Quist and Marshall,[4] in 1965, produced an estimation of the dielectric constant of water up to 1073 K in terms of the Kirkwood equation, to be discussed in Sec. 2. Tabulated values of the density of water were used to convert pressure to density. Values of $\mu^2 g$ were backed out from all available data in the liquid up to 623 K and 1200 MPa, and fitted with a function of density and pressure that contained four to five adjustable parameters. There were no data available in the supercritical regime at that time. Tabulated values were presented at temperatures up to 1073 K, at densities up to 1 g cm^{-3}.

Helgeson and Kirkham,[5] in 1974, developed a correlation of the dielectric constant of water up to high pressures and temperatures for the purpose of developing the Born model[2] of solvation for aqueous solutions. This model characterizes the water solvent solely by its dielectric constant. For geochemical purposes it was important to extend the model to supercritical states. These authors formulated the dielectric constant itself as a polynomial in density and temperature with 15 adjustable parameters. They fitted this function to data of Oshry,[6] Owen *et al.*,[7] and Heger.[8] The latter data extend into the supercritical regime. The range of the correlation is up to 600 MPa and 773 K. The equation of state used to convert pressure to density appears to have been that of Keenan *et al.*[9] Pressure and temperature derivatives of the dielectric constant were calculated and tabulated.

A correlation of the dielectric constant of water as a function of pressure and temperature was developed by Bradley and Pitzer[10] in 1979. A somewhat different selection of data in the liquid phase below 623 K was made than that of Helgeson and Kirkham, and the Heger data were fitted in the supercritical regime. The functional form chosen had nine adjustable parameters. Debye–Hückel slopes were calculated and tabulated for the range up to 623 K and 100 MPa.

Uematsu and Franck,[11] in 1980, recognized the need for a formulation of the dielectric constant of water and steam that would encompass the entire fluid region, including not only the supercritical state but also the subcritical vapor. A key role was played by the data of Heger *et al.*, since published.[12] The conversion from measured pressures to densities was achieved by means of the formulation for scientific and general use (IFC68) that was adopted by the International Association for the Properties of Steam in 1968. This equation is now recognized to have shortcomings, and has been supplanted by more recent high-quality formulations. Uematsu and Franck included several data sets in the near- and supercritical state that had not been considered before. The dielectric constant was formulated as a polynomial in density and inverse temperature, with ten adjustable parameters for the range up to 500 MPa and from 273 K to 823 K. The emphasis of Uematsu and Franck was on the dielectric constant in the supercritical regime. The issue of the derivatives was not considered. At the low-temperature end in liquid water, the temperature slope of the Uematsu–Franck correlation is smaller in absolute value than the slope displayed by most of the data.

A recent correlation of the static dielectric constant of all fluid states of water is that of Archer and Wang[13] in 1990. These authors used the relation proposed for the g-factor by Kirkwood (Sec. 2) as a starting point, and the high-quality equation of state of Hill,[14] which we will denote as Hill90, to convert pressure to density. They fit the quantity $(g-1)/\rho$. Their fitting expression contains nine adjustable parameters for the range from 238 K to 823 K up to ~500 MPa, including data in supercooled water. The data available at pressures

higher than 500 MPa were not included in the fit. The Archer–Wang formulation has unusual features. First of all, it uses not only density and temperature, but also pressure as variables (obviously not all independent). Second, it uses three anomalous terms that diverge strongly at a temperature of 215 K (well outside the range of available data); this temperature is also well below that of 228 K at which the compressibility and viscosity diverge according to the analysis of Angell and co-workers (see Sec. 1.6). The correlation of Archer and Wang gives an accurate representation of all dielectric constant data known at the time, and includes a tabulation of Debye–Hückel coefficients.

Johnson and Norton,[15] in a recent review, discuss the relationship of the various formulations, and offer refinements of the Helgeson and Kirkham and of the Uematsu and Franck equations that reflect a better knowledge of critical behavior and of the equation of state.

1.4. Need for a New Correlation

There are a number of reasons why it is desirable to revisit the issue of the dielectric constant formulation. The first reason is the availability of new experimental data in liquid water.[16] For the first time, accurate data are available in the steam phase,[17] see Ref. 3. Also, a vexing discrepancy between two groups of data sets in liquid water, reducing the precision with which derivatives of the dielectric constant and Debye–Hückel coefficients can be obtained, has been at least partially resolved.[16]

The second reason is the revision of the international temperature scale to the ITS-90.[18] The Archer–Wang formulation cannot be consistently adjusted to the new scale by a simple shift of the temperature variable, because of the implicit and explicit use of the Hill equation of state of water, which is not on the new scale. The revision requires a new formulation of the equation of state, which again is not a matter of a simple shift of scale, since a variety of thermodynamic data enters the formulation of the Helmholtz function from which the equation of state is derived. A new Helmholtz function of water on ITS-90 has become available since: that of Wagner and Pruss.[19] It has been adopted by the International Association for the Properties of Water and Steam.[20]

Third, we considered it desirable to extend the formulation over the full pressure range, up to 1190 MPa, for which data are available, rather than cutting off at 500 MPa. Finally, we considered the dependence on three variables, p, T, and ρ in the formulation of the g-factor an undesirable feature, and have decided not to use this approach.

1.5. Choice of Functional Form

We have experimented with many possible functional forms for the correlation. An empirical polynomial in density and temperature, as used by Uematsu and Franck, was certainly an option, and we performed some not completely satisfactory fits with roughly ten adjustable parameters.

We have tried a 4-5 parameter dependence on the scaled variable ρ/T, as suggested by Mulev *et al.*,[17] and found it adequate for vapor and supercritical data, but not sufficiently precise and flexible for the liquid phase.

Some previous correlations have been based on the g-factor of Kirkwood (Sec. 2). It should be understood that none of the existing correlations is based on a theoretical expression for the Kirkwood g-factor. The expression is simply inverted, and values of g are calculated from the measured experimental data. The advantage of such a procedure is that the g-factor varies only over a factor of 5 at most, while the dielectric constant varies over 2 orders of magnitude.

We finally decided to correlate the dielectric constant by means of the g-factor in the form proposed by Harris and Alder (see Sec. 2). We do incorporate the known dipole moment and average polarizability of the isolated water molecule. The Harris–Alder g-factor is again treated as an empirical property backed out from the experimental dielectric constant data.

1.6. Further Assumptions Made

In the present formulation, possible anomalies of the dielectric constant near the critical point have been ignored, while that in the supercooled liquid has been accounted for to some extent. As far as the latter anomaly is concerned, as Speedy and Angell[21] have shown, many properties of supercooled water, such as compressibility and viscosity, appear to diverge at a temperature of $\sim$228 K.

Hodge and Angell[22] measured the dielectric constant of emulsified supercooled water down to 238 K. This was a very difficult experiment, because it is hard to avoid partial crystallization of the water. The authors estimate the reliability of their data as 2%. The data do agree well within this uncertainty with other data that penetrate deeply into the supercooled state.[23,24]

Hodge and Angell fitted their data with a power law of the form:

$$\epsilon = A_{\epsilon}(T/T_s - 1)^{-q} \tag{1}$$

with $q = 0.126$, a weak divergence at most. Here T is the temperature, and T_s the glass transition temperature. Hodge and Angell also fitted their data with a quadratic in temperature, measured in °C. In their Fig. 3, the quadratic appears slightly too flat, missing the lowest-temperature point by -1%. The power-law expression, however, curves too strongly, underestimating all points in the middle range by a percent or more, and overshooting the lowest-temperature point by a percent. We therefore considered the evidence for a power-law divergence to be weak.

As a practical matter, however, we found that the Hodge and Angell data are fitted better over the whole range when one divergent term was used in addition to the set of regular terms that defines the surface over most of the range. The divergent term selected by our algorithm has a strong divergence at 228 K, with an exponent of -1.2.

As far as the critical behavior of the dielectric constant is concerned, it should be noted that in any formulation, such as Refs. 4, 5, 11, and the present one, in which the leading variation of the dielectric constant is proportional to the density, the strong critical divergence of the pressure and temperature derivatives of the dielectric constant will be (trivially) included. In the present formulation, the additional subtle $(1-\alpha_c)$-type critical anomaly

$$\epsilon = \epsilon_c + A(1-T/T_c)^{1-\alpha_c}, \tag{2}$$

which is expected to occur in the dielectric constant of fluids[25,26] along the critical isochore, has not been included. Here α_c is the critical exponent for the isochoric heat capacity, the best estimate for its value being 0.11, a small number characteristic of a weak anomaly; and ϵ_c is the value of the dielectric constant at the critical point. The anomalous term is subtle, reaching a value of zero at the critical point, but leading to a weak divergence of the first temperature derivative of the dielectric constant at constant volume. An anomaly of this type has not been detected in the best experiments in nonpolar pure fluids (He, Ref. 27; SF_6, Ref. 28; Ne and N_2, Ref. 29), but it has been seen in CO, a weakly polar fluid.[30] There is no theoretical prediction for the amplitude of this anomaly in terms of the molecular dipole moment. The experimental dielectric constant data in near- and supercritical steam are much too imprecise to allow an estimate of the amplitude. Moreover, building into a formulation the appropriate scaled behavior in terms of both density and temperature is a nontrivial problem. For all these reasons, we have decided not to incorporate the expected critical anomaly into our formulation. The large size of the molecular dipole moment of water, however, is a warning that the effect potentially could be substantial. Only new more accurate measurements near the critical point of water could justify the introduction of a term reflecting the critical anomaly.

2. Physical Models

2.1. Dielectric Behavior of Polar, Polarizable Dipolar Molecules

The first descriptions of the dielectric properties of materials were formulated in the 19th century. An example is the well-known Clausius–Mossotti relation

$$\frac{\epsilon-1}{\epsilon+2} = \frac{n\alpha}{3\epsilon_0} \tag{3}$$

for the dielectric constant ϵ of a medium of number density $n=N/V$ and molecular polarizability α. Lorentz[31] presented a derivation of this equation by considering the internal field E_i, which acts on an individual polarizable molecule and differs from the Maxwell field E inside the dielectric. The Maxwell field E can be related to the external field E_0 for a given shape of the dielectric. The dielectric constant is a measure of the polarization $\boldsymbol{P}$ per unit volume induced by the Maxwell field:

$$\epsilon = 1 + \frac{\boldsymbol{P}}{\epsilon_0 E}. \tag{4}$$

Lorentz[31] developed a procedure for calculating the internal field by surrounding the molecule by a microscopic cavity, a sphere large enough to contain many molecules, but outside of which the medium can be replaced by a homogeneous dielectric. The net effect of the external field on an empty cavity inside the dielectric is to build up a polarization charge on the cavity wall, which reduces the electric field strength inside the cavity. In addition, Lorentz calculated the contribution of the fields of the polarized molecules inside the cavity to the internal field, found that it averaged to zero for a distribution of the molecules on a regular lattice and also for a completely random arrangement of the molecules, and concluded that it could be set equal to zero. In both cases, the Clausius–Mossotti relation, Eq. (3), results. In fact, this proof is not valid[32] because it ignores the correlation between the induced dipole moment on the molecule considered and the polarization this dipole induces into surrounding volume elements inside the cavity.

It was Debye[33] who, in the early part of this century, noted that an important characteristic of dielectric materials was not described by Eq. (3), namely the temperature dependence of the dielectric constant found for many fluids. Debye proposed that this feature is due to the presence of permanent electric dipoles and he modified the Clausius–Mossotti equation by assuming that the same internal field that polarizes the molecules also torques the dipoles. The result is

$$\frac{\epsilon-1}{\epsilon+2} = \frac{n}{3\epsilon_0}\left(\alpha + \frac{\mu^2}{3kT}\right). \tag{5}$$

This linear relation of the dielectric constant and the inverse temperature permits the extraction of the values of both the molecular polarizability α and the dipole moment μ from experimental data for the temperature dependence of the dielectric constant of a fluid.

Bell[32,34] calculated the interaction of a nonpolarizable point dipole with its environment by considering it imbedded in a molecular-size spherical cavity. The dipole polarizes its environment, which produces a reaction field at the position of the dipole; this reaction field adds to the dipole field.

Onsager[35] pointed out undesirable features in the Debye equation, namely the prediction of the existence of a Curie point below which a permanent electric moment exists not found in real liquids. Also, the dipole moments derived by Debye's method from experimental data in high-dielectric liquids are smaller than those found in the gas phase of the same compound. Onsager traced these problems to the assumption that the same internal field that polarizes the molecule also torques its dipole. In reality, the torquing or directing field is smaller than the internal field. Onsager,[35] generalizing Bell's method to the case of an external field and a polarizable dipolar molecule, calculated the reaction field due to polarization of the cavity wall. The reaction field is parallel to the dipole and does not contribute to the torque. It does enhance both the dipole moment and the induced

moment, causing an effective dipole moment typically 20%–40% larger, in common polar organic liquids, than that of the isolated molecule.

Böttcher's[32] form of Onsager's equation for a pure fluid consisting of polarizable dipoles is

$$\frac{(\epsilon-1)(2\epsilon+1)}{9\epsilon}=\frac{n}{\epsilon_0}\left(\alpha^*+\frac{(\mu^*)^2}{3kT}\right),$$

$$\alpha^*/\alpha=\mu^*/\mu=\frac{(\nu^2+2)}{(2\epsilon+\nu^2)}\,\frac{(2\epsilon+1)}{3}, \tag{6}$$

$$\alpha=a^3\frac{\nu^2-1}{\nu^2+2}.$$

Here the symbol ν stands for the refractive index of the medium. Onsager introduced this quantity to eliminate both the polarizability and the unspecified radius a of the cavity from the expressions.

Bell's and Onsager's descriptions of the dielectric behavior of dipolar fluids are mean-field theories in the sense that an individual dipole is considered in interaction with a continuum. Considerable generalization is required for application to the case of water, for which the molecules have strong specific interactions. These generalizations are introduced in Sec. 2.2.

2.2. Statistical–Mechanical Theories of Dielectrics

The statistical mechanical treatment of the dielectric behavior of a medium consisting of polar and/or polarizable molecules, initiated by Kirkwood,[36] may be viewed as a generalization of the Lorentz approach in which only two limiting cases, total order and total disorder, were assumed for the molecules inside the cavity, and permanent dipoles were not present.

In general, these statistical–mechanical theories[32] assume that the polarization $\boldsymbol{P}$ is equal to the dipolar density P, and neglect the influence of higher multipolar densities. For a sample with volume V, the dipole density P is then related to the statistical average of the instantaneous total dipole moment M, $\langle M\rangle$, by

$$PV=\langle M\rangle. \tag{7}$$

Equations (4) and (7) are the starting point for the microscopic description of the static permittivity. The total intermolecular potential, including specific interactions such as hydrogen bonding, can in principle be included in the calculation of the statistical average. With the external electric field E_0 as the independent variable, Eqs. (4) and (7) result in

$$\epsilon=1+\frac{1}{\epsilon_0 V}\left(\frac{\partial E_0}{\partial E}\right)_{E=0}\left(\frac{\partial}{\partial E_0}\langle \boldsymbol{M}\cdot\boldsymbol{e}\rangle\right)_{E_0=0}, \tag{8}$$

where $\boldsymbol{M}$ is the total dipole moment vector and $\boldsymbol{e}$ is the unit vector in the direction of the field. In Eq. (8) only the linear term in the power series expansions of P and $\boldsymbol{M}$ in powers of E has been retained.

For special shapes of the dielectric, typically a sphere, the internal field E can be straightforwardly related to the external field E_0. The total dipole moment $\boldsymbol{M}$ is composed of N instantaneous molecular vectors, each of them made up from permanent and induced parts. The induced dipole moment is the product of a scalar polarizability and the instantaneous local electric field E_l at the position of the molecule. The internal field E_i is the average of the local field E_l over time and position of all molecules. The permanent dipole moment is that of the isolated molecule. The average $\langle \boldsymbol{M}\cdot\boldsymbol{e}\rangle$, as a function of E_o, then has to be calculated as the average of the sum of the instantaneous dipole moments of the N molecules. The total intermolecular energy U is included in the Boltzmann factor for the statistical average. U is composed of electrostatic, V_{el}, as well as nonelectrostatic energies, V_o. The electrostatic energy, in this case, originates from dipolar forces, with contributions from the potential energy of the dipoles in the external field and in each other's field, and from polarization work required to bring the molecular dipoles from the isolated-molecule value to the total value including the induced contribution.

Because of the relatively short range of specific bonding forces in liquids such as water, the Lorentz prescription, in which only a number N_c of molecules inside a spherical cavity from the total number of molecules N is considered in the average, should be a good approximation. The remaining $N-N_c$ molecules are replaced by a continuum of dielectric constant ϵ in which the spherical cavity is immersed. The external field working on the sphere with N_c molecules and volume V is the cavity field E_c,

$$E_o=E_c=\frac{3\epsilon}{2\epsilon+1}\,E, \tag{9}$$

where E is the Maxwell field in the material outside the sphere.

For a liquid composed of nonpolarizable molecules with permanent dipole moment μ one obtains

$$\epsilon=1+\frac{1}{\epsilon_0 V}\,\frac{3\epsilon}{2\epsilon+1}\,\frac{\langle M^2\rangle_o}{3kT}, \tag{10}$$

where $M^2=\boldsymbol{M}\cdot\boldsymbol{M}$, $\boldsymbol{M}$ being now the sum of the dipole moments for the N_c molecules inside the spherical cavity of volume V. $\langle\ \rangle_o$ denotes the statistical average in the absence of an external field. Equation (10) is obtained by writing V_{el} in terms of E_o, taking the derivative in Eq. (8) and using Eq. (9). The average $\langle M^2\rangle_o$ can be rewritten by defining the Kirkwood[36] correlation factor g,

$$g=\frac{1}{|\mu|^2}\int p(X^i)\mu_i\cdot\boldsymbol{M}_i^*\,\mathrm{d}X^i, \tag{11}$$

where X^i represents the positional and orientational coordinates for the molecule i, and the weight factor $p(X^i)$ and the average moment $\boldsymbol{M}_i^*$ are defined according to

$$p(X^i)=\frac{\int \mathrm{d}X^{N-i}\exp(-U/kT)}{\int \mathrm{d}X^N\exp(-U/kT)}, \tag{12}$$

$$\boldsymbol{M}_i^* = \frac{\int \mathrm{d}X^{N-i} \boldsymbol{M} \exp(-U/kT)}{\int \mathrm{d}X^{N-i} \exp(-U/kT)}, \tag{13}$$

where X^{N-i} represent the positional and orientational coordinates of the N_c molecules, except for molecule i. With Eqs. (11)–(13), Eq. (10) is rewritten as the so-called Kirkwood equation[36]

$$\frac{(\epsilon-1)(2\epsilon+1)}{\epsilon} = \frac{n}{\epsilon_0 kT} g\mu^2, \tag{14}$$

where $n=N/V$ is the number density of the sample. The quantity $\boldsymbol{M}_i^*$, given by Eq. (13), represents the average moment of the sphere containing N_c molecules in the field of the dipole of molecule i, held with fixed orientation. The Kirkwood correlation factor g, given in Eq. (11), characterizes the correlation between the molecular orientations due to nondipolar interactions. Equation (14) reduces to the Onsager equation, Eq. (6), for nonpolarizable molecules ($\nu=1$) and for $g=1$.

For polarizable molecules, the above definitions are no longer valid. The induced moment depends on the local field acting on molecule i, $(E_1)_i$, and is a function of the orientations and positions of all other molecules. The average moment $\boldsymbol{M}_i^*$, given in Eq. (13), no longer depends on the coordinates of molecule i alone. Kirkwood[36] explained that in this case the dipole moment μ is not that of the isolated molecule because of the polarization of the molecule by its neighbors, but no rigorous procedure was given to relate this moment to that of the isolated molecule. Noting that the contribution of the induced polarization to the dielectric constant for polar polarizable fluids is in general small, Kirkwood[36] supplemented Eq. (14) with another term proportional to the polarizability α:

$$\frac{(\epsilon-1)(2\epsilon+1)}{3\epsilon} = \frac{n}{\epsilon_0}\left(\alpha + \frac{1}{3kT} g\mu^2\right). \tag{15}$$

This is only an approximate result for systems of polar polarizable molecules. Equation (15) does not reduce to the Clausius–Mossotti equation in the absence of a permanent dipole. A different alternative was proposed by Harris and Alder,[37]

$$\frac{(\epsilon-1)(2\epsilon+1)}{3\epsilon} = \frac{n}{\epsilon_0}\left(\frac{(2\epsilon+1)(\epsilon+2)}{9\epsilon}\alpha + \frac{1}{3kT} g\mu^2\right). \tag{16}$$

Equation (16) does reduce to the Clausius–Mossotti formula in the absence of a permanent dipole. It does not, however, reduce to the Onsager equation for $g=1$. As in the case of Eq. (15), the dipole moment μ is not that of the isolated molecule, and it is not possible to evaluate it without further approximations. The procedure leading to Eq. (16) was criticized by various authors,[38,39] and others concurred with the criticism.[40,41]

The model conceived by Fröhlich[42] for a system of polar polarizable molecules is a continuum with dielectric constant ϵ_∞ in which molecules with dipole moment μ_d and specific nonelectrostatic interactions are immersed. The molecular dipole moment μ_d is not that of the isolated molecule, but includes that part of the induced dipole moment that arises from the presence of permanent dipoles. μ_d can be related to the dipole moment μ of the isolated molecule by

$$\mu_d = \frac{\epsilon_\infty + 2}{3}\mu. \tag{17}$$

Again, a spherical cavity with N_c molecules and volume V is considered, now embedded in a continuum with dielectric constant ϵ_∞. The external field working on this cavity is, in this case,

$$E_o = \frac{3\epsilon}{2\epsilon + \epsilon_\infty} E. \tag{18}$$

Finally, the Kirkwood–Fröhlich equation[32] is

$$\frac{(\epsilon-\epsilon_\infty)(2\epsilon+\epsilon_\infty)}{\epsilon(\epsilon_\infty+2)^2} = \frac{1}{9}\frac{n}{\epsilon_0 kT} g\mu^2, \tag{19}$$

where g is the Kirkwood correlation factor of Eqs. (11), (14), and (15). In the derivation of Eq. (19) the contribution of the induced polarization to the dielectric constant is rigorously included for Fröhlich's model, which is essentially Onsager's model with specific correlations added. The Kirkwood–Fröhlich equation reduces to the Onsager equation for $g=1$.

The model of a continuum with dielectric constant ϵ_∞ is a mean-field theory and thus implies the neglect of the correlations between the positions and the induced dipole moment of the molecules.[32] As noticed by Hill,[40] Eq. (19) is very sensitive to the value selected for ϵ_∞. For instance, if the value arising from dielectric relaxation measurements for liquid water, $\epsilon_\infty \approx 4.5$, is used together with the isolated-molecule value for μ, g values result unrealistically close to unity. There are many different interpretations for ϵ_∞, associated with the far-infrared dispersion of the water molecule.[41,43,44] Repeatedly, ϵ_∞ has been approximated by the better known optical permittivity

$$\epsilon_\infty = \nu^2, \tag{20}$$

where ν is the refractive index.

In summary, the statistical–mechanical treatment of the dielectric constant of water, a system of polar, polarizable molecules with specific interactions, is a daunting problem for which only approximate solutions are available at present.

2.3. Theoretical and Phenomenological Estimates for the *g*-Factor

The correlation factor g for water has been estimated on the basis of a variety of models. The first value, $g=2.63$ in liquid water, was calculated by Oster and Kirkwood,[45] who included only the contribution of first neighbors. Early models of (a) bond-bending and (b) bond-breaking assumed a tetrahedral ice-I tridymite structure for the liquid phase, and produced similar values for g, namely of 2.60 (a) and 2.81 (b), respectively, for liquid water at 273.15 K.[43] The bond-

TABLE 1. Comparison of calculated and experimental high-temperature values for the dielectric constant of water.

T/K	ρ/kg m^{-3}	Goldman *et al.*[50]	Franck[46]	Heger[8]	Deul[48]	This work
673	854	22.2	22.9	22.1	21.9	21.77
673	792	19.4	19.5	20.0	19.4	19.40
673	693	15.8	16.7	16.5	15.5	15.82
773	871		19.0	18.8		19.16
782	1000	23.4	22.9			23.56
810	257	3.76	3.74			3.33
1091	702	8.35	8.56			9.65
1278	1000	11.1	11.1			14.47

breaking model is able to reproduce the dielectric constant of liquid water up to the critical point fairly well with only one adjustable parameter.

For even higher temperatures, a break-up of the hydrogen bonding network is expected. In this case, simpler models may be appropiate to describe the static dielectric behavior of the fluid. Franck *et al.*[46] used the linearized hypernetted-chain analytic result for a collection of hard spheres with embedded dipoles.[47] The equation obtained by Patey *et al.*[47] was fitted by Franck *et al.*[46] to experimental data at 673 K and 823 K obtained by Heger[8,12] and by Deul.[48,49] The effective dipole moment, an adjustable parameter, was taken to be 2.33 D. The authors presented ϵ values for temperatures up to 1273 K and densities up to 1000 kg m^{-3} (see Table 1).

Goldman *et al.*[50] developed a second-order perturbation theory for the Kirkwood correlation factor and obtained the dielectric constant by means of a series expansion of the dielectric constant in terms of the dipolar strength $\mu^2\rho/(3kT)$. They used the SPC/E intermolecular potential for water.[51] This model consists of three-point, nonpolarizable rigid charges embedded in a Lennard-Jones core, with a dipole moment of 2.35 D. Results were presented at temperatures up to 1278 K and densities up to 1000 kg m^{-3}, and showed good agreement with simulation values.[52] The values obtained from the different theories for the average dipole moment and the correlation factor g in the liquid can be compared with those calculated with good accuracy for ice-1h, namely $\mu = 2.434$ D and $g = 3.00$, respectively.[53]

Table 1 shows the comparison of results obtained by Goldman *et al.*[50] with the prediction of Franck *et al.*[46] and with experimental data. The prediction by Franck *et al.* was recalculated by us on the basis of Franck's equation.

Much effort was recently expended in calculating the static dielectric constant of liquid water by means of simulation techniques,[52,54–57] The evaluation of the dipole correlation is a time-consuming task, because an average has to be obtained of the total instantaneous dipole moment of the entire system. The actual values obtained for the static dielectric constant have been found to be highly sensitive to details of the intermolecular potential used. The most succesful intermolecular potential nowadays is the SPC/E,[51] by means of which it has been possible to reproduce ϵ along the coexistence curve up to the critical point to within 10% of the experimental value.[55] For recent calculations with SPC/E, see Ref. 57. For a critical intercomparison of all literature results for SPC/E, and a comparison with the present formulation, see Ref. 58.

There are at present no predictive methods for the g- factor and the apparent dipole moment over the full range of state parameters for which dielectric constant data are available or desired. In practice, the g-factor is backed out from the experimental data after a choice of the dipole moment μ is made.

Figure 2(A) shows a comparison of the correlation factor g when calculated from the experimental data by means of Eqs. (15), (16), or (19). The dipole moment μ was taken to be equal to that of the isolated molecule, $6.138\cdot10^{-30}$ C m, and the polarizability $\alpha/\epsilon_0 = 18.1459\cdot10^{-30}$ m^3. For Eq. (19), the Kirkwood–Fröhlich equation, the dielectric constant of induced polarization ϵ_∞ was set equal to ν^2, Eq. (20), the square of the refractive index of water calculated for a wavelength of 1.2 μm, the low-frequency limit of the correlation given in Ref. 59. The three correlation factors were calculated from the data of Lees,[60] Deul[48] (above 473 K), Hodge and Angell,[22] Mulev[3,17] and Fernández *et al.*[3] The data are discussed in Sec. 3.

The high-density region of Fig. 2(A) is displayed in more detail in Fig. 2(B) for the data of Lees[60] in the compressed liquid and for the Harris–Alder g-factor [Eq. (16)] as a function of ρ/T. There are rather small, but quite significant departures from the scaling as ρ/T proposed by Mulev *et al.*[17] The Kirkwood g-factor shows similar nonscaling behavior in this range.

Figure 3 shows for the Harris–Alder Eq. (16) the representation of $(g-1)/\rho$, the expression fitted by Archer and Wang, as a function of the pressure p, for the data by Lees in the compressed liquid. Similar results would have been obtained for the Kirkwood g-factor, Eq. (15). It appears that the data collapse onto a single curve, with only a small systematic temperature dependence remaining. In selecting pressure as a third variable, Archer and Wang[13] were able to represent the data with relatively few empirical terms. The three state variables, T, p and ρ, however, are not independent.

We have no conclusive evidence that any of the proposed forms for the dielectric constant, Eqs. (15), (16), or (19), is vastly superior to the others if used as a correlation method of what essentially are empirical values of g. In all three cases, an equivalent number of adjustable parameters is re-

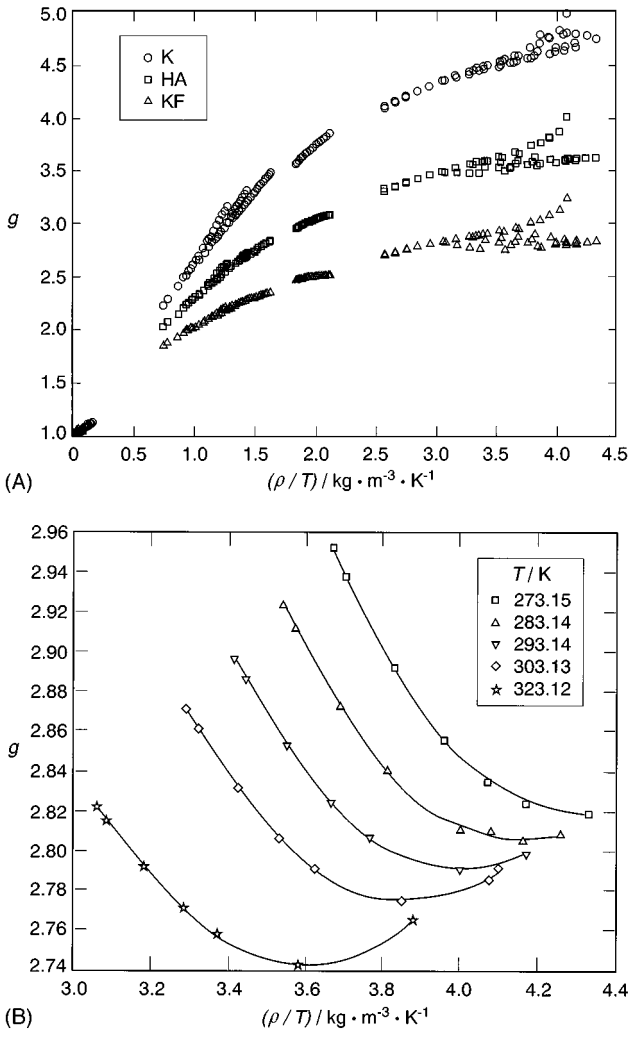

FIG. 2. (A) The Kirkwood g-factor [○], modified to include polarizability, Eq. (15), the Harris–Alder (Ref. 37) g-factor [□], Eq. (16), and the Kirkwood–Fröhlich (Ref. 32) g-factor [△], Eq. (19), as functions of the variable ρ/T for a subset of the data in Figs. 1. Symbols: Table 6. (B) The Harris–Alder g-factor for the high-density Lees data (Ref. 60) as a function of ρ/T.

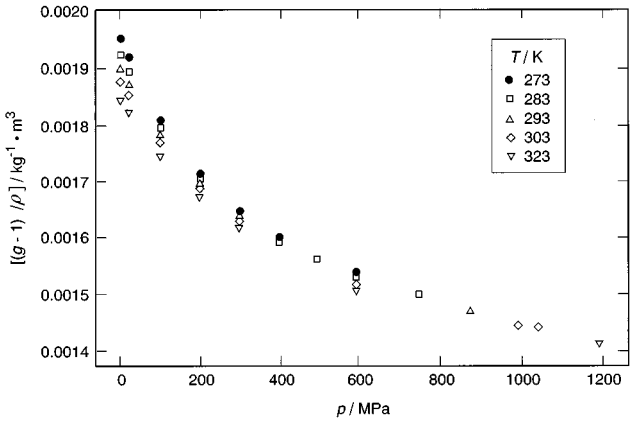

FIG. 3. Harris–Alder, Eq. (16), $(g-1)/\rho$ versus pressure, Lees data (Ref. 60).

quired to produce a correlation of similar quality in the same range. We arbitrarily decided to base the new correlation on the Harris–Alder equation, Eq. (16).

3. Review of the Data

All experimental values for the dielectric constant of water obtained since 1930, excluding solid and amorphous phases, were compiled, compared and evaluated in a previous work.[3] The different data sets were tabulated according to the region in the phase diagram in which the data were obtained. The regions include: liquid water at temperatures below the normal boiling point, saturated liquid water and steam, one-phase data above 373.12 K, and supercooled water. The data extend over a temperature range from 238 K to 873 K, over a pressure range from 0.1 MPa to 1189 MPa, and over a density range from 2.55 kg m^{-3} to 1253 kg m^{-3}. Both original and corrected values were presented. Corrections included the transformation to the new temperature scale,[18] ITS-90; recalculation of the pressures of Lees[60] to correct the reference pressure at the freezing point of mercury; recalculation of the dielectric constant values presented relative to air or to a literature value; recalculation of the values for Milner[61] and Cogan[62] who reported resonance frequency values as the primary experimental result; and correction of the values obtained by Rusche[63] according to the criticism of Kay *et al.*[64]

Figures 1(A) and 1(B) display all data for the dielectric constant ϵ of water as a function of temperature T and density ρ. Most of the data tabulated in Ref. 3 were obtained by measuring the temperature and the pressure as the experimental variables. The density for each data point was then calculated from the recent equation of state of Wagner and Pruss.[19,20]

As was mentioned before, the data compiled in Ref. 3 are not all of comparable quality. Reference 3 already indicated the data sets considered to be the most consistent within each of the regions mentioned above, by considering the accuracy claimed by the authors, together with a careful intercomparison of the data and assessment of the methods used.

Not all of the data sets marked in Ref. 3 were fully used in the present formulation. Figure 4 displays, in ρ, T variables, the data selected for the correlation. These data were obtained by Lees[60] in the liquid region, for temperatures between 273.15 K and 323.13 K and pressures up to the freezing curve; by Fernández *et al.*[16] also in the liquid region, at ambient pressure and temperatures between the normal freezing and boiling points; by Hodge and Angell[22] in the supercooled region at ambient pressure; by Lukashov[65] in the one-phase region between 726 K and 871 K and pressures between 14.1 MPa and 579 MPa, and for saturated liquid at temperatures between 523 K and 573 K; by Heger[8,12] in the one-phase region at 573 K and 500 MPa, and at 823 K and 500 MPa; by Deul[48,49] in the one-phase region at 573 K and pressures between 8.6 MPa and 300 MPa; and by Mulev[3,17] for saturated steam at temperatures between 510.3 K and 614.8 K. Also, not all the data points obtained by the authors

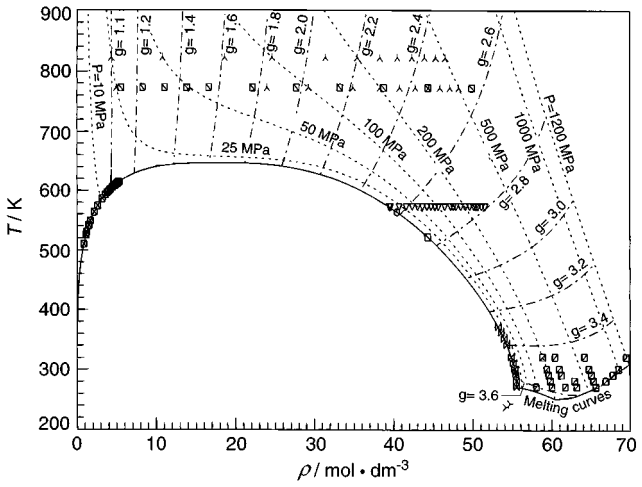

FIG. 4. Location of the selected dielectric constant data used in the correlation. Iso-g lines for the Harris–Alder g-factor are indicated in the plot. Symbols: Table 6.

mentioned before were used in the correlation. We have preferred a sparse data set, retaining only the most reliable and consistent data in each subregion. For instance, only the data obtained with one of the two methods used by Fernández *et al.*[16], those with the higher accuracy, were considered. Heger[8,12] presented an extensive set of measurements, but two data points were included here, at temperatures and pressures where no other measurements exist. At 673 K, no data were included because of the large discrepancy between the different data sets. For the complete data sets and the comparison between them, see Ref. 3. For the data displayed in Fig. 4 and used in the correlation procedure, see Section 4.

The data were weighted in two stages. As a first trial a weight w_1 was calculated by means of an estimated uncertainty $d\epsilon$, according to the usual rule $w_1 = 1/(d\epsilon)^2$. The estimated uncertainty $d\epsilon$ was evaluated from the accuracy claimed by the authors in each particular case, together with our judgement based on the method employed and the comparison between different sets obtained for the same conditions.

Table 2 shows the relations we used to estimate the uncertainty $d\epsilon$ of the dielectric constant values of each data set considered in the correlation, from which the first weight w_1 can be computed. Second, an additional weighting factor was used in the correlation, to allow further emphasis or deemphasis of individual data sets in the global fit. For the weight assigned to the Harris–Alder correlation factor g, see Sec. 4.4.

TABLE 2. Initial absolute uncertainties assigned to the static dielectric constant measurements from each source based on Ref. 16.

Source	Uncertainty, $d\epsilon$
Åkerlöf[66]	$0.25+0.2\lvert T/\mathrm{K}-298.15\rvert/75$
Albright[67]	$0.25+0.2\lvert T/\mathrm{K}-298.15\rvert/75$
Albright and Gosting[68]	$0.25+0.2\lvert T/\mathrm{K}-298.15\rvert/75$
Bertolini *et al.*[24]	0.005ϵ
Cogan[62]	$0.1+0.05\lvert T/\mathrm{K}-298.15\rvert/25+(p/\mathrm{MPa})0.05/100.9$
Deul[48]	$T/\mathrm{K}<299$ 0.002ϵ $373<T/\mathrm{K}<375$ $0.25+(p/\mathrm{MPa})0.2/500$ $470<T/\mathrm{K}<575$ $0.005+(p/\mathrm{MPa})0.005/500\epsilon$ $620<T/\mathrm{K}<625$ $[0.01+0.005\lvert(\rho/\mathrm{mol\ dm^{-3}})18.0153-800\rvert/200]\epsilon$ $670<T/\mathrm{K}<675$ $[0.02+0.02\lvert(\rho/\mathrm{mol\ dm^{-3}})18.0153-900\rvert/400]\epsilon$
Drake *et al.*[69]	0.25
Dunn and Stokes[70]	$0.05+0.1\lvert T/\mathrm{K}-298.15\rvert/74+(p/\mathrm{MPa})0.1/206.8$
Fernández *et al.*[16]	Uncertainty for each data point assigned individually
Fogo *et al.*[71]	0.03ϵ
Gier and Young[72]	0.3
Golubev[73]	0.02ϵ
Grant *et al.*[74]	$(0.005+0.001\lvert T/\mathrm{K}-303.15\rvert/30)\epsilon$
Harris *et al.*[75]	$0.25+0.5\lvert T/\mathrm{K}-287\rvert/60+(p/\mathrm{MPa})0.5/14$
Hasted and Shahidi[23]	0.02ϵ
Heger[8]	$T/\mathrm{K}<400$ $0.25+(p/\mathrm{MPa})0.2/500$ $400<T/\mathrm{K}<574$ $0.5+(p/\mathrm{MPa})0.2/500$ $T/\mathrm{K}>623$ $0.25+0.5(\rho/\mathrm{mol\ dm^{-3}})18.0153/900$
Hodge and Angell[22]	$(0.005+0.015\lvert T/\mathrm{K}-273\rvert/35)\epsilon$
Kaatze and Uhlendorf[76]	0.05
Lees[60]	$0.01+0.01\lvert T/\mathrm{K}-296.6\rvert/75+(p/\mathrm{MPa})0.05/1176.8$
Lukashov *et al.*[77]	0.03ϵ
Lukashov[65]	0.03ϵ Saturated liquid 0.02ϵ Saturated vapor 0.01ϵ
Malmberg and Maryott[78]	$0.05+0.1\lvert T/\mathrm{K}-298.15\rvert/74$
Milner[61]	$0.1+0.05\lvert T/\mathrm{K}-298.15\rvert/25+(p/\mathrm{MPa})0.05/100.9$
Muchailov[79]	0.008ϵ
Mulev *et al.*[17]	0.004ϵ
Oshry[6]	$0.5+0.5\lvert T/\mathrm{K}-371.6\rvert/282.6$
Rusche[63]	0.1
Scaife[80]	$[0.03+(p/\mathrm{MPa})0.01/588]\epsilon$
Schadow and Steiner[81]	$0.1+0.2\lvert T/\mathrm{K}-293.15\rvert/25+(p/\mathrm{MPa})0.1/125.53$
Srinivasan and Kay[82,83]	$0.05+0.1\lvert T/\mathrm{K}-298.15\rvert/74+(p/\mathrm{MPa})0.1/300$
Svistunov[84]	0.02ϵ
Tyssul Jones[85]	0.25
Vidulich *et al.*[86,87]	$0.01+0.01\lvert T/\mathrm{K}-298.15\rvert/75$
Wyman and Ingalls[88]	$0.25+0.2\lvert T/\mathrm{K}-298.15\rvert/75$
Wyman[89]	0.25

4. Correlation Procedure

4.1. Development of a Dielectric Constant Equation for Water

As has been described in Sec. 2, in this work we have chosen the Harris and Alder equation, Eq. (16), for the static dielectric constant of polar substances. It can be written in the form:

$$\frac{(\epsilon-1)}{(\epsilon+2)} = \frac{N_A\rho}{3}\left(\frac{\alpha}{\epsilon_0} + \frac{g\mu^2}{3kT\epsilon_0}\frac{9\epsilon}{(2\epsilon+1)(\epsilon+2)}\right). \quad (21)$$

In Eq. (21), ϵ is the dimensionless relative permittivity or static dielectric constant, the actual permittivity having been divided by ϵ_0, the permittivity of free space. Furthermore, α represents the mean molecular polarizability, μ the dipole moment of the molecule in the absence of all electric fields, k Boltzmann's constant, N_A Avogadro's number, ρ the amount of substance density (mol m^{-3}), T the temperature (K), and the correlation factor g an empirical function of the state variables. The values of g are extracted from the experimental dielectric-constant data. Table 3 lists the values of

TABLE 3. Constants used in the dielectric constant correlation.

Parameter	Value	Reference
Permittivity of free space, ϵ_o	$[4\cdot10^{-7}\pi(299\,792\,458)^2]^{-1}$ $C^2\ J^{-1}\ m^{-1}$	90
Elementary charge, e	$1.602\,177\,33\cdot10^{-19}$ C	90
Boltzmann's constant, k	$1.380\,658\cdot10^{-23}$ J K^{-1}	90
Avogadro's number, N_A	$6.022\,136\,7\cdot10^{23}$ mol^{-1}	90
Molar mass of water, M_w	0.018 015 268 kg mol^{-1}	91
Mean molecular polarizability of water, α	$1.636\cdot10^{-40}$ $C^2\ J^{-1}\ m^{-2}$	92
Dipole moment of water, μ	$6.138\cdot10^{-30}$ C m	43

the above constants as used in this work. The molar mass of water needed to convert the unit-mass densities of the Wagner–Pruss equation to molar units was taken to be that of Vienna Standard Mean Ocean Water (V-SMOW)[91] namely 18.015 268 g mol^{-1}. Equation (21) can be simplified to

$$\frac{\epsilon-1}{\epsilon+2}=A\frac{\epsilon}{(2\epsilon+1)(\epsilon+2)}+B, \tag{22}$$

where A and B are given by

$$A=\frac{N_A\mu^2}{\epsilon_0 k}\frac{\rho g}{T}, \tag{23}$$

$$B=\frac{N_A\alpha}{3\epsilon_0}\rho. \tag{24}$$

Equation (22) can be rearranged to

$$\epsilon^2(2-2B)-\epsilon(1+A+5B)-(1+2B)=0. \tag{25}$$

The physically correct root of Eq. (25) for the dielectric constant is

$$\epsilon=\frac{1+A+5B+\sqrt{9+2A+18B+A^2+10AB+9B^2}}{4-4B}. \tag{26}$$

Values of g can be determined from values of ϵ with the following equation:

$$g=\left(2+\frac{1}{\epsilon}\right)\frac{kT}{3\mu^2}\left(\frac{3\epsilon_0}{N_A\rho}(\epsilon-1)-\alpha(\epsilon+2)\right). \tag{27}$$

4.2. Adaptive Regression Algorithm

Our approach to obtaining a functional form for g was purely empirical, except for some physical constraints. We required that $g=1$ at $\rho=0$. Also, we spent considerable effort on making sure that the dielectric constant and g-factor display acceptable behavior, such as a monotonic decrease along isochores, when extrapolating to high temperatures. We assumed that $g-1$ could be represented by a sum of terms of the form $[(\rho/\rho_c)^i(T_c/T)^j]$, where $\rho_c=322/M_w$ mol m^{-3}, with M_w from Table 3, and $T_c=647.096$ K. By means of a weighted adaptive linear regression algorithm,[93] the most significant terms were selected from a large bank of terms of the appropriate form; the weight assignments will be discussed in Sec. 4.4. To adequately accommodate the supercooled water data, we included a bank of additional ''power-law'' terms of the form proposed by Hodge and Angell[22]

$$\frac{\rho}{\rho_c}\left(\frac{T}{228\ \mathrm{K}}-1\right)^{-q}. \tag{28}$$

The temperature of 228 K is the singular temperature introduced by Speedy and Angell.[21] Terms of this form were found by us to contribute significantly only at temperatures well below 273.15 K. The prefactor ρ/ρ_c in Eq. (28) insures that only the liquid phase is affected by the anomalous term.

4.3. Equation of State for Water

In this work, the densities have been calculated from the equation of state of Wagner and Pruss.[19] It has been adopted by the International Association for the Properties of Water and Steam (IAPWS) as the formulation for general and scientific use.[20] The International Temperature Scale of 1990[18] (ITS-90) was used in this formulation and has been used throughout this paper.

4.4. Weight Assignment

The uncertainty dg in the value of g, used in the regression analyses was obtained by combining in quadrature the uncertainties in ϵ, T and ρ with the following equation:

$$dg=\sqrt{\left(\frac{\partial g}{\partial\epsilon}d\epsilon\right)^2+\left(\frac{\partial g}{\partial\rho}d\rho\right)^2+\left(\frac{\partial g}{\partial T}dT\right)^2}. \tag{29}$$

In this case we arbitrarily set the uncertainties $dT=0.1$ K, $d\rho=0.5$ mol dm^{-3} and took $d\epsilon$ from Table 2. The derivatives of g required in Eq. (29) were determined from the following relationships:

$$\left(\frac{\partial g}{\partial T}\right)_{\rho,\epsilon}=\left(2+\frac{1}{\epsilon}\right)\frac{k}{3\mu^2}\left(\frac{3\epsilon_0}{N_A\rho}(\epsilon-1)-\alpha(\epsilon+2)\right), \tag{30}$$

$$\left(\frac{\partial g}{\partial\rho}\right)_{T,\epsilon}=-\left(2+\frac{1}{\epsilon}\right)\frac{kT}{3\mu^2}\frac{3\epsilon_0}{N_A\rho^2}(\epsilon-1), \tag{31}$$

and

$$\left(\frac{\partial g}{\partial\epsilon}\right)_{T,\rho}=\frac{kT}{3\mu^2}\left[\frac{3\epsilon_0}{N_A\rho}\left(2+\frac{1}{\epsilon^2}\right)-\alpha\left(2-\frac{2}{\epsilon^2}\right)\right]. \tag{32}$$

TABLE 4. Values of the dielectric constant ϵ at temperatures T, pressures p and densities ρ, determined from the equation of state, calculated g obtained from Eq. (16), and final assigned weights.

Author	T/K	p/MPa	ρ/mol dm^{-3}	ε	g	$100 \cdot wt$
Deul[48]	573.11	8.6	39.536 264	20.1	2.538 957	0.005 129 1
	573.11	10.0	39.709 55	20.25	2.545 543	0.005 133 4
	573.11	20.0	40.787 042	21.05	2.567 493	0.005 227 3
	573.11	30.0	41.671 746	21.8	2.595 640	0.005 254 2
	573.11	40.0	42.432 143	22.39	2.611 605	0.005 301 5
	573.11	50.0	43.104 308	22.92	2.625 867	0.005 335 7
	573.11	60.0	43.709 938	23.4	2.638 311	0.005 362 2
	573.11	70.0	44.263 241	23.88	2.653 959	0.005 364 1
	573.11	80.0	44.774 104	24.29	2.663 999	0.005 378 5
	573.11	90.0	45.249 720	24.68	2.673 892	0.005 385 2
	573.11	100.0	45.695 507	25.08	2.686 681	0.005 373 8
	573.11	120.0	46.513 525	25.77	2.704 209	0.005 365 2
	573.11	140.0	47.252 612	26.43	2.722 998	0.005 333 4
	573.11	150.0	47.597 886	26.71	2.728 383	0.005 327 1
	573.11	160.0	47.929 138	27.04	2.739 899	0.005 294 4
	573.11	180.0	48.554 664	27.67	2.761 647	0.005 225 8
	573.11	200.0	49.137 694	28.2	2.775 200	0.005 178 1
	573.11	220.0	49.684 684	28.65	2.782 571	0.005 144 4
	573.11	240.0	50.200 665	29.12	2.793 731	0.005 090 0
	573.11	250.0	50.448 311	29.36	2.800 364	0.005 056 8
	573.11	260.0	50.689 642	29.6	2.807 320	0.005 021 3
	573.11	280.0	51.154 854	30.0	2.814 262	0.004 970 6
	573.11	300.0	51.598 969	30.45	2.827 219	0.004 895 2
Fernández *et al.*[16]	273.174	p_0*	55.499 852	87.883	3.647 568	3.456 808 6
	283.142	p_0*	55.491 996	84.014	3.612 379	3.524 059 6
	293.143	p_0*	55.409 034	80.239	3.576 082	3.585 507 1
	298.139	p_0*	55.344 747	78.401	3.557 593	3.615 394 5
	298.154	p_0*	55.344 534	78.414	3.558 389	3.613 606 9
	303.132	p_0*	55.267 282	76.631	3.540 434	3.641 368 5
	313.125	p_0*	55.076 944	73.235	3.507 631	3.687 766 6
	323.129	p_0*	54.844 843	69.946	3.472 787	3.734 955 8
	323.139	p_0*	54.844 592	69.934	3.472 308	3.736 085 1
	343.127	p_0*	54.274 949	63.827	3.403 857	3.820 287 8
	343.134	p_0*	54.274 728	63.790	3.401 930	3.824 539 3
	343.147	p_0*	54.274 316	63.806	3.402 962	3.822 202 2
	353.128	p_0*	53.943 361	60.946	3.367 749	3.862 241 2
	353.13	p_0*	53.943 292	60.919	3.366 249	3.865 629 1
	353.154	p_0*	53.942 462	60.878	3.364 229	3.870 116 1
	363.137	p_0*	53.583 346	58.137	3.328 250	3.906 314 3
	373.113	p_0*	53.197 966	55.503	3.291 169	3.932 318 5
	373.147	p_0*	53.196 609	55.515	3.292 303	3.929 498 3
Heger[8]	773.15	25.0	4.981 529	1.7	1.367 106	0.000 238 3
	773.15	50.0	14.269 709	3.7	1.589 509	0.001 562 2
	773.15	75.0	24.049 460	7.0	1.929 083	0.003 224 6
	773.15	100.0	29.323 759	9.3	2.117 029	0.004 101 1
	773.15	150.0	34.970 589	12.0	2.279 219	0.005 028 4
	773.15	200.0	38.380 237	13.8	2.373 334	0.005 581 8
	773.15	250.0	40.865 463	15.05	2.415 249	0.005 993 5
	773.15	300.0	42.841 001	16.1	2.451 078	0.006 319 5
	773.15	350.0	44.491 957	16.95	2.472 018	0.006 596 0
	773.15	400.0	45.917 463	17.65	2.482 223	0.006 838 8
	773.15	450.0	47.176 919	18.3	2.494 231	0.007 052 6
	773.15	500.0	48.308 755	18.8	2.491 645	0.007 251 5
	823.152	25.0	4.358 312	1.5	1.203 311	0.000 156 9
	823.152	50.0	10.846 791	2.65	1.422 085	0.000 881 4
	823.152	75.0	18.713 108	4.9	1.787 130	0.002 049 5
	823.152	100.0	24.676 279	6.95	1.977 066	0.002 953 1
	823.152	150.0	31.497 089	9.85	2.209 228	0.003 961 0
	823.152	200.0	35.513 728	11.6	2.294 971	0.004 555 0
	823.152	250.0	38.367 489	12.85	2.338 668	0.004 979 5
	823.152	300.0	40.594 479	13.9	2.378 251	0.005 308 6
	823.152	350.0	42.429 787	14.75	2.402 243	0.005 582 6
	823.152	400.0	43.997 206	15.45	2.414 872	0.005 819 6
	823.152	450.0	45.369 866	16.05	2.421 761	0.006 029 1
	823.152	500.0	46.594 511	16.6	2.428 890	0.006 216 2
Hodge and Angell[22]	238.157	p_0*	54.141 910	106.3	3.979 086	0.050 208 8
	244.356	p_0*	54.699 601	101.5	3.845 995	0.066 304 2

TABLE 4. Values of the dielectric constant ϵ at temperatures T, pressures p and densities ρ, determined from the equation of state, calculated g obtained from Eq. (16) and final assigned weights—Continued

Author	T/K	p/MPa	ρ/mol dm^{-3}	ε	g	$100 \cdot wt$
Lees[60]	273.15	99.09	58.001 257	91.778	3.602 552	1.080 697 4
	273.15	198.17	60.023 304	95.278	3.579 951	1.149 365 0
	273.15	297.26	61.707 332	98.518	3.572 306	1.200 134 6
	273.15	396.35	63.157 902	101.565	3.573 677	1.238 506 8
	273.15	594.53	65.598 915	107.262	3.591 865	2.581 927 7
	283.144	198.17	59.813 425	90.969	3.556 776	1.157 780 0
	283.144	396.35	62.894 786	96.919	3.552 029	1.245 534 5
	283.144	594.53	65.320 162	102.300	3.568 833	1.299 204 6
	283.144	743.16	66.870 830	106.076	3.588 141	1.326 185 4
	293.138	198.17	59.586 871	86.901	3.532 469	1.166 578 1
	293.138	297.26	61.206 331	89.828	3.528 068	1.214 668 0
	293.138	594.53	65.035 939	97.671	3.545 697	1.307 462 6
	293.138	871.97	67.790 006	104.211	3.582 110	1.353 639 0
	303.133	198.17	59.346 956	83.039	3.506 258	1.176 287 2
	303.133	297.26	60.943 844	85.832	3.503 105	1.223 557 5
	303.133	594.53	64.750 435	93.308	3.520 848	1.316 861 1
	303.133	990.88	68.527 427	101.925	3.569 192	1.381 227 1
	323.127	198.17	58.830 959	75.972	3.452 943	1.195 548 4
	323.127	297.26	60.401 874	78.571	3.453 056	1.241 084 6
	323.127	594.53	64.181 204	85.417	3.471 099	1.335 799 6
	323.127	1189.05	69.522 290	96.992	3.547 484	1.420 329 2
Lukashov[65]	773.071	27.104 065	5.550 930	1.68	1.176 701	0.000 488 2
	773.071	35.897 927	8.326 395	2.116	1.223 181	0.000 959 4
	773.071	42.968 070	11.101 860	2.656	1.305 619	0.001 408 3
	773.071	49.141 869	13.877 324	3.31	1.407 327	0.001 766 7
	773.071	55.104 104	16.652 789	4.06	1.508 998	0.002 042 0
	773.071	68.964 086	22.203 719	6.2	1.834 535	0.002 085 2
	773.071	90.957 351	27.754 649	8.4	2.012 873	0.002 221 9
	773.071	131.669 202	33.305 579	11.2	2.239 132	0.002 135 5
	773.071	208.508 795	38.856 508	14.1	2.393 065	0.002 105 0
	773.071	347.134 958	44.407 438	17.1	2.501 186	0.002 097 7
	773.071	582.069 333	49.958 368	19.6	2.496 270	0.002 233 9
	523.11	3.973 490	44.348 696	26.75	2.721 860	0.031 058 7
Mulev *et al.*[17]	510.27	3.180 748	0.883 105	1.125	1.032 179	0.010 606 6
	525.09	4.108 069	1.146 229	1.162	1.048 917	0.017 258 4
	530.10	4.464 192	1.249 422	1.176	1.050 900	0.020 397 7
	541.06	5.325 323	1.504 591	1.211	1.057 139	0.029 142 6
	541.30	5.345 499	1.510 672	1.215	1.073 621	0.028 557 4
	541.73	5.381 793	1.521 623	1.216	1.071 162	0.029 090 0
	548.78	6.004 140	1.711 967	1.235	1.040 732	0.038 705 0
	563.60	7.490 683	2.188 337	1.302	1.057 079	0.061 100 7
	574.35	8.734 037	2.614 215	1.358	1.054 174	0.087 216 2
	586.67	10.347 813	3.212 504	1.450	1.082 146	0.124 830 0
	593.28	11.303 732	3.596 024	1.506	1.087 529	0.154 456 4
	596.65	11.816 846	3.812 325	1.540	1.094 576	0.171 235 9
	599.14	12.207 551	3.982 426	1.566	1.097 926	0.185 542 5
	601.94	12.658 954	4.185 230	1.595	1.097 647	0.204 654 8
	605.73	13.290 854	4.481 459	1.645	1.109 944	0.229 362 4
	608.50	13.768 336	4.715 807	1.684	1.117 276	0.250 459 0
	609.48	13.940 506	4.802 716	1.698	1.118 990	0.258 864 5
	609.91	14.016 591	4.841 550	1.704	1.119 319	0.262 842 1
	610.86	14.185 868	4.928 914	1.717	1.119 238	0.272 252 2
	611.61	14.320 663	4.999 460	1.727	1.118 388	0.280 325 6
	612.77	14.531 176	5.111 434	1.745	1.120 201	0.291 891 7
	613.58	14.679 647	5.191 774	1.758	1.121 536	0.300 289 4
	613.91	14.740 485	5.225 031	1.763	1.121 511	0.304 078 1
	614.20	14.794 118	5.254 515	1.768	1.122 305	0.307 049 7
	614.71	14.888 820	5.306 962	1.779	1.126 691	0.310 860 0
Oshry[6]	564.23	7.559 563	40.512 412	21.273	2.576 942	0.331 446 7

*Liquid state at 0.101 325 MPa.

The weight wt for each experimental data point was obtained from:

$$wt = \frac{1}{(dg)^2}. \tag{33}$$

We based our initial weighting scheme on our data evaluations described in Ref. 3. The uncertainties in the dielectric constant determined from Ref. 3 are listed in Table 2.

In a preliminary regression analysis with our bank of terms and the initial weights, we were unable to obtain a satisfactory equation that represented the dielectric constant over the entire surface. We therefore adjusted, numerous times, the bank of terms and found no significant improvement in the equation. Finally, we added additional weights to key data sets until we obtained an accurate representation of all dielectric constant data. The data sets, values of g, and final weights used in the regression analysis and normalized to sum to unity, are listed in Table 4.

Table 4 shows that while the experimental static dielectric constant varies between 1 and 110, the corresponding values of g lie between 1 and 4 in the available temperature and pressure range. Because of its limited range, g is a more favorable dependent variable for regression analysis.

5. Results

5.1. Results of the Regression Analysis

The terms selected to represent g were

$$g = 1 + \sum_{k=1}^{11} N_k(\rho/\rho_c)^{i_k}(T_c/T)^{j_k} + N_{12}(\rho/\rho_c)\left(\frac{T}{228\ \mathrm{K}} - 1\right)^{-q}. \tag{34}$$

The values of N_k, i_k, j_k, and q are given in Table 5. Each term entered with a high degree of significance (>0.9995) and no further significant terms remained unselected at the conclusion of the analysis.

TABLE 5. Coefficients N_k and exponents i_k, j_k, and q of Eq. (34) for the g-factor.

k	N_k	i_k	j_k
1	0.978 224 486 826	1	0.25
2	−0.957 771 379 375	1	1
3	0.237 511 794 148	1	2.5
4	0.714 692 244 396	2	1.5
5	−0.298 217 036 956	3	1.5
6	−0.108 863 472 196	3	2.5
7	$0.949\ 327\ 488\ 264 \cdot 10^{-1}$	4	2
8	$-0.980\ 469\ 816\ 509 \cdot 10^{-2}$	5	2
9	$0.165\ 167\ 634\ 970 \cdot 10^{-4}$	6	5
10	$0.937\ 359\ 795\ 772 \cdot 10^{-4}$	7	0.5
11	$-0.123\ 179\ 218\ 720 \cdot 10^{-9}$	10	10
12	$0.196\ 096\ 504\ 426 \cdot 10^{-2}$	$q = 1.2$	

TABLE 6. Dielectric constant data sources corresponding to the symbols in the deviation plots.

Symbol	Author	Reference(s)
+	Åkerlöf	66
×	Albright	67
□	Albright and Gosting	68
○	Bertolini *et al.*	24
△	Cogan	62
▽	Deul	48
◁	Drake *et al.*	69
▷	Dunn and Stokes	70
⧖	Fernández *et al.* (TB)	16
⋈	Fernández *et al.* (LCR)	16
◇	Fogo *et al.*	71
*	Gier and Young	72
◺	Golubev	73
◹	Grant *et al.*	74
◿	Harris *et al.*	75
Y	Hasted and Shahidi	23
⅄	Heger	8
≻	Hodge and Angell	22
≺	Kaatze and Uhlendorf	76
⍁	Lees	60
⍂	Lukashov	65
⍃	Lukashov *et al.*	77
⍀	Malmberg and Maryott	78
⍄	Milner	61
⍅	Muchailov	79
⍆	Mulev *et al.*	17
⍇	Oshry	6
⍈	Rusche	63
⍉	Scaife	80
⍊	Schadow and Steiner	81
⍋	Srinivasan and Kay	82, 83
⍌	Svistunov	84
⍍	Tyssul Jones and Davis	85
⍎	Vidulich *et al.*	86, 87
⍏	Wyman and Ingalls	88
↑	Wyman	89
———	This work	
- - - - -	Archer and Wang	13

5.2. Deviation Plots

The dielectric constant data from virtually the entire data base[3] are shown in Figs. 5–11 along with the correlation of Archer and Wang, as deviations from our formulation. The symbols used are explained in Table 6. In each figure, the experimental data span small regions of pressure and temperature; the temperature or pressure at which the correlation

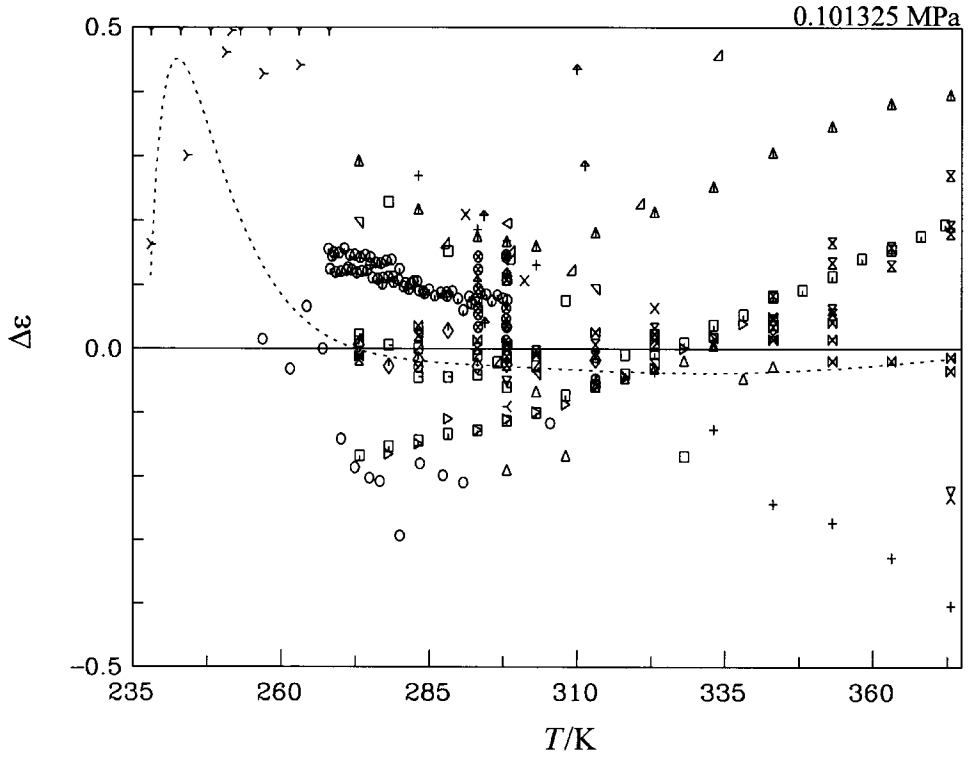

FIG. 5. Deviations $\Delta\epsilon = \epsilon - \epsilon$(calc.) of dielectric constant ϵ data from Eqs. (21) and (34) (and coefficients listed in Table 5) for water at a pressure of 0.101325 MPa and temperatures in the range 235–373 K. Symbols: Table 6.

is calculated is indicated in parentheses. Only the data of Scaife *et al.*[80] and of Schadow and Steiner[81] were omitted because they were out of range.

The dielectric constant data at ambient pressure, including those in the supercooled region, are shown in Fig. 5 as deviations from Eqs. (21) and (34) plotted against temperature.

For the supercooled state, the data of Hodge and Angell[22] differ from 0.15 to 0.5 from our formulation. This difference is of similar magnitude as the discrepancy between the Hodge and Angell data and those of Bertolini *et al.*[24] at 260 K. The latter measurements and those of Rusche span both the low temperature liquid and supercooled state, although the minimum temperature reached is well above that of Hodge and Angell. The Bertolini data lie within ± 0.1 of Eqs. (21) and (34) in the supercooled region but depart from the correlation at the higher temperatures, to lie at worst 0.3 below our equation at 283 K. The data of Rusche shows an opposite trend, converging from an offset of $+0.2$ at 265 K to less than $+0.1$ at about 300 K.

Above 273 K and below 340 K the results of Fernández *et al.*,[16] Milner,[61] Cogan,[62] Srinivasan and Kay,[82,83] Lees,[60] and Vidulich *et al.*[86,87] differ by less than 0.05 from Eqs. (21) and (34), while the data of Malmberg and Maryott[78] and those of Dunn and Stokes[70] depart systematically below 340 K, to -0.2 below Eqs. (21) and (34) at 273.15 K. At temperatures above 340 K the LCR meter data of Fernández *et al.*[17] lie within 0.05 of Eqs. (21) and (34) and follow the trend indicated by the data of Lukhashov,[65] while the Fernández *et al.*[17] transformer bridge data follow the trend of Malmberg and Maryott.[78] At 373 K the latter two data sets depart from our equation by about $+0.2$. Above 273 K, the correlation of Archer and Wang is consistent with ours and passes through the LCR meter results of Fernández *et al.* This agreement implies that the data of Malmberg and Maryott are inconsistent with the other data sets in that range.

The data in liquid water up to 570 K and high pressures are compared with the formulation in Figs. 6–8. Here comparisons are made at narrow temperature intervals around the nominal values indicated, and the deviations are plotted as a function of the amount-of-substance density.

The data of Lees[60] extend to densities of about 70 mol dm^{-3} at temperatures between 273 K and 320 K and therefore anchor the high-density end of the formulation. They are shown in Figs. 6 and 7. The departures lie within ± 0.1 of Eqs. (21) and (34), exceeding Lees's estimated uncertainty in the measurements (0.01) but reflecting the actual scatter of the data. At temperatures between 370 K and 520 K, shown in Fig. 8, the data of Heger[8,12] and Deul[48,49] are inconsistent. At 370 K these two data sets differ by up to 0.5 and they grow further apart at higher temperatures.

The near- and supercritical data are compared in Figs. 9 and 10. The largest difference between the Heger and Deul data is at 673 K, up to one unit in ϵ. At this temperature, systematic differences from the formulation are of the order of ± 0.5. Notwithstanding strenuous effort on our part, the formulation could not be forced to follow the curvature displayed by the Heger data at the high densities. At the highest temperatures, up to 873 K, the available data are within ± 0.5

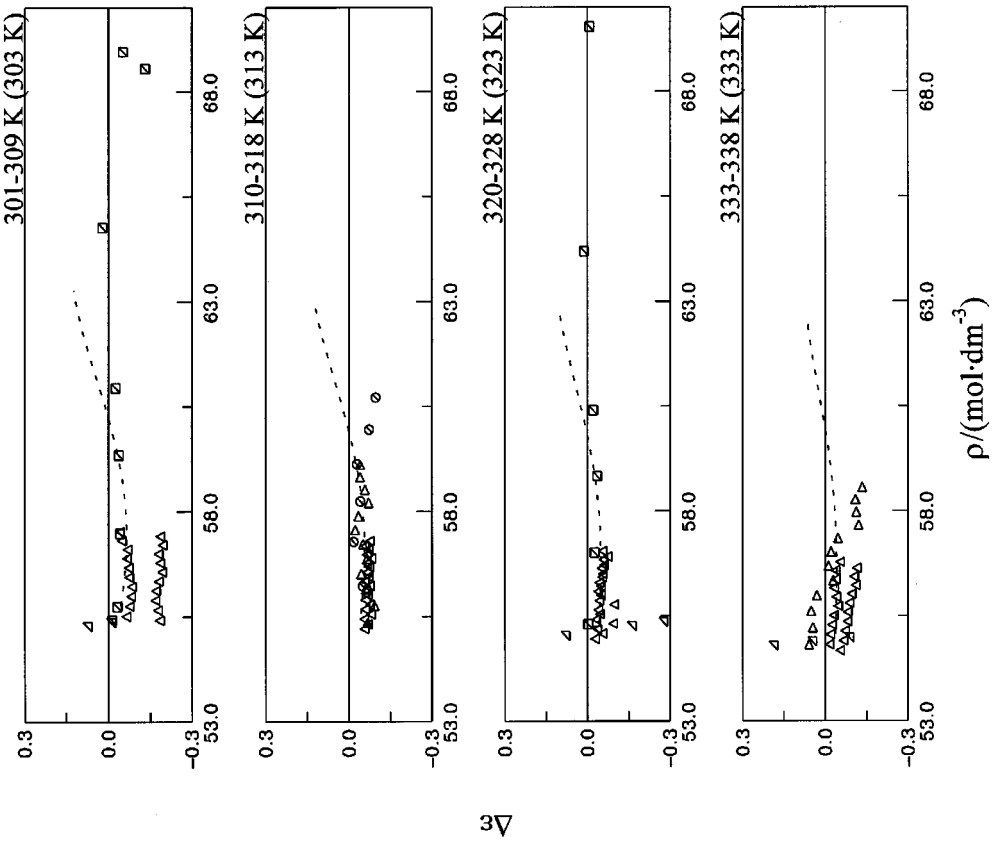

FIG. 7. Deviations $\Delta\epsilon = \epsilon - \epsilon(\text{calc.})$ of dielectric constant ϵ data from Eqs. (21) and (34) (with coefficients listed in Table 5) for water at temperatures between 301 K and 338 K. Symbols: Table 6.

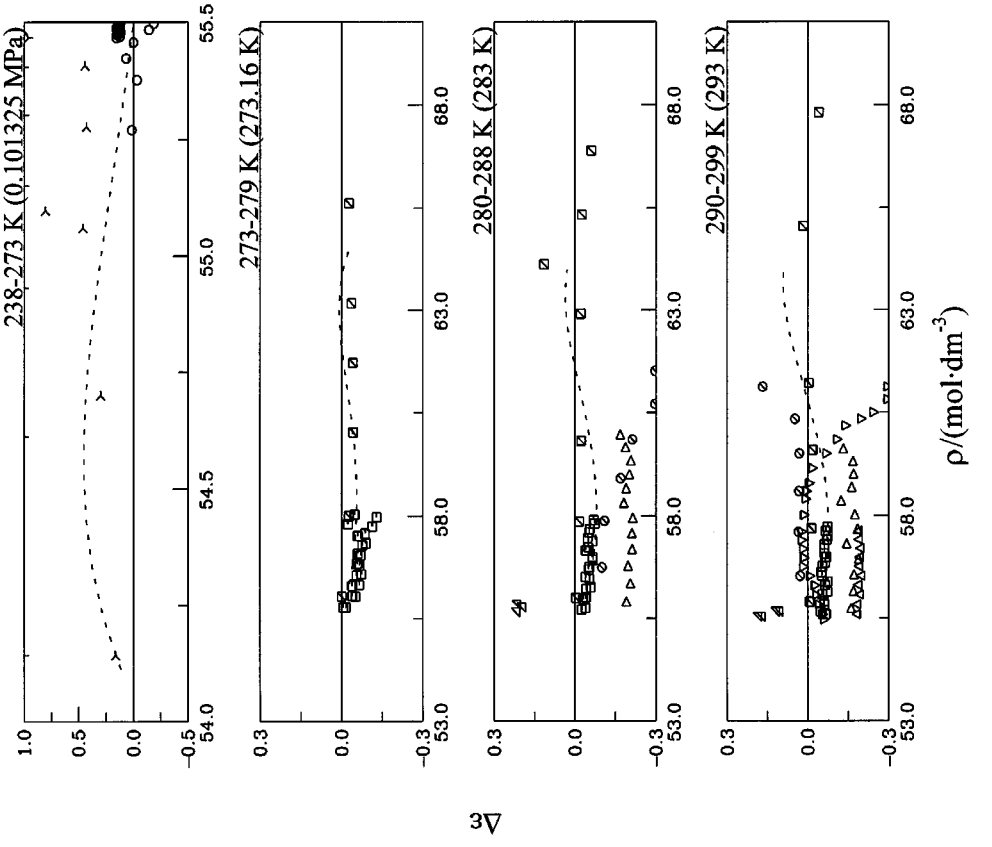

FIG. 6. Deviations $\Delta\epsilon = \epsilon - \epsilon(\text{calc.})$ of dielectric constant ϵ data from Eqs. (21) and (34) (with coefficients listed in Table 5) for water at temperatures between 238 K and 299 K. Symbols: Table 6.

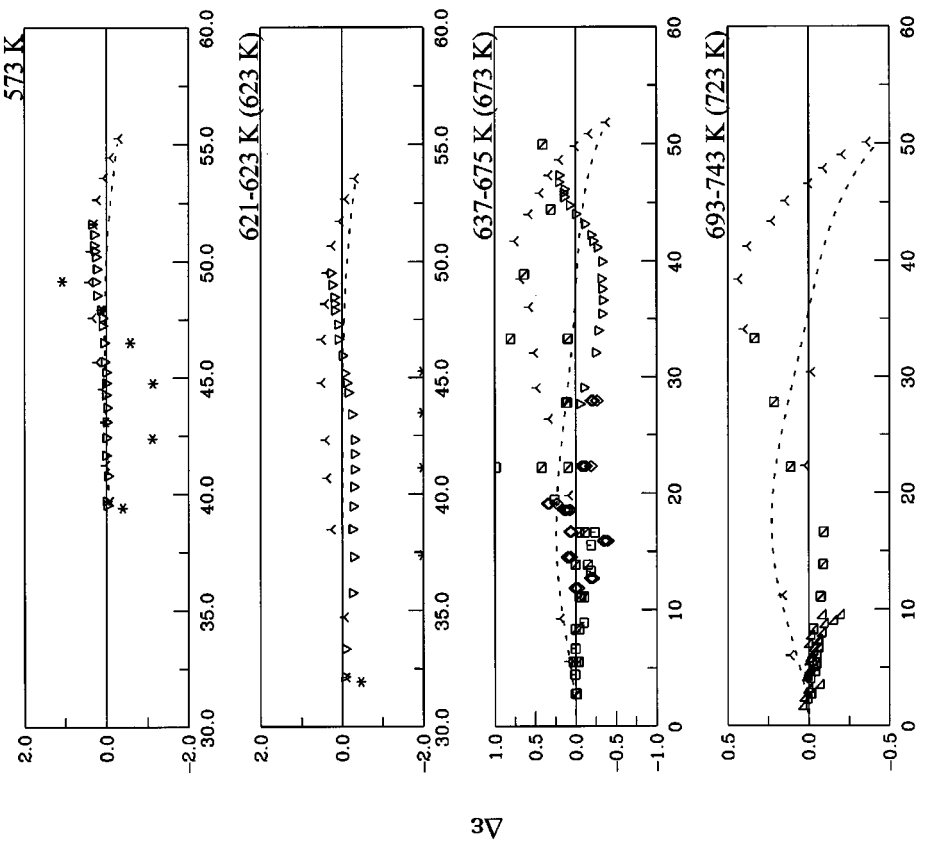

FIG. 9. Deviations $\Delta\epsilon = \epsilon - \epsilon$(calc.) of dielectric constant ϵ data from Eqs. (21) and (34) (with coefficients listed in Table 5) for water at temperatures between 573 K and 743 K. Symbols: Table 6.

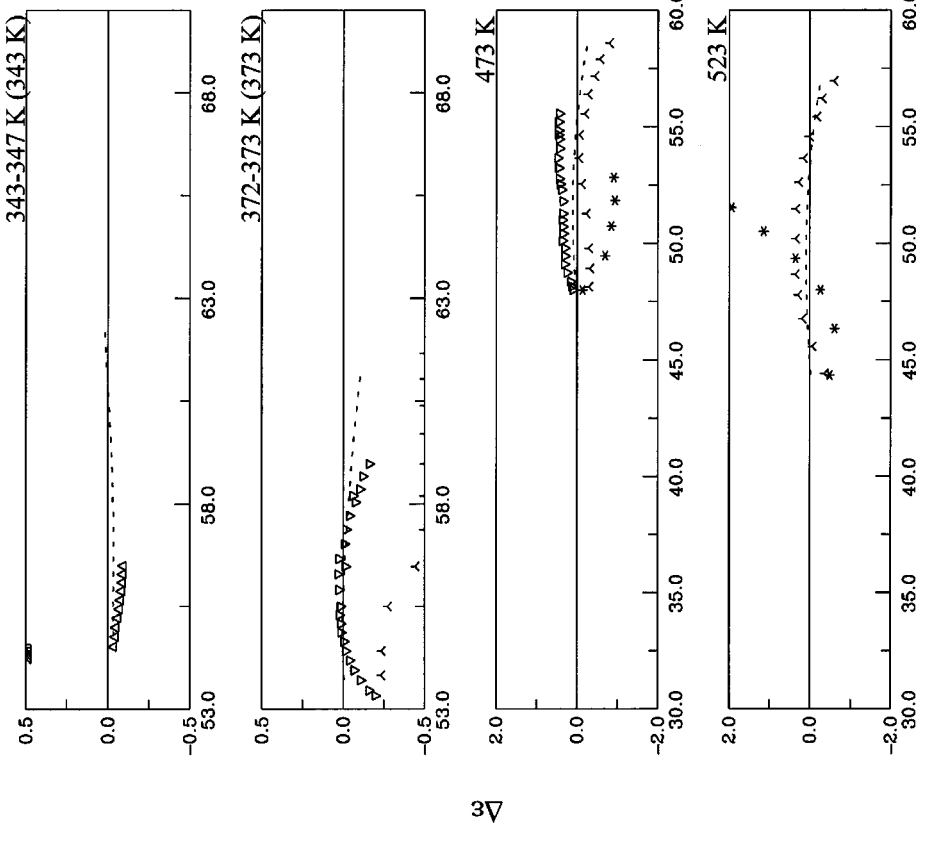

FIG. 8. Deviations $\Delta\epsilon = \epsilon - \epsilon$(calc.) of dielectric constant ϵ data from Eqs. (21) and (34) (with coefficients listed in Table 5) for water at temperatures between 343 K and 523 K. Symbols: Table 6.

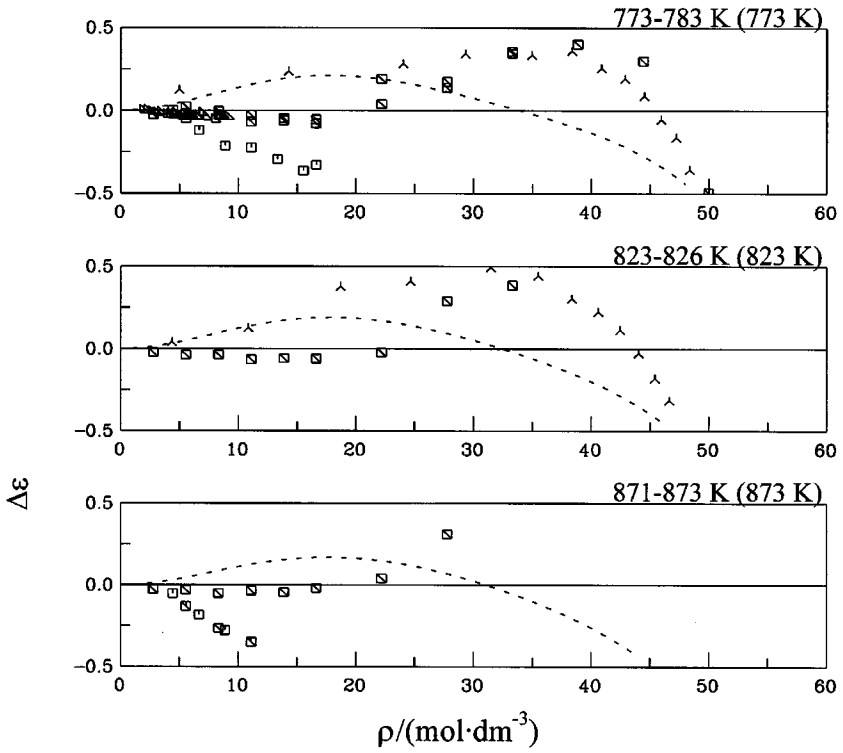

FIG. 10. Deviations $\Delta\epsilon = \epsilon - \epsilon$(calc.) of dielectric constant ϵ data from Eqs. (21) and (34) (with coefficients listed in Table 5) for water at temperatures between 773 K and 873 K. Symbols: Table 6.

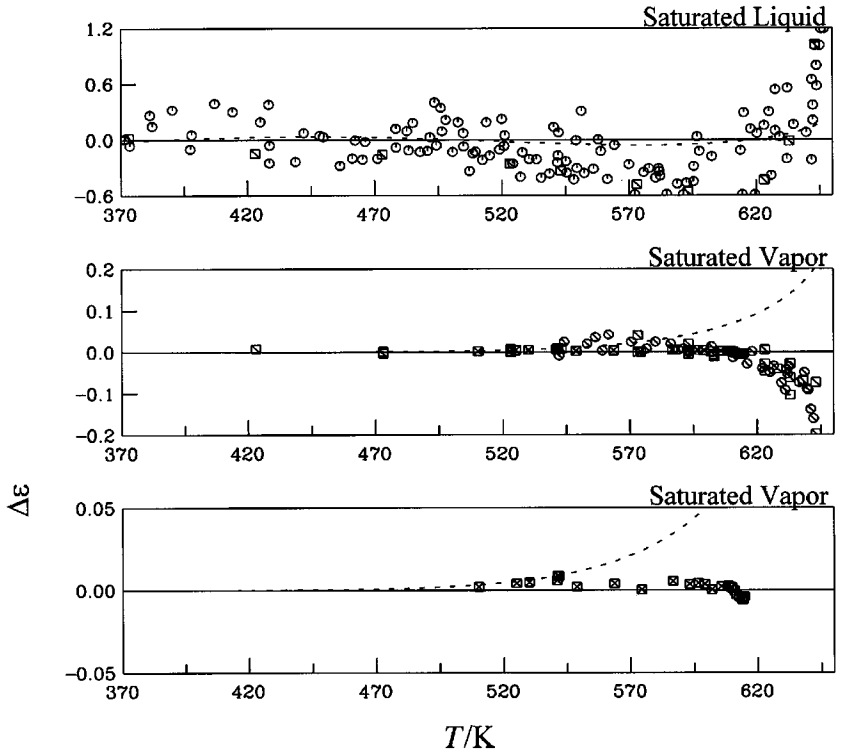

FIG. 11. Deviations $\Delta\epsilon = \epsilon - \epsilon$(calc.) of dielectric constant ϵ data from Eqs. (21) and (34) (with coefficients listed in Table 5) for saturated liquid water and steam. Symbols: Table 6.

from the formulation. In this range, the actual dielectric constant values are of the order of 10 only, so this uncertainty is substantial.

The saturated liquid and vapor data are shown in Fig. 11. The saturated liquid data of Lukashov,[65] which were included in our regression, and those of Oshry,[6] which were not, show, albeit small, systematic departures from Eqs. (21) and (34). These departures increase within the last 25 K from the critical point, with values up to 1.2 for the liquid, and down to −0.2 for the vapor, roughly twice the scatter of the data. The most recent data in the saturated vapor by Mulev,[3,17] which reach up to 614 K, are in excellent agreement with Eqs. (21) and (34), while the values reported by Lukashov,[65] Svistunov *et al.*,[84] and Muchailov[79] depart from it increasingly as the temperature approaches the critical, and end up about 0.2 below our formulation.

The theoretical predictions of Goldman *et al.*[50] are compared with the present formulation in Table 1. In the range of the data, the theoretical predictions and the formulation differ by less than one unit in ϵ, but the correlation develops positive departures from the theoretical predictions at the higher temperatures. For a detailed comparison of SPC/E computer simulation data with our formulation, see Ref. 59.

The differences between the values obtained from Eqs. (21) and (34) and from the correlation of Archer and Wang[13] are less than 0.3 under all conditions. At temperatures below 470 K the differences are less than 0.1 except for the supercooled liquid. The two formulations show small systematic differences at the higher temperatures and densities, which result from the choice (and availability) of different data sets as well as different upper density limits. Archer and Wang, for instance, included the Heger data[8,12] at subcritical temperatures (Figs. 8 and 9), which results in the systematic, but still quite modest departures between the two formulations in the high-density range where we choose to follow the Deul data.[48,49] Nevertheless, the agreement is quite exceptional and indicates that any uncertainties associated with the selection of functional form are small compared to the systematics in the experimental values.

5.3. Comparison with Previous Correlations

At a number of state points, we have compared the current formulation with the previous formulations of Helgeson and

TABLE 7. Comparison of previous formulations with the present one. (H&K: Ref. 5: B&P: Ref. 10, U&F: Ref. 11, A&W: Ref. 13).

T/K (ITS-90)	p/MPa	H&K	B&P	U&F	A&W	This work
238.00	p_0*		102.69		106.42	106.31
273.15	p_0*		87.86	87.81	87.90	87.90
273.15	100		91.69	92.04	91.79	91.84
273.15	500		103.65	101.42	104.71	104.59
273.15	1000		114.23			117.73
298.14	p_0*	78.47	78.38	78.46	78.38	78.41
298.14	50	80.20	80.17	80.36	80.15	80.21
298.14	100	81.78	81.84	82.08	81.83	81.90
298.14	200	84.38	84.87	84.94	85.00	85.02
298.14	500	90.35	92.24	91.16	93.31	93.09
298.14	1000		101.11			104.60
373.12	p_0*	55.47	55.46		55.51	55.53
373.12	100	58.55	58.61	58.55	58.67	58.67
373.12	500	66.17	66.95	66.57	67.67	67.78
373.12	1000		*73.25*			*76.39*
473.11	100	38.27	38.19	38.17	38.33	38.23
573.11	100	25.46	25.36	25.17	25.10	25.07
673.10	10			1.17	1.25	1.24
673.10	50	12.13	11.24	12.16	12.04	11.99
673.10	100	16.27	17.15	16.05	15.80	15.82
673.10	500	24.68	25.51	24.96	24.63	24.95
673.10	1000		*28.64*			*30.50*
773.07	10			1.11	1.17	1.17
773.07	50	3.94		3.45	3.65	3.46
773.07	100	9.27	11.83	9.29	9.05	8.96
773.07	500	18.56		19.14	18.73	19.13
773.07	1000					*24.25*
873.04	10				1.13	1.13
873.04	50				2.21	2.11
873.04	100	5.53			5.06	4.90
873.04	500	15.83			14.53	14.99
873.04	1000					*19.79*
1272.96	500				*6.34*	6.66

*Liquid state at 0.101 325 MPa.

Kirkham,[5] Bradley and Pitzer,[10] Uematsu and Franck,[11] and Archer and Wang.[13] We took tabulated values from the published formulations. The results are presented in Table 7. Blank values in Table 7 indicate entries not present in the relevant published tables. Data in italics indicate extrapolated values.

5.4. Auxiliary Formulations for Saturated States

Although the formulation gives a complete description of the dielectric constant both for unsaturated and saturated water and steam, it seemed useful to develop separate formulations for the dielectric constant as a function of temperature for the saturated states, thus circumventing the needs of generating the saturation boundary from the IAPWS-95 formulation, and incorporating the formulation of the g-factor. The functional form chosen is such that the limiting behavior at the critical point is close to theoretical expectations: a 1/3 power law in reduced temperature, with an amplitude of the same absolute value on the vapor and liquid sides. Defining the variable

$$\theta=(1-T/T_c)^{1/3} \tag{35}$$

the equation we used to describe the dielectric constant of the saturated liquid is

$$\epsilon_{\rm liq}=5.36058\left(1+\sum_{i=1}^{i=8} L_i\theta^{\,i}\right), \tag{36}$$

while that for the saturated vapor is given by

$$\epsilon_{\rm vap}=1+4.36058\left(\sum_{i=1,2,7,14,24} V_i\theta^{\,i}\right). \tag{37}$$

The coefficients in these equations were determined by fitting the functional forms to a dense set of saturation values generated from the full formulation. The coefficients L_i and V_i are listed in Table 8. The auxiliary equations (36) and (37) represent the dielectric constant values generated by the full formulation for temperatures up to 634 K to within 0.05%.

Between 634 K and 643 K, the representation agrees with the full formulation to within 0.1%, and between 643 K and the critical point, to within 0.5%.

TABLE 8. Coefficients L_i and V_i for Eqs. (36) and (37).

i	L_i	V_i
1	2.725 384 249 466	−3.350 389 240 1
2	1.090 337 041 668	−3.472 776 251 5
3	21.452 598 367 36	
4	−47.127 595 811 94	
5	4.346 002 813 555	
6	237.556 188 697 1	
7	−417.735 307 739 7	−12.061 801 495
8	249.383 400 313 3	
14		−25.430 358 103
24		−48.297 009 442

TABLE 9. Estimated absolute uncertainty of the predicted dielectric constant, $\epsilon_{\rm pred}$, at various state points.

p/MPa	T/K	ρ/kg m^{-3}, Ref. 20	$\epsilon_{\rm pred}$	U_ϵ
p_0*	238	975.06	106.31	1
p_0*	256	995.25	95.20	0.3
p_0*	273	999.83	87.96	0.04
585.3	273	1180	107.06	0.05
p_0*	323	988.10	69.96	0.04
1189	323	1253	97.02	0.04
p_0*	373	958.46	55.57	0.2
495.8	373	1110	67.73	0.5
3.16 541	510	15.832 0	1.122	0.003
141.68	523	900	32.23	1
14.757	614	94.3	1.77	0.02
22.038 6	647	357	6.17	0.3
19.933 7	673	100	1.75	0.1
407.896	673	900	23.60	0.5
27.099	773	100	1.66	0.2
581.908	773	900	20.16	0.5
124.707	873	450	6.28	0.4

*Liquid state at 0.101 325 MPa.

5.5. Reliability Estimates in Various Regions

The reliability estimate of the correlation in each region of the phase diagram is based on the following three considerations: (1) our judgement of the quality of the selected data, if any, for the considered region; (2) how well the correlation represents these data; and (3) the assumption that global averaging tends to yield a result with less uncertainty than that of the individual data sets. The reliability is quantified by assigning an uncertainty $U_\epsilon(\rho,T)$, for each region in the phase diagram. This quantification is not rigorous, and does not follow the procedures recommended to express experimental uncertainties[94] because the statistical information needed is mostly not available. The reliability estimates proposed should therefore be considered only as a guideline. We expect that the dielectric constant for each thermodynamic condition will be, with a probability close to 1, within the interval $\epsilon_{\rm corr}\pm U_\epsilon$, where $\epsilon_{\rm corr}$ is the predicted value from the present correlation.

Table 9 shows our reliability estimates for the present correlation as a function of temperature and density. Undoubtedly the best known region is the liquid phase between 273.15 K and 323.14 K, and pressures up to the freezing curve. See Ref. 3 for an extensive review and intercomparison of the data. At 0.101325 MPa, the data of Lees,[60] Vidulich and Kay,[86,87] and Fernández *et al.*[16] in this temperature range agree to within 0.04 units of ϵ at 273.15 K, and somewhat closer at the higher temperatures. At 100 MPa, the data of Lees[60] agree with those of Milner[61] and Cogan[62] within 0.03 units of ϵ, or 0.04, at the five temperatures measured by Lees: 273.15 K, 283.14 K, 293.14 K, 303.13 K and 323.13 K. The formulation fits these data sets closely, and the uncertainty of the formulation in this range was estimated on the basis of the agreement with these data sets (Figs. 6 and 7).

Above 100 MPa, no direct comparison can be made, but it

may be expected that the data of Lees retain an excellent accuracy. The scatter of the Lees data in this range is less than 0.1 unit of ϵ, or 0.1%, see Figs. 6 and 7, and Fig. 6 in Ref. 17. These data are fitted to within this scatter, which forms the basis for an uncertainty estimate in this region.

Above 323.14 K, the uncertainty increases steeply. At the normal boiling point, the scatter of the most reliable data sources is at least 0.2 units of ϵ, or 0.4%. At pressures higher than 0.101325 MPa, the uncertainty is higher, due in part to the discrepancy, close to 1% at 200 MPa, of the only two data sets, those of Heger[8,12] and Deul.[48,49] For a detailed discussion of the best values at 298.14 K and 373.12 K, at 0.101325 MPa, see Ref. 3.

At temperatures above 473.12 K and below 873 K, the dielectric constant is predicted with an uncertainty exceeding 1, with the exception of the vapor phase for temperatures below 615 K. The saturated-steam state has been investigated accurately[3,17] and a reliability of 0.003 ϵ units (better than 0.3%) is expected for the correlation.

The situation in the rest of the high-temperature region is fairly uniform. At densities above 500 $\mathrm{kg\,m^{-3}}$ (28 $\mathrm{mol\,m^{-3}}$), up to the experimental limit corresponding to pressures of 500 MPa, an uncertainty of 0.5 units of ϵ, about 1%, can be expected on the basis of the departures of the data from the correlation (Figs. 8–10). The disagreement between the Heger and Deul data sets at 673 K, however, occasionally exceeds 1 ϵ unit or 5% (Fig. 9). For the lower densities, the absolute departures are below 0.5 ϵ units (Figs. 9 and 10), but the relative departures may be several percent, because of the lower values of ϵ.

We have refrained from speculating about the uncertainty in regions above 873 K. Although we have made sure both ϵ and g extrapolate reasonably, there are no data to compare with. We refer to Sec. 8 for further discussion of this range.

The supercooled region can be divided into two parts. From 256 K to the normal freezing point, accurate data by Bertolini *et al.*[24] measured in the bulk phase agree with the prediction of the correlation within 0.2 units of ϵ, even though these data were not considered in the fit. Below 256 K, only measurements in dilute emulsions have been obtained[22] with experimental uncertainties exceeding 1%.

5.6. Tabulation of the Dielectric Constant

Values of the dielectric constant have been calculated on a grid in p-T space. These values are displayed in Table 19 (Appendix). Outside the range where data exist, the values are given in italics and should be considered with caution. We have taken care to ensure that the equation extrapolates smoothly as function of temperature and density, but nothing is known about the uncertainty of the extrapolation. Liquid–vapor and liquid–solid phase boundaries are indicated. The values in the supercooled liquid are indicated in bold face.

For the near- and supercritical region, the dielectric constant varies steeply with pressure on isotherms, making interpolation awkward. Representation in a density-temperature grid (Table 20) leads to easier interpolation.

6. Derivatives of the Dielectric Constant

6.1. Derivatives Calculated from Experimental Information

The temperature and pressure derivatives of the dielectric constant have assumed a huge (and perhaps somewhat overblown[95]) importance in the formulation of properties of aqueous electrolytes because of their role in the Debye–Hückel limiting law and in applications of the Born model. It was therefore deemed important to compare derivatives obtained from our formulation with ''experimental'' values and with those derived from other formulations.

Several different techniques were employed by us to calculate the first and second derivatives of the dielectric constant with respect to temperature and pressure for experimental data. All experimental data were sorted by author on isotherms and isobars. Data that were not isothermal or isobaric were not used.

It is important to note that derivatives are not experimentally measured, and that what is termed ''experimental value of the derivative'' is, in fact, a value depending on the method used to derive it from the data. The first technique we used is a Lagrange interpolation using three and five points. The method tends to magnify the errors in the experimental data since the polynominal is forced to go through all points. The second technique we used is a polynomial regression of the data using three to nine terms, which tends to smooth the data. We tested out the two methods by calculating the first and second temperature derivatives of the dielectric constant at ambient pressure for the recent data of Fernández *et al.*[16]

As to the Lagrangian interpolation method, an $(n-1)^{\mathrm{th}}$-degree polynomial is used to fit a curve through every point of a set of n unevenly spaced data

$$\epsilon_n(x)=\sum_{i=1}^{n} L_i(x)\,\epsilon(x_i), \tag{38}$$

where $L_i(x)$ is given by

$$L_i(x)=\prod_{j=1,j\neq i}^{n}\frac{x-x_j}{x_i-x_j} \tag{39}$$

and x represents the pressure for isothermal data, or the absolute temperature for isobaric data. The value of the number n is the number of data points used in the interpolation. We have calculated the derivatives at the experimental data points themselves, although the Lagrangian interpolation can be used at any point in the interval. For $n=5$, we choose two data points on each side of the current data point, and for $n=3$, one data point on each side. Near the ends of the interval, the first, respectively last n data points were used. The first and second derivatives of ϵ with repect to x are readily obtained from algebraic expressions for the derivatives of $L(x)$.

TABLE 10. Values of $(\partial\epsilon/\partial T)_p$ determined from the results of Fernández *et al.* (Ref. 16) with five methods at $p=0.101325$ MPa and at temperatures between 273 K and 373.2 K.

Method	273.174 K	373.113 K
3-point Lagrange	−0.3935	−0.2571
5-point Lagrange	−0.3860	−0.2555
3-term polynomial	−0.3939	−0.2525
4-term polynomial	−0.4011	−0.2606
5-term polynomial	−0.4003	−0.2615
mean[a]	-0.39_5 $\pm 0.01_2$	-0.25_5 $\pm 0.01_2$

[a]Mean $\pm 2\sigma$, where σ is the standard deviation.

TABLE 11. Values of $(\partial^2\epsilon/\partial T^2)_p$ determined from the results of Fernández *et al.* (Ref. 16) with five methods at $p=0.101325$ MPa and at temperatures between 273 K and 373.2 K.

Method	273.174 K	373.113 K
3-point Lagrange	0.003209	0.004195
5-point Lagrange	−0.001543	0.001910
3-term polynomial	0.001415	0.001415
4-term polynomial	0.001809	0.001003
5-term polynomial	0.001723	0.000917
mean[a]	0.001_2 $\pm 0.003_3$	0.002_1 $\pm 0.002_9$

[a]Mean $\pm 2\sigma$, where σ is the standard deviation.

In the second method, an n^{th}-degree polynomial is fitted to all data in the experimental range of interest as a function of one independent variable, while another independent variable is kept constant.

The first and second derivatives of the dielectric constant with respect to temperature for the Fernández[16] LCR data at 11 different temperatures in the range of 273–373.2 K and at ambient pressure were determined from 3- and 5-point Lagrangian interpolations, and 3–5 term polynomial fits at 273.174 and 373.113 K. The results are shown in Table 10 for the first and in Table 11 for the second temperature derivative.

Tables 10 and 11 indicate that if all interpolation methods were considered equivalent, at 273 K, which is the lower edge of the interval, the first derivative has a 3% uncertainty at 273 K, and the second derivative is simply not reliably known. As we mentioned, however, Lagrangian and polynomial interpolations are not at all equivalent, the first method being the easiest to implement by computer, but having a tendency to exaggerate the scatter in the derivative, the second one smoothing the data, but requiring individual judgment. There are, therefore, no exact guidelines as to how to choose the proper method. In the case of temperature derivatives of the data of Fernández *et al.*, Tables 10 and 11, we have opted for the low degree and smoothing features of the 3rd-degree polynomial, and have chosen the uncertainty estimates associated with it.[16] In all other calculations of ''experimental derivatives'' (see Section 6.3), we have opted for Lagrangian 5-point interpolation for the sake of computation.

6.2. Derivatives from the Correlation

The partial derivative of the dielectric constant with respect to pressure at constant temperature is

$$\left(\frac{\partial\epsilon}{\partial p}\right)_T=\left(\frac{\partial\epsilon}{\partial\rho}\right)_T\left(\frac{\partial\rho}{\partial p}\right)_T. \tag{40}$$

The partial derivative of the dielectric constant with respect to temperature at constant pressure is

$$\left(\frac{\partial\epsilon}{\partial T}\right)_p=\left(\frac{\partial\epsilon}{\partial T}\right)_\rho-\left(\frac{\partial\epsilon}{\partial\rho}\right)_T\left(\frac{\partial p}{\partial T}\right)_\rho\left(\frac{\partial\rho}{\partial p}\right)_T. \tag{41}$$

From Eqs. (23), (24), and (26), the partial derivative of the dielectric constant with respect to density at constant temperature is

$$\left(\frac{\partial\epsilon}{\partial\rho}\right)_T=4B_1\frac{\epsilon}{4-4B}+\frac{A_1+5B_1+0.5C^{-0.5}[2A_1+18B_1+2AA_1+10(A_1B+AB_1)+18BB_1]}{4-4B}, \tag{42}$$

A and B are defined in Eqs. (23) and (24), respectively, and

$$A_1=A/\rho+(A/g)\left(\frac{\partial g}{\partial\rho}\right)_T,$$

$$B_1=B/\rho, \tag{43}$$

$$C=9+2A+18B+A^2+10AB+9B^2.$$

The partial derivative of the dielectric constant with respect to temperature at constant density is

$$\left(\frac{\partial\epsilon}{\partial T}\right)_\rho=\frac{A_2+0.5C^{-0.5}A_2[2+2A+10B]}{4-4B}, \tag{44}$$

where

$$A_2=-A/T+(A/g)\left(\frac{\partial g}{\partial T}\right)_\rho. \tag{45}$$

The first derivatives were therefore calculated analytically from the formulation in terms of ρ and T variables, after which they were converted to derivatives in p, T variables by multiplying by the appropriate derivatives of the equation of state. The second derivatives were calculated numerically.

Table 12 presents values of the dielectric constant, and the two first and three second derivatives. The first part of the table has integer temperature values on ITS-90, and can be

TABLE 12. Predicted values of the dielectric constant and its first and second derivatives with respect to pressure and temperature, at selected values of temperature and pressure.

T/K (ITS-90)	p/MPa	ρ/mol dm^{-3}	ϵ	$(\partial\epsilon/\partial p)_T$/MPa^{-1}	$(\partial\epsilon/\partial T)_p$/K^{-1}	$(\partial^2\epsilon/\partial p^2)_T$/MPa^{-2}	$(\partial^2\epsilon/\partial T^2)_p$/K^{-2}	$(\partial^2\epsilon/\partial p\partial T)$/MPa^{-1} K^{-1}
270	p_0*	55.482 7	89.182 1	0.042 680 5	−0.409 375	$-0.567\,45\times10^{-4}$	$0.226\,55\times10^{-2}$	$-0.284\,74\times10^{-3}$
300	p_0*	55.317 4	77.747 4	0.037 186 0	−0.355 908	$-0.571\,34\times10^{-4}$	$0.157\,32\times10^{-2}$	$-0.110\,07\times10^{-3}$
300	10.0	55.561 5	78.112 7	0.036 634 3	−0.357 011	$-0.543\,89\times10^{-4}$	$0.160\,84\times10^{-2}$	$-0.112\,78\times10^{-3}$
300	100.0	57.572 9	81.215 9	0.032 574 8	−0.367 852	$-0.374\,92\times10^{-4}$	$0.190\,41\times10^{-2}$	$-0.124\,92\times10^{-3}$
300	1000.0	68.692 7	103.696	0.021 287 2	−0.481 815	$-0.503\,41\times10^{-5}$	$0.357\,60\times10^{-2}$	$-0.121\,20\times10^{-3}$
350	p_0*	54.050 2	61.788 9	0.034 827 3	−0.284 834	$-0.777\,69\times10^{-4}$	$0.128\,05\times10^{-2}$	$-0.248\,20\times10^{-5}$
350	10.0	54.292 2	62.129 9	0.034 083 4	−0.284 884	$-0.726\,39\times10^{-4}$	$0.129\,33\times10^{-2}$	$-0.755\,56\times10^{-5}$
350	100.0	56.262 0	64.951 0	0.029 038 3	−0.286 956	$-0.434\,40\times10^{-4}$	$0.139\,09\times10^{-2}$	$-0.339\,72\times10^{-4}$
350	1000.0	67.295 1	83.608 4	0.016 893 2	−0.334 865	$-0.444\,15\times10^{-5}$	$0.215\,76\times10^{-2}$	$-0.574\,91\times10^{-4}$
400	10.0	52.312 2	49.385 0	0.035 083 9	−0.227 249	$-0.106\,47\times10^{-3}$	$0.101\,24\times10^{-2}$	$0.461\,03\times10^{-4}$
400	100.0	54.499 5	52.200 9	0.028 247 8	−0.225 663	$-0.546\,19\times10^{-4}$	$0.107\,52\times10^{-2}$	$-0.152\,32\times10^{-5}$
400	1000.0	65.942 2	69.124 9	0.014 787 2	−0.251 380	$-0.423\,34\times10^{-5}$	$0.131\,47\times10^{-2}$	$-0.320\,72\times10^{-4}$
450	10.0	49.744 7	39.171 6	0.038 933 6	−0.183 607	$-0.177\,95\times10^{-3}$	$0.734\,30\times10^{-3}$	$0.113\,97\times10^{-3}$
450	100.0	52.372 9	42.149 5	0.028 741 0	−0.178 549	$-0.731\,29\times10^{-4}$	$0.816\,62\times10^{-3}$	$0.211\,91\times10^{-4}$
450	1000.0	64.598 3	58.020 0	0.013 401 1	−0.195 865	$-0.402\,22\times10^{-5}$	$0.943\,87\times10^{-3}$	$-0.246\,40\times10^{-4}$
500	10.0	46.517 5	30.794 1	0.047 663 0	−0.153 818	$-0.362\,98\times10^{-3}$	$0.453\,62\times10^{-3}$	$0.256\,63\times10^{-3}$
500	100.0	49.914 0	34.149 0	0.030 425 4	−0.143 247	$-0.104\,11\times10^{-3}$	$0.603\,42\times10^{-3}$	$0.472\,11\times10^{-4}$
500	1000.0	63.253 0	49.301 7	0.012 264 8	−0.154 787	$-0.390\,98\times10^{-5}$	$0.712\,69\times10^{-3}$	$-0.210\,35\times10^{-4}$
550	10.0	42.287 5	23.530 8	0.069 541 0	−0.139 993	$-0.109\,16\times10^{-2}$	$0.487\,65\times10^{-4}$	$0.733\,66\times10^{-3}$
550	100.0	47.114 6	27.667 2	0.033 596 6	−0.117 403	$-0.157\,34\times10^{-3}$	$0.438\,23\times10^{-3}$	$0.812\,80\times10^{-4}$
550	1000.0	61.909 0	42.377 5	0.011 287 8	−0.123 594	$-0.390\,18\times10^{-5}$	$0.543\,04\times10^{-3}$	$-0.180\,89\times10^{-4}$
600	100.0	43.934 6	22.290 3	0.038 745 0	−0.098 672 4	$-0.251\,40\times10^{-3}$	$0.318\,10\times10^{-3}$	$0.126\,80\times10^{-3}$
600	1000.0	60.571 5	36.819 5	0.010 451 9	−0.099 791 5	$-0.397\,00\times10^{-5}$	$0.415\,10\times10^{-3}$	$-0.153\,89\times10^{-4}$
650	100.0	40.310 9	17.717 3	0.046 488 1	−0.084 898 7	$-0.419\,46\times10^{-3}$	$0.239\,96\times10^{-3}$	$0.184\,54\times10^{-3}$
650	1000.0	59.246 1	32.305 8	0.009 7437 7	−0.081 552 1	$-0.408\,42\times10^{-5}$	$0.319\,14\times10^{-3}$	$-0.129\,95\times10^{-4}$
700	100.0	36.179 0	13.754 4	0.057 134 6	−0.073 855 7	$-0.699\,43\times10^{-3}$	$0.211\,78\times10^{-3}$	$0.236\,22\times10^{-3}$
700	1000.0	57.937 2	28.595 1	0.009 146 26	−0.067 471 6	$-0.421\,91\times10^{-5}$	$0.247\,59\times10^{-3}$	$-0.109\,69\times10^{-4}$
750	100.0	31.557 5	10.336 0	0.068 683 4	−0.062 523 6	$-0.102\,20\times10^{-2}$	$0.254\,47\times10^{-3}$	$0.198\,46\times10^{-3}$
750	1000.0	56.648 9	25.507 2	0.008 640 69	−0.056 489 7	$-0.435\,57\times10^{-5}$	$0.194\,28\times10^{-3}$	$-0.931\,41\times10^{-5}$
800	100.0	26.767 6	7.562 25	0.073 445 0	−0.047 827 0	$-0.980\,76\times10^{-3}$	$0.322\,80\times10^{-3}$	$-0.301\,96\times10^{-4}$
800	1000.0	55.384 2	22.907 7	0.008 209 19	−0.047 821 0	$-0.448\,01\times10^{-5}$	$0.154\,37\times10^{-3}$	$-0.799\,81\times10^{-5}$
273.150	p_0*	55.499 8	87.903 5	0.041 829 7	−0.402 570	$-0.550\,72\times10^{-4}$	$0.206\,74\times10^{-2}$	$-0.256\,17\times10^{-3}$
273.150	100.0	58.021 8	91.838 0	0.037 176 5	−0.426 331	$-0.401\,52\times10^{-4}$	$0.261\,83\times10^{-2}$	$-0.219\,82\times10^{-3}$
298.144	p_0*	55.344 7	78.410 6	0.037 396 6	−0.358 840	$-0.566\,06\times10^{-4}$	$0.158\,70\times10^{-2}$	$-0.116\,89\times10^{-3}$
298.144	50.0	56.532 1	80.211 4	0.034 873 6	−0.364 953	$-0.453\,77\times10^{-4}$	$0.176\,68\times10^{-2}$	$-0.126\,88\times10^{-3}$
298.144	200.0	59.500 1	85.017 5	0.029 695 0	−0.384 517	$-0.256\,72\times10^{-4}$	$0.221\,95\times10^{-2}$	$-0.130\,70\times10^{-3}$
373.124	p_0*	53.197 5	55.533 3	0.035 099 4	−0.256 700	$-0.925\,18\times10^{-4}$	$0.115\,25\times10^{-2}$	$0.252\,66\times10^{-4}$
373.124	100.0	55.496 2	58.672 7	0.028 474 7	−0.256 655	$-0.479\,09\times10^{-4}$	$0.123\,41\times10^{-2}$	$-0.160\,42\times10^{-4}$
473.110	100.0	51.277 4	38.231 7	0.029 358 8	−0.160 903	$-0.854\,49\times10^{-4}$	$0.712\,14\times10^{-3}$	$0.324\,58\times10^{-4}$
673.102	100.0	38.467 6	15.818 0	0.051 073 6	−0.079 613 0	$-0.533\,99\times10^{-3}$	$0.219\,52\times10^{-3}$	$0.212\,05\times10^{-3}$
773.071	100.0	29.331 4	8.964 72	0.072 338 6	−0.056 201 7	$-0.107\,33\times10^{-2}$	$0.293\,68\times10^{-3}$	$0.110\,28\times10^{-3}$

*Liquid state at 0.101 325 MPa.

used for code checking and other purposes. In the second part of the table, the temperature entries, all on the ITS-90 scale, have been chosen to correspond with integer Centigrade values on the IPTS-68 scale. This part of the table permits easy comparison with correlations performed prior to the acceptance of the ITS-90 scale.

The values of the first derivatives with respect to pressure and temperature are displayed in Figs. 12–21 over the whole range of the present correlation; the predictions of Ref. 13 are also shown. The first derivatives have a strong infinity at the water critical point, and are therefore somewhat awkward to plot in the supercritical regime.

6.3. Comparison of Derivatives from Experiment and from Correlations

''Experimental'' values of the first derivatives, obtained by 5-point Lagrangian interpolation (Sec. 6.1) are displayed in Figs. 12–16 (first pressure derivative), Figs. 17–21 (first temperature derivative). As argued in Sec. 6.1, Lagrangian interpolation tends to exaggerate the uncertainty of the derivatives. Therefore, we have additionally performed comparisons of first and second temperature and pressure derivatives of the dielectric constant at values of the independent variables such that experimental information is sufficient to determine experimental derivatives by polynomial interpola-

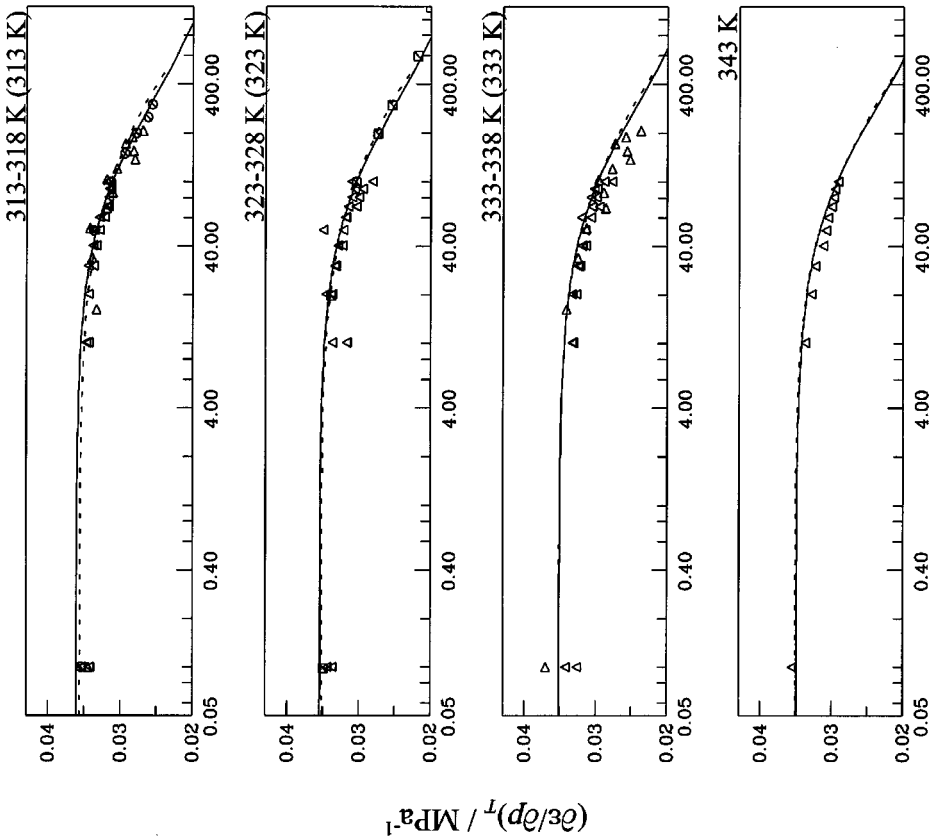

FIG. 13. First derivative of the dielectric constant with respect to pressure at constant temperature $(\partial\epsilon/\partial p)_T$ for water at temperatures between 313 K and 343 K. Symbols: Table 6; ''experimental'' values: 5-point Lagrangian interpolation. Dashed curve: Ref. 13.

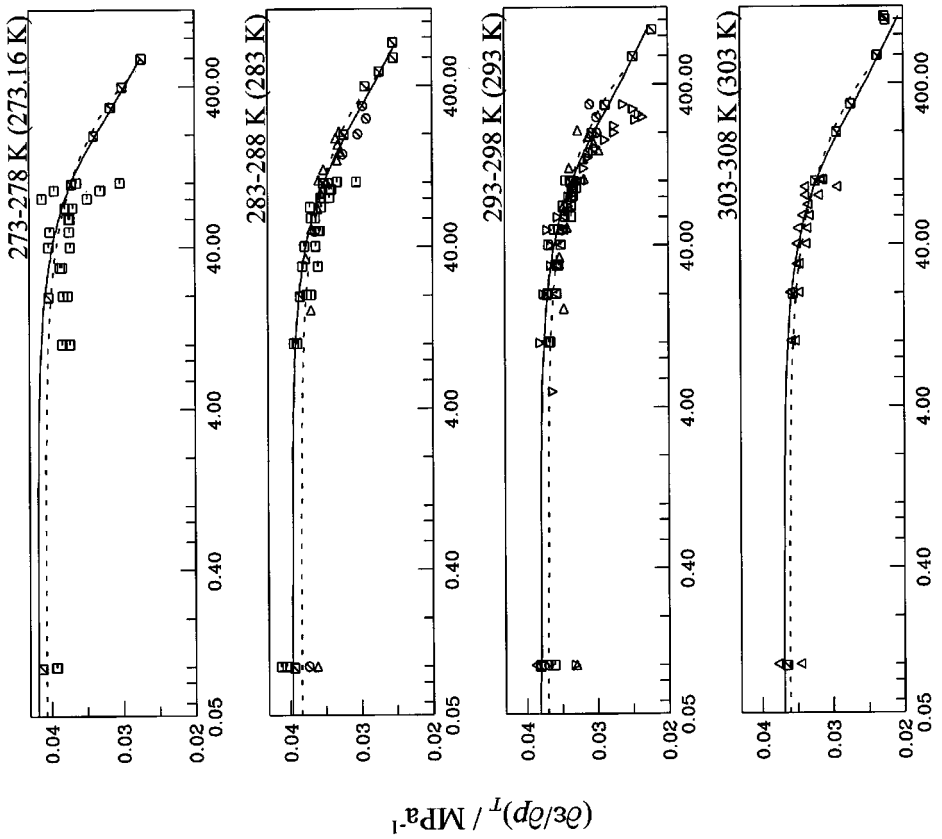

FIG. 12. First derivative of the dielectric constant with respect to pressure at constant temperature $(\partial\epsilon/\partial p)_T$ for water at temperatures between 273 K and 308 K. Symbols: Table 6; ''experimental'' values: 5-point Lagrangian interpolation. Dashed curve: Ref. 13.

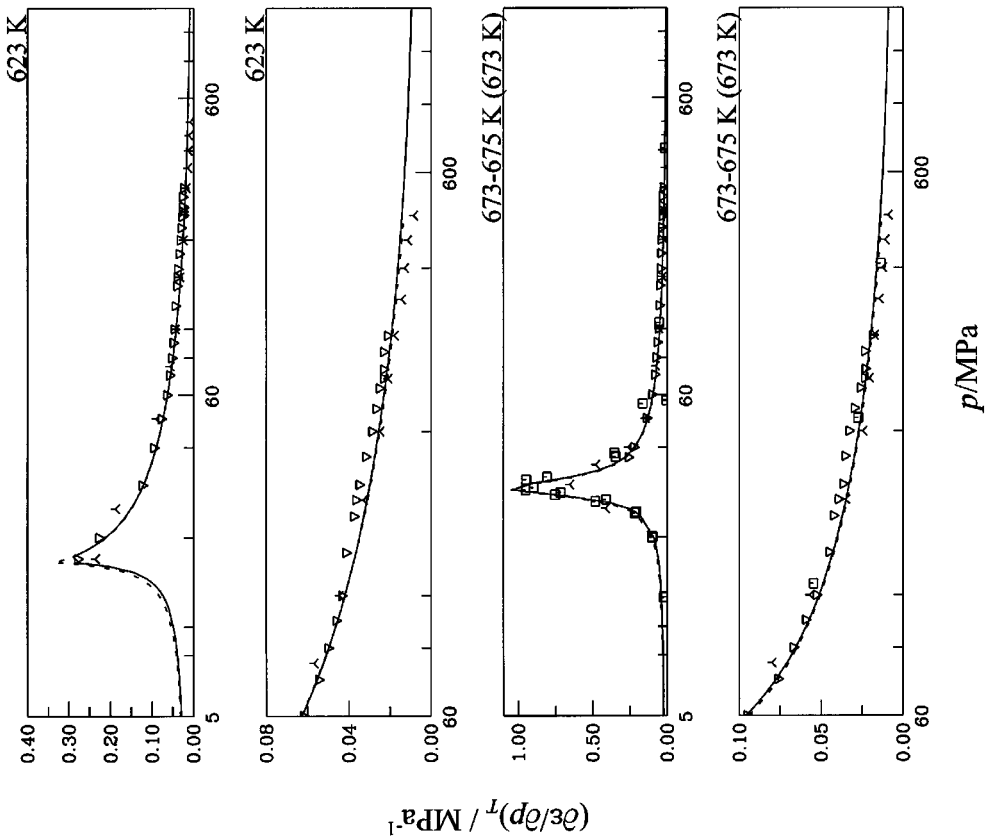

FIG. 15. First derivative of the dielectric constant with respect to pressure at constant temperature $(\partial\epsilon/\partial p)_T$ for water at temperatures between 623 K and 675 K. Symbols: Table 6; ''experimental'' values: 5-point Lagrangian interpolation. Dashed curve: Ref. 13.

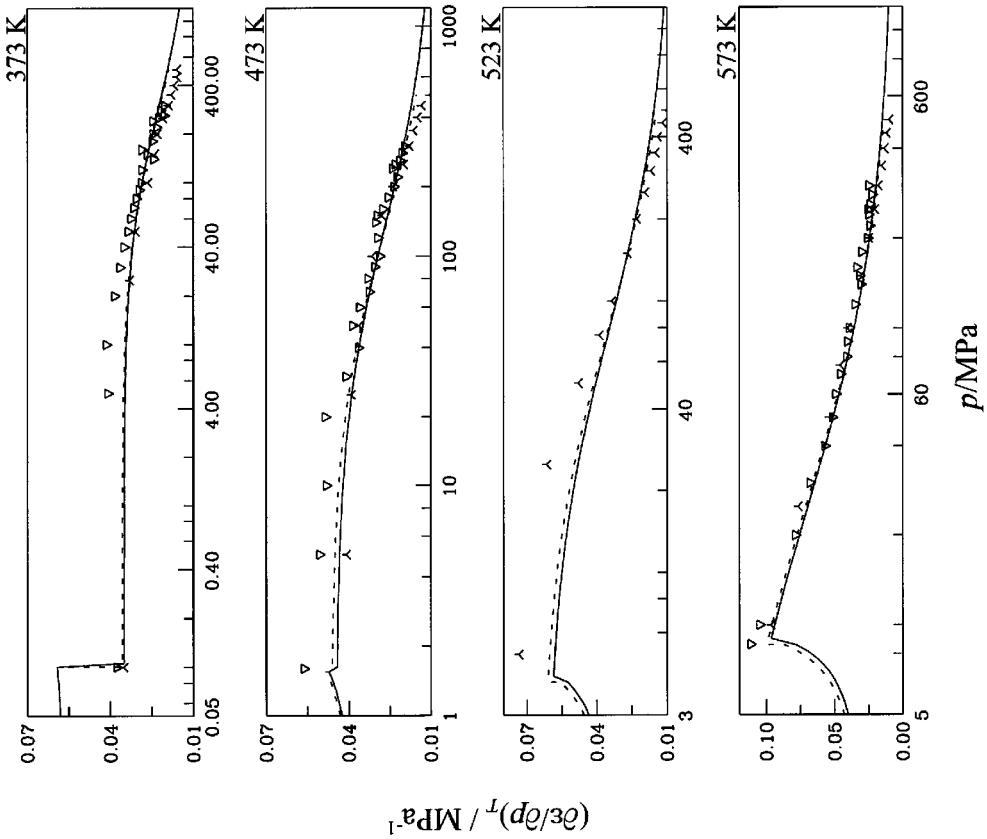

FIG. 14. First derivative of the dielectric constant with respect to pressure at constant temperature $(\partial\epsilon/\partial p)_T$ for water at temperatures between 373 K and 573 K. Symbols: Table 6; ''experimental'' values: 5-point Lagrangian interpolation. Dashed curve: Ref. 13.

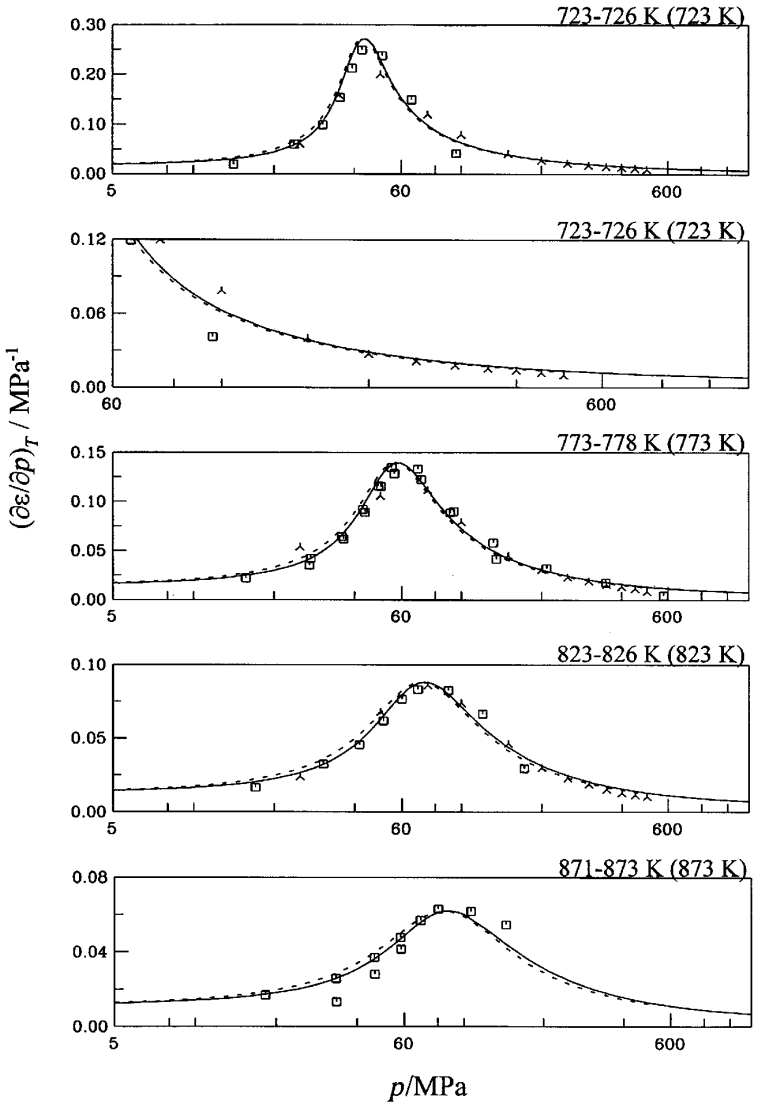

FIG. 16. First derivative of the dielectric constant with respect to pressure at constant temperature $(\partial\epsilon/\partial p)_T$ for water at temperatures between 723 K and 873 K. Symbols: Table 6; ''experimental'' values: 5-point Lagrangian interpolation. Dashed curve: Ref. 13.

tion. Six isotherms in the range 273–673.1 K have been selected, and one to three target pressures have been chosen at each temperature.

Tables 13–16 contain values for first and second pressure and temperatures derivatives derived from experimental data by low-degree polynomial fits along isotherms or isobars (Sec.6.2); they are listed under the heading ''experiments.'' In addition, derivative values for the same table entries have been calculated for the correlations of Helgeson and Kirkham,[5] Bradley and Pitzer,[10] and Archer and Wang.[13] The last line in the tables contains the values predicted by the present correlation.

At 273.15 K and 0.1 MPa, the first temperature derivative values shown in Table 13 agree within 1%, except for the values derived from Milner's data. The values obtained by polynomial fits to the data of Lees,[60] Vidulich *et al.*,[86,87] and Fernández *et al.*[16] agree to the third digit. The value resulting from the correlation of Bradley and Pitzer[10] is somewhat low in absolute value, probably because the authors relied on the data by Dunn and Stokes[70] in this region; these data, and those by Malmberg and Maryott,[78] depart from those of Refs. 60, 85, 86, and 16, which were preferred by us. The value resulting from the Archer and Wang correlation, $-0.405\ \mathrm{K}^{-1}$, seems somewhat high in absolute value with respect to the experimental average (Milner's data excluded) of $-0.402\ \mathrm{K}^{-1}$. These authors did not have the new data[16] available when they did their correlation.

At 298.14 K and ambient pressure, uncertainties in the first temperature derivative are below 1%, with some deterioration at elevated pressures.

At temperatures higher than 373.12 K, first temperature derivative values obtained from the Heger[8,12] and the Deul[48,49] data disagree sharply, and so do the differences between the various correlations. The predictions of the two most recent correlations, however, agree remarkably well, notwithstanding vastly different functional forms.

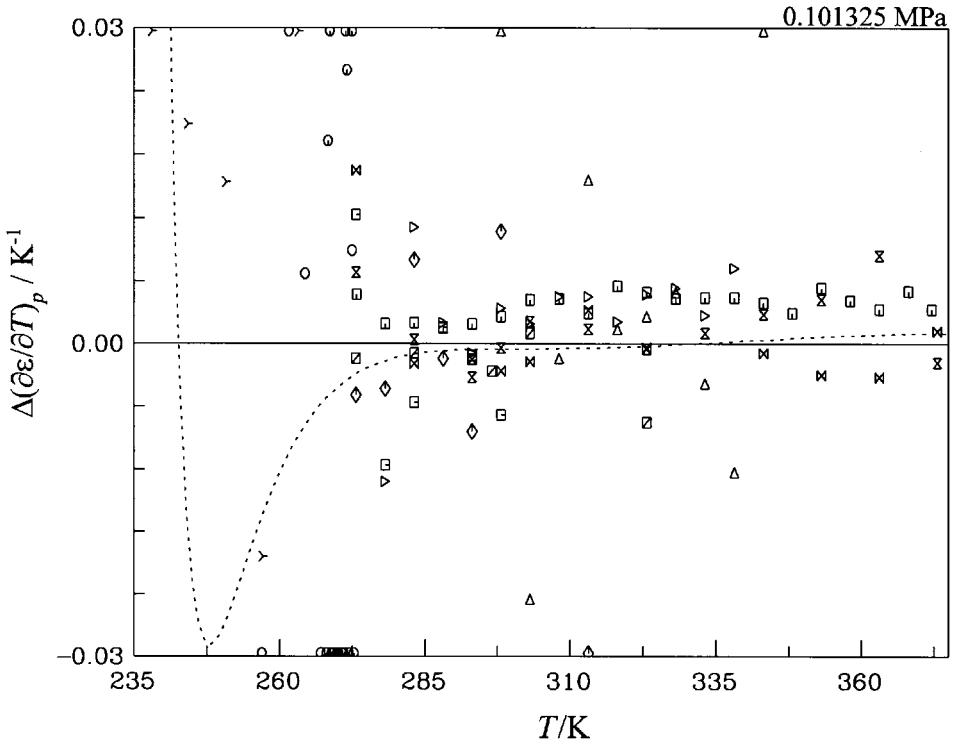

FIG. 17. Departure from the formulation for the first derivative of the dielectric constant with respect to temperature at constant pressure $(\partial\epsilon/\partial T)_p$ for water at 0.101325 MPa in the range of 235–373 K. Symbols: Table 6; ''experimental'' values: 5-point Lagrangian interpolation. Dashed curve: Ref. 13.

The second temperature derivative at ambient pressure and up to the boiling point is shown in Table 14. At the normal freezing point, the spread of experimental derivative values and predictions from correlations exceeds 10%. The uncertainty in the second temperature derivative in the supercooled regime must be at least that large. As the temperature increases above the freezing point, the uncertainty of the second temperature derivative falls, and at 298.14 K the spread of values is well below 10%.

Above 373.12 K, the predictions from the different correlations agree in the order of 10%, much better than the values calculated from the various data sets. The agreement between the two most recent formulations, however, is remarkable.

The values of the first and second pressure derivatives are shown in Tables 15 and 16, respectively. Especially for the second derivatives, the experimental values show large scatter.

It is worth noting that the derivative values obtained from the correlations are generally much better defined than the values derived from individual experimental data sets. The various correlations, though of very different algebraic forms, apparently do comparable jobs of smoothing the data, even in regions where there are few and not very consistent data. This is especially striking for the two most recent formulations.

6.4. Reliability of the Derivatives of the Dielectric Constant

Tables 13–16 permit us to estimate the reliability of the dielectric constant derivatives, by comparing values obtained from the four different high-quality correlations. This is, of course, a somewhat optimistic estimate of uncertainty since all these formulations, in regions where data are sparse or inconsistent, might try to fit to a set of unconfirmed data which could be wrong.

The first temperature derivative (Table 13) is defined within 1% up to the boiling point, with a somewhat larger spread (1.5%) at 273 K, at the low end of the range. At the higher temperatures, up to 673 K, the differences mostly remain within 10%. The definition of the second temperature derivative (Table 14) is, of course, much worse, with a percent-level definition only in the middle of the range, 298–373 K. At the 273 K end, the derivative values scatter by 25%.

The first pressure derivative (Table 15) spreads no more than 3% up to 473 K. Above that temperature, the spread is within 10%. The second pressure derivative is poorly defined almost everywhere.

In general, the differences between the present formulation and that of Archer and Wang are smaller than the overall spread between formulations.

A legitimate question is that of the effect of the equation

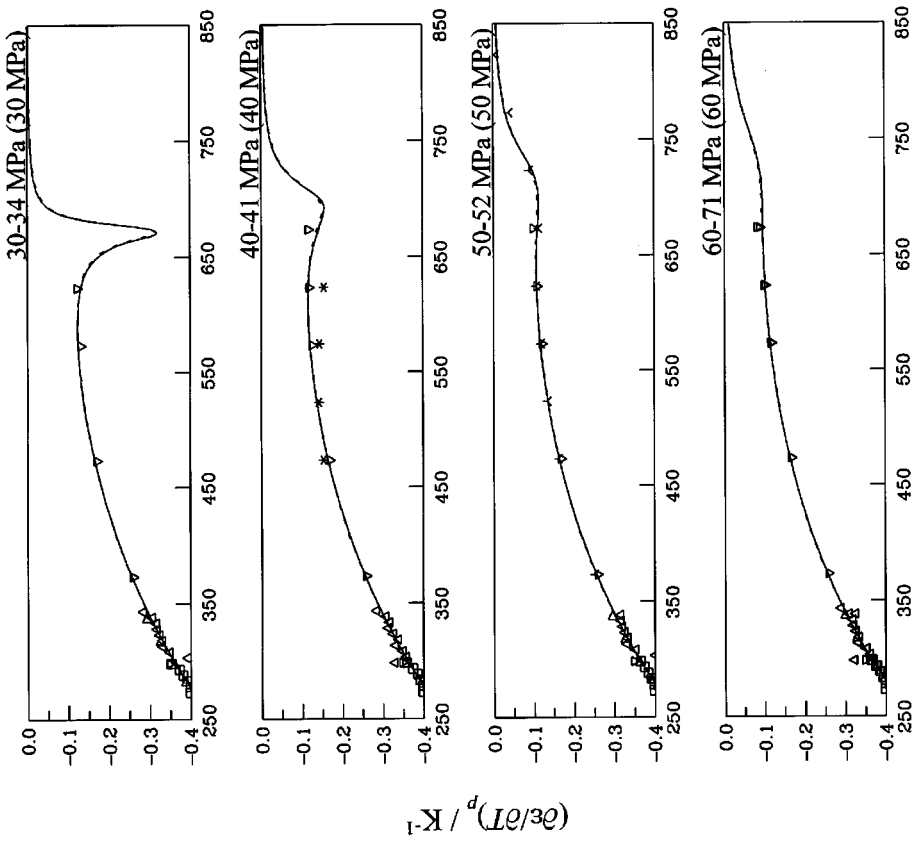

FIG. 19. First derivative of the dielectric constant with respect to temperature at constant pressure $(\partial\epsilon/\partial T)_p$ for water at pressures between 30 MPa and 71 MPa. Symbols: Table 6; ''experimental'' values: 5-point Lagrangian interpolation. Dashed curve: Ref. 13.

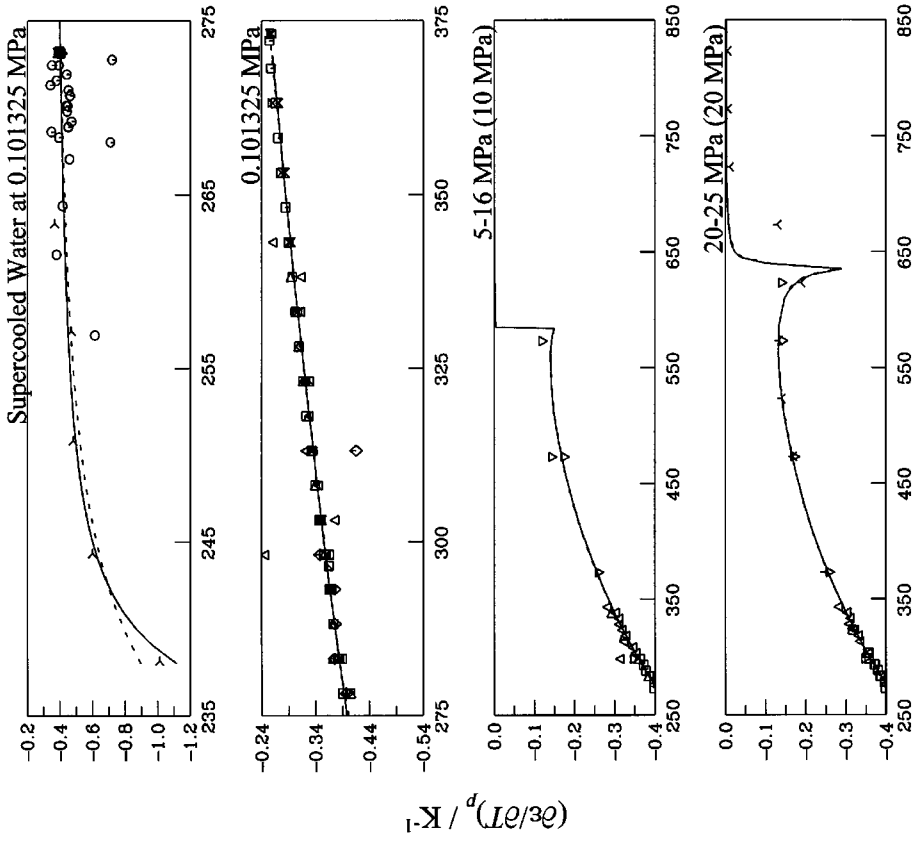

FIG. 18. First derivative of the dielectric constant with respect to temperature at constant pressure $(\partial\epsilon/\partial T)_p$ for water at pressures between 0.1 MPa and 25 MPa. Symbols: Table 6; ''experimental'' values: 5-point Lagrangian interpolation. Dashed curve: Ref. 13.

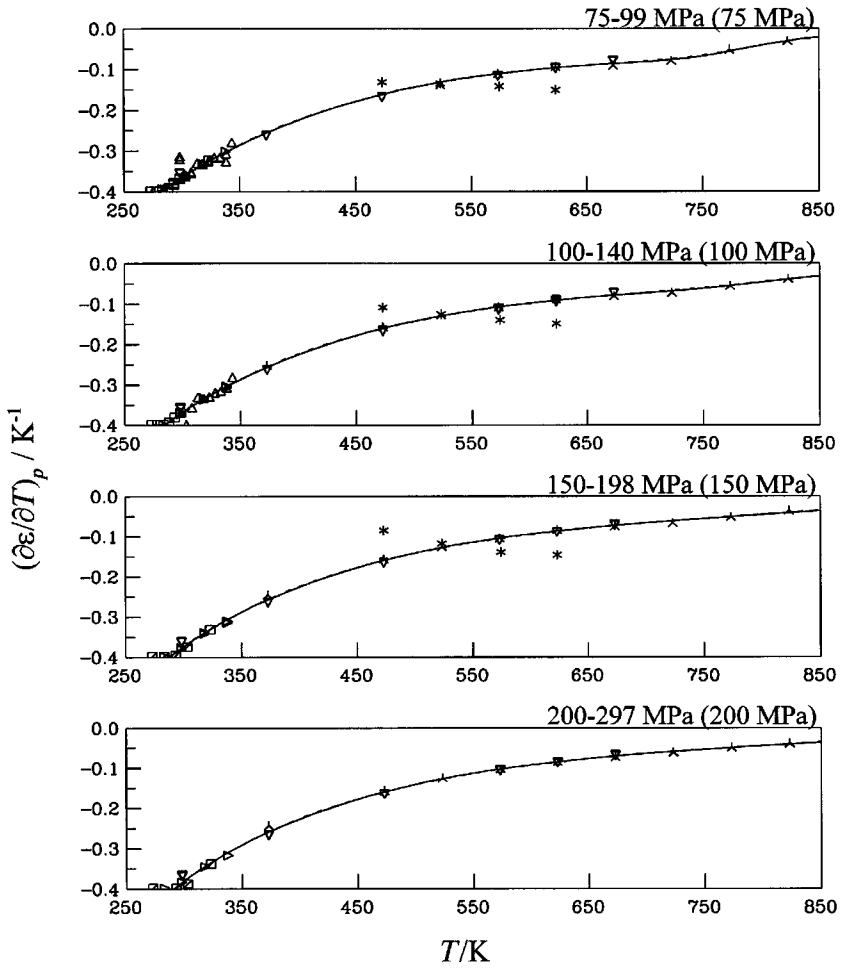

FIG. 20. First derivative of the dielectric constant with respect to temperature at constant pressure $(\partial\epsilon/\partial T)_p$ for water at pressures between 75 MPa and 297 MPa. Symbols: Table 6; ''experimental'' values: 5-point Lagrangian interpolation. Dashed curve: Ref. 13.

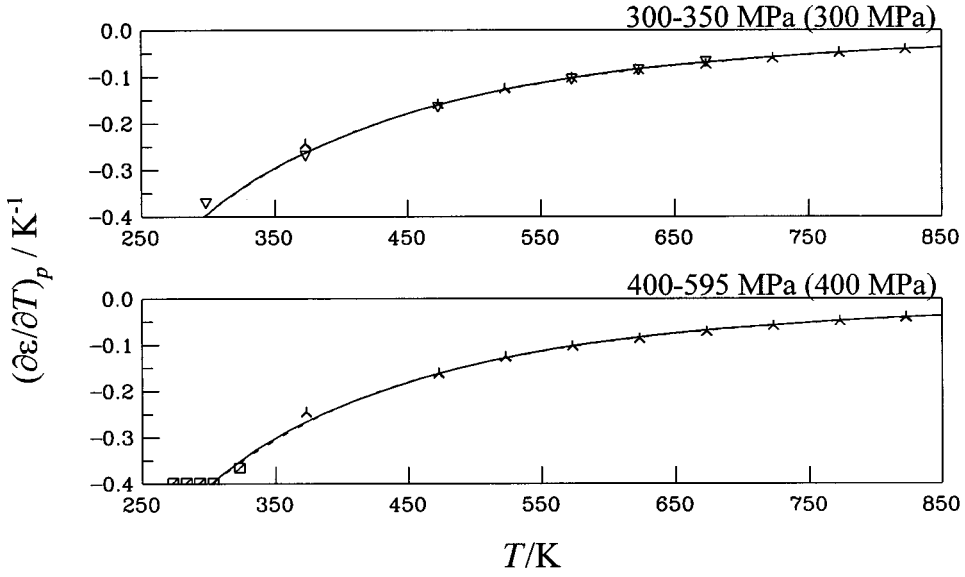

FIG. 21. First derivative of the dielectric constant with respect to temperature at constant pressure $(\partial\epsilon/\partial T)_p$ for water at pressures between 300 MPa and 595 MPa. Symbols: Table 6; ''experimental'' values: 5-point Lagrangian interpolation. Dashed curve: Ref. 13.

TABLE 13. First temperature derivative of the dielectric constant at constant pressure.

	$-10^3(\partial\epsilon/\partial T)_p/\mathrm{K}^{-1}$									
T/K→	273.15		298.14			373.12		473.11	573.11	673.10
p/MPa→	p_0*	100	p_0*	100	200	p_0*	100	100	100	100
Experiments										
Wyman[89]			360			257				
Lees[60]	402	422	360	373	386					
Milner[61]	411	428	358	366	382					
Vidulich *et al.*[87]	402		360							
Heger[8]							262	156	104	81
Deul[48]				377	385		253	160	114	75
Fernández *et al.*[16]	402		359			258				
Correlations										
Helgeson & Kirkham[5]			357	368	371	258	258	157	104	81
Bradley & Pitzer[10]	398	419	359	370	382	257	257	160	101	65
Archer & Wang[13]	405	432	359	370	384	256	255	161	109	79
This work	403	426	359	371	385	257	257	161	108	80

*Liquid state at 0.101 325 MPa.

TABLE 14. Second temperature derivative of the dielectric constant at constant pressure.

	$10^5(\partial^2\epsilon/\partial T^2)_p/\mathrm{K}^{-2}$									
T/K→	273.15		298.14			373.12		473.11	573.11	673.10
p/MPa→	p_0*	100	p_0*	100	200	p_0*	100	100	100	100
Experiments										
Wyman[89]										
Lees[60]		196	170	196	219					
Milner[61]		250	202	250	180					
Vidulich *et al.*[87]			166							
Heger[8]							143	74	33	19
Deul[48]					215		129	63	36	50
Fernández *et al.*[16]	185		165			109				
Correlations										
Helgeson & Kirkham[5]			130			117	128	73	34	19
Bradley & Pitzer[10]	154	209	155	183	208	114	124	74	45	
Archer & Wang[13]	240	351	159	194	218	116	125	69	38	24
This work	207	262	159	193	222	115	123	711	38	22

*Liquid state at 0.101 325 MPa.

TABLE 15. First pressure derivative of the dielectric constant at constant temperature.

	$10^4(\partial\epsilon/\partial p)_T/\mathrm{MPa}^{-1}$									
T/K→	273.15		298.14			373.12		473.11	673.10	773.07
p/MPa→	p_0*	100	p_0*	50	200	p_0*	100	100	100	100
Experiments										
Lees[60]	406	371								
Milner[61]	383		370	347						
Cogan[62]			369	347						
Heger[8]					327		273	315	487	640
Srinivasan[82]			372	349	301					
Lukashov[65]										787
Deul[48]			381	358	278	378	291	300	528	
Correlations										
Helgeson & Kirkham[5]			366	329	262	352	281	299	568	746
Bradley & Pitzer[10]	407	361	371	345	286	353	283	301		
Archer & Wang[13]	407	371	365	344	305	357	284	294	503	695
This work	418	372	374	349	297	351	285	294	511	723

*Liquid state at 0.101 325 MPa.

TABLE 16. Second pressure derivative of the dielectric constant at constant temperature.

	$-10^6(\partial^2\epsilon/\partial p^2)_T$/MPa^{-2}									
T/K→	273.15		298.14			373.12		473.11	673.10	773.07
p/MPa→	p_0*	100	p_0*	50	200	p_0*	100	100	100	100
Experiments										
Lees[60]	41	35								
Milner[61]	30	23	66	51						
Cogan[62]			68	43						
Heger[8]						66	54	90	343	483
Srinivasan[82]			63	52	11					
Lukashov[65]										860
Deul[48]			59	57	50	117	78	103	418	
Correlations										
Helgeson & Kirkham[5]			104	54		124	45	109	586	971
Bradley & Pitzer[10]	51	40	55	48	33	87	56	104		
Archer & Wang[13]	39	31	46	35	21	106	51	95	529	1047
This work	55	40	57	45	26	93	48	85	534	1073

*Liquid state at 0.101 325 MPa.

TABLE 17. Predicted values of the Debye–Hückel coefficients at selected values of temperature and pressure. Values in italics are outside the range of experimental data.

T/K (ITS-90)	p/MPa	A_ϕ (kg mol^{-1})$^{1/2}$	A_V (cm^3 kg$^{1/2}$ mol$^{-3/2}$)	A_H/RT (kg mol^{-1})$^{1/2}$	A_K (cm^3 kg$^{1/2}$ mol$^{-3/2}$ MPa^{-1})	A_C/R (kg mol^{-1})$^{1/2}$
270	p_0*	0.374 75	1.537 5	0.564 28	−0.002 473 6	1.761 1
300	p_0*	0.392 51	1.927 5	0.814 48	−0.004 340 9	3.901 4
300	10.0	0.390 62	1.885 7	0.803 15	−0.004 110 1	3.813 9
300	100.0	0.375 05	1.585 4	0.726 66	−0.002 720 0	3.152 4
300	1000.0	0.283 96	0.702 18	0.600 01	−0.000 435 37	1.257 5
350	p_0*	0.434 57	3.118 3	1.409 8	−0.010 397	6.132 7
350	10.0	0.431 96	3.019 1	1.382 1	−0.009 657 1	5.956 4
350	100.0	0.411 39	2.362 5	1.189 1	−0.005 527 3	4.783 9
350	1000.0	*0.308 07*	*0.864 45*	*0.655 07*	*−0.000 555 01*	*1.303 0*
400	10.0	0.489 72	5.223 4	2.129 1	−0.023 563	9.021 8
400	100.0	0.459 96	3.752 2	1.748 5	−0.011 390	6.611 4
400	1000.0	*0.332 02*	*1.131 9*	*0.797 37*	*−0.000 793 40*	*2.205 0*
450	10.0	0.566 54	9.671 8	3.182 3	−0.064 731	14.964
450	100.0	0.520 81	6.113 2	2.421 2	−0.024 311	9.184 7
450	1000.0	*0.358 14*	*1.492 3*	*0.981 33*	*−0.001 130 0*	*2.636 7*
500	10.0	0.671 09	20.023	4.981 1	−0.219 66	29.970
500	100.0	0.595 28	10.230	3.293 4	−0.054 486	13.512
500	1000.0	*0.386 30*	*1.933 1*	*1.156 3*	*−0.001 579 7*	*2.797 3*
550	10.0	0.830 30	52.399	9.159 3	−1.160 8	86.227
550	100.0	0.687 41	17.800	4.544 7	−0.130 08	21.426
550	1000.0	*0.415 68*	*2.452 0*	*1.308 4*	*−0.002 167 2*	*2.853 6*
600	100.0	0.805 62	32.686	6.512 8	−0.335 65	36.568
600	1000.0	*0.445 57*	*3.052 6*	*1.438 8*	*−0.002 922 2*	*2.895 5*
650	100.0	0.965 77	64.214	9.843 7	−0.946 29	66.458
650	1000.0	*0.475 52*	*3.742 1*	*1.553 4*	*−0.003 878 5*	*2.967 7*
700	100.0	1.196 9	135.69	15.739	−2.883 6	124.09
700	1000.0	*0.505 27*	*4.529 3*	*1.658 4*	*−0.005 071 9*	*3.088 0*
750	100.0	1.547 2	299.47	25.776	−8.726 7	209.94
750	1000.0	*0.534 74*	*5.424 4*	*1.759 1*	*−0.006 538 9*	*3.257 9*
800	100.0	2.066 9	616.62	38.835	−20.833	239.33
800	1000.0	*0.563 92*	*6.437 4*	*1.859 2*	*−0.008 315 3*	*3.469 5*
273.150	p_0*	0.376 41	1.570 8	0.580 68	−0.002 615 4	2.191 9
273.150	100.0	0.360 40	1.352 3	0.538 60	−0.001 884 7	1.924 9
298.144	p_0*	0.391 26	1.897 8	0.795 51	−0.004 196 5	3.820 3
298.144	50.0	0.382 19	1.713 2	0.747 24	−0.003 274 5	3.423 9
298.144	200.0	0.359 32	1.346 3	0.664 57	−0.001 815 0	2.566 8
373.124	p_0*	0.459 69	4.010 1	1.741 5	−0.015 715	7.439 5
373.124	100.0	0.432 34	2.914 0	1.436 3	−0.007 695 9	5.581 2
473.110	100.0	0.553 37	7.724 9	2.791 3	−0.035 059	10.882
673.102	100.0	1.061 3	89.955	12.151	−1.572 3	88.779
773.071	100.0	1.764 7	425.76	31.748	−13.633	238.49

*Liquid state at 0.101 325 MPa.

of state in those formulations that use a g-factor as a function of density. It is our opinion that the variations in the equations of state used will have a rather minor effect, because any uncertainties introduced into the density when calculated from measured pressures will be compensated for by the fit of the g-factor. In other words, the fit is to the dielectric constant data, and if they are fitted well, it does not matter if the equation of state was not perfect. The quality of the equation of state, however, definitely affects the reliability of the Debye–Hückel coefficients.

7. Debye–Hückel Coefficients

7.1. Definition and Values

The Debye–Hückel limiting law for electrolyte solutions was originally formulated in terms of a Helmholtz free energy framework,[1] and describes the concentration dependence of thermodynamic properties due to the presence of ionic charges in the limit of infinite dilution. In applications to aqueous electrolyte solutions, the limiting-law term is incorporated in the Gibbs free energy. This is allowed as long as the fluid has low compressibility, see, however, Ref. 95. The limiting law defines an initial slope for the concentration dependence of each of the excess thermodynamic properties: Gibbs free energies of solvent and solute, and apparent molar volume, enthalpy, heat capacity and compressibility of the solute. When formulated in terms of the excess Gibbs free energy, it is based on the pure-solvent and infinite-dilution solute standard states and on the molality scale for concentration.[96–99] The coefficient A_γ multiplying the Debye–Hückel composition dependence for the logarithm of the activity coefficient of the solute has the following form:[96,97]

$$A_\gamma=(2\pi N_A\rho M_w)^{1/2}[e^2/(4\pi\epsilon\epsilon_0 kT)]^{3/2}. \quad (46)$$

From the Debye–Hückel coefficient for the limiting slope of the activity, Debye–Hückel coefficients for the limiting slopes of other thermodynamic properties are derived by differentiation, as follows. For that of the osmotic coefficient[97]

$$A_\phi=A_\gamma/3. \quad (47)$$

For that of the apparent molar volume[98]

$$A_V=-4RT(\partial A_\phi/\partial p)_T. \quad (48)$$

For that of the apparent molar compressibility[10]

$$A_K=(\partial A_V/\partial p)_T. \quad (49)$$

For that of the apparent molar enthalpy[10,97]

$$A_H/RT=4T(\partial A_\phi/\partial T)_p. \quad (50)$$

For that of the apparent molar heat capacity[97]

$$A_C=(\partial A_H/\partial T)_p. \quad (51)$$

Here e is the charge of the electron, R is the universal gas constant, ρ is the molar density, and M_w the molar mass of water, see Table 3.

The expressions used to calculate the Debye–Hückel coefficients for the apparent molar volume and enthalpy are, respectively,

$$A_V=2A_\phi RT[3(\partial\epsilon/\partial p)_T/\epsilon-(\partial\rho/\partial p)_T/\rho], \quad (52)$$

$$A_H=-6A_\phi RT[1+T(\partial\epsilon/\partial T)_p/\epsilon-T(\partial\rho/\partial T)_p/3\rho]. \quad (53)$$

The higher-order derivatives were calculated numerically.

The units of A_ϕ, A_H/RT, and A_C/R are $(\mathrm{kg\,mol^{-1}})^{1/2}$, that of A_V is $\mathrm{cm^3\,kg^{1/2}\,mol^{-3/2}}$ and that of A_K, $\mathrm{cm^3\,kg^{1/2}\,mol^{-3/2}\,MPa^{-1}}$.

The expressions for the Debye–Hückel coefficients contain, in addition to the first and second pressure and temperature derivatives of the dielectric constant, also the first and second derivatives of the equation of state.

Table 17 displays the values of the Debye–Hückel coefficients derived from the present formulation for the same choices of temperature and density entries as in Table 12. As in Table 12, the bottom part of Table 17 is produced at ITS-90 temperatures that correspond with integer values of the IPTS-68 Centigrade scale. It can be used for comparison with predictions made on that scale by earlier workers. The top part of the table is at integer temperatures on the ITS-90 Kelvin scale. An excessive number of decimals is given, several more than the reliability of these values warrants; the purpose is to permit code checking.

7.2. Reliability

As a first measure of the reliability of the Debye–Hückel coefficients, the uncertainty of the derivatives of the dielectric constant, as determined in Section 6, can be used as a guide. This implies a few percent or less uncertainty in the first derivatives, 10% or more in the second temperature derivative except for the range of ambient-pressure liquid water (1%–1.5%), 10% or less in the first pressure derivative, and an undefined second pressure derivative.

In addition, however, the derivatives of the equation of state itself explicitly enter into the picture, see, for instance, Eqs. (52) and (53). It is natural to assume that the equation of state, being based on a very large body of excellent thermodynamic data, does not contribute to the uncertainty of the Debye–Hückel coefficients. This is, however, not true. As an example, in Fig. 22, the second temperature derivative, as calculated from different high quality equations of state, those of Haar *et al.*,[100] Saul and Wagner,[101] Hill,[14] and Wagner and Pruss,[19,20] is displayed as a function of the pressure along isotherms at 253 K, 273 K, and 298 K. It is obvious that at 253 K and 273 K, this derivative is not defined at the higher pressures. Also, second derivatives of some of these accurate equations of state display unphysical oscillations in the subcooled liquid.

An exhaustive investigation of the behavior of the derivatives of the equation of state is beyond the scope of this paper, and will be the topic of future research. A cursory check in other regions of phase space, including the super-

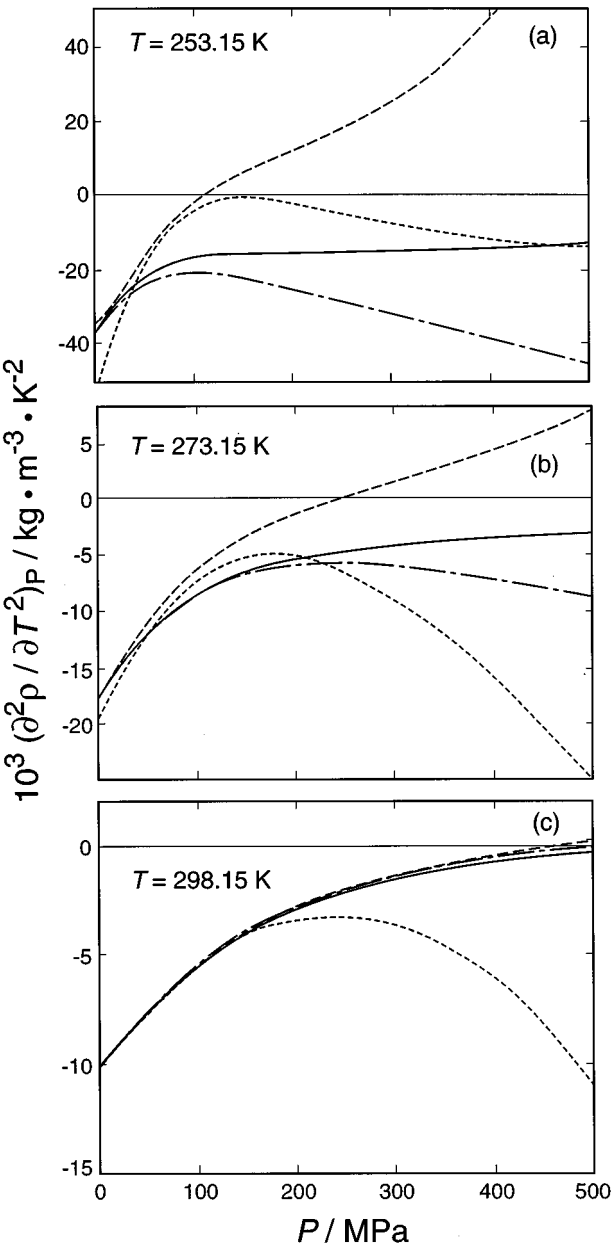

FIG. 22. The second temperature derivative of the density, according to a variety of high-quality equations of state. . . . Ref. 100; - - - -Ref. 101; full curve, Ref. 19; -· -· - Ref. 14.

critical regime, reveals that the agreement between the various formulations, in general, is better than that shown in Fig. 22.

Another estimate of the reliability of the Debye–Hückel coefficients is obtained by comparing values derived from an independent formulation of the dielectric constant, such as that of Archer and Wang,[13] which used a different equation of state. Such a comparison is made in Table 18.

We find that in the range of liquid water up to 473 K, the values for A_V agree on the level of 2%–3%, while those for A_H agree to within 1%, except at 273 K, where the differences are from 3% to 6%. These differences are slightly larger than those for the first pressure derivative of the dielectric constant, Table 13, thus confirming that the equation of state contributes to the uncertainty of the Debye–Hückel coefficients. In the supercritical regime, the spread is much larger, especially for A_V, where the difference between predictions from the two correlations is of the order of the value itself at 773 K and 100 MPa. Since the values of the first pressure derivative of the dielectric constant, according to the two formulations, agree to within 4% at this state point (Table 15), the large additional uncertainty must be due to the difference between the equations of state used.

The coefficient A_K appears to be defined on a level of 25% in the range up to 473 K, and somewhat better, within 10%, in the supercritical range. This is roughly consistent with the agreement of the second temperature derivative of the dielectric constant displayed in Table 16.

The value of A_C, of importance in heat capacity measurements, is not well defined at 273 K. In the middle range, 298–473 K, the two formulations agree to its value to better than 4%, and at supercritical temperatures to within 5%–15%. The second temperature derivative of the dielectric constant (Table 14), however, shows a smaller spread between these two formulations, consistent with the idea that the equation of state makes an additional contribution to the uncertainty of the Debye–Hückel coefficients. Comparisons of the Debye–Hückel coefficients obtained from earlier correlations can be found elsewhere.[98]

TABLE 18. Percentage difference of our predicted Debye–Hückel coefficient values from those of Archer and Wang (Ref. 13).

T/K	p/MPa	A_ϕ	A_V	A_H	A_K	A_C
273.150	0.1	−0.002	4.09	−3.38	31.6	23.5
273.150	100	−0.091	−0.09	−6.82	26.5	69.4
298.144	0.1	−0.056	3.54	−0.80	20.0	−0.41
298.144	50	−0.117	1.50	0.17	24.2	1.33
298.144	200	−0.041	−3.70	0.61	10.8	−3.73
373.124	0.101 325	−0.044	−2.63	0.92	−17.3	2.41
373.124	100	0.003	0.61	1.66	−5.08	4.11
473.110	100	0.409	0.49	1.16	−8.70	−2.37
673.102	100	−0.162	1.64	0.38	2.03	5.01
773.071	100	1.44	7.37	6.74	10.3	13.2

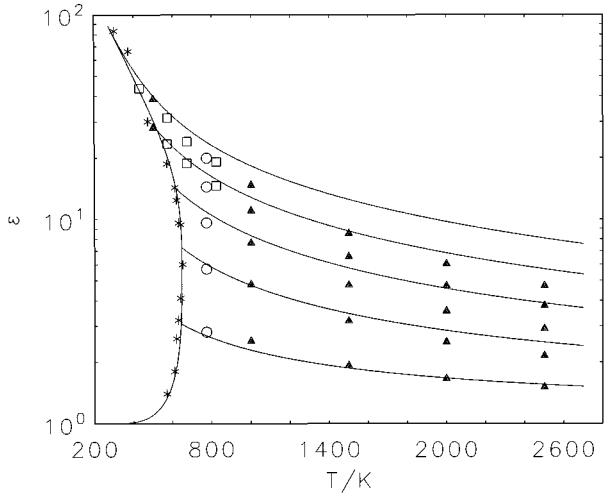

FIG. 23. Comparison of high-temperature computer simulation data for the SPC/E model with our correlation. Isochores are for 1.0, 0.8, 0.6, 0.4, and 0.2 kg dm^{-3}, respectively, from top to bottom. ○, Wallqvist (Ref. 58); □, Mountain (Ref. 58); ▲, Neumann (Ref. 57); ⋆, simulated coexistence curve, Guissani (Ref. 56); solid curves: the present correlation.

8. High-Temperature Behavior and Extrapolation

The behavior of the dielectric constant of water at high temperature and in the supercritical regime is of importance to geological and hydrothermal applications. The upper limit of the data is presently at 873 K, while information at even higher temperatures is urgently desired. Experiments under these conditions, however, become more arduous as temperature and pressure increase, while, on the other hand, the molecular behavior is expected to become simpler because of the diminishing importance of hydrogen bonding. Thus there have been several theoretical efforts at describing the supercritical regime in such a way that extrapolation to higher temperatures becomes feasible. We have described some of these efforts in Section 2.2, and have seen that their predictions are reasonably consistent with the experimental data available well above the critical point (Table 1), and must therefore also be consistent with our formulation in the range where data exist. Table 1 bears this out. It is also clear from Table 1 that the theoretical predictions, on extrapolation, have the dielectric constant decline at a faster rate than the extrapolation from our formulation.

As also discussed in Section 2.2, computer simulation has recently been making substantial inroads into the realm of supercritical water. A large body of information is now available for the dielectric constant of water according to the SPC/E model, see Sec. 2.2 and Refs. 51 and 53–57.

In Fig. 23, we compare the high-temperature simulation results with our formulation in the range where data exist as well as at higher temperatures. The simulation results are shown along selected isochores in the density range up to 1000 kg m^{-3} and at temperatures up to 2600 K. The solid lines give the results of our correlation along the same isochores in the same regime.

There is an obvious mismatch in slope between simulation and formulation, the simulation data declining more steeply with temperature than the formulation, especially at the higher densities. This mismatch, however, already occurs in the range below 873 K, where experimental data exist, and may, therefore, reflect the approximate character of the SPC/E model. Had we chosen to follow the SPC/E results, we would have had an appreciable departure from the available supercritical experimental data. It is no surprise that the SPC/E model is not accurate at high densities.[58] In addition, SPC/E predictions must be expected to deviate as well at very low densities, since SPC/E does not take into account the polarizability of the water molecule, and assumes an effective dipole moment higher than that of isolated water molecules. Given the low values of the dielectric constant in the dilute steam phase, such departures would not be visible on the scale of Fig. 23.

It is obvious that our correlation extrapolates smoothly to high temperatures. In the absence of data, it is impossible to assess the uncertainty of the values produced. In using the formulation for predictions of the dielectric costant values as a function of pressure and temperature in that range, one needs to realize that the range of validity of the Wagner equation of state does not exceed 1273 K. This limitation is not a concern when density and temperature are used as variables.

9. Conclusions

A new formulation of the dielectric constant of water and steam, including supercooled and supercritical states has been presented; pressure and temperature derivatives of the dielectric constant and the associated Debye–Hückel coefficients have been calculated, and their reliability has been evaluated. The formulation is based on selected and carefully evaluated experimental data, some of which has recently been acquired. Use has been made of the most recent formulation of the equation of state of water and steam which is based on the new temperature scale ITS-90.

At the end of a large project such as the present one, authors tend to focus on the deficits more than on the achievements. The lack of a sound physical basis for formulating the behavior of the dielectric constant of water and steam is painfully clear, notwithstanding a long and concentrated effort by some of the greatest minds in the field of physical chemistry. Although computer simulation has shown major improvement, and offers promise, especially at high temperatures, it is not yet quite at the cutting edge.

Data gaps and discrepancies between the two most important data sources[8,12,48,49] affect the liquid range above 373 K, and most of the supercritical regime. Except for the limited range of liquid water at atmospheric pressure, the derivatives of the dielectric constant, especially the second ones, are known with quite limited reliability. In addition to the uncertainty of the dielectric constant derivatives, that of the

equation-of-state derivatives contributes to the uncertainty of the Debye–Hückel coefficients. Particularly troublesome is the region of supercooled water, in which the second derivatives of the equation of state tend to develop unwanted oscillations.

It is, nevertheless, gratifying to see that the worst-case scenario, based on estimates of uncertainty of experimental dielectric constant and equation-of-state derivatives, does not appear to play out. A comparison of the Debye–Hückel coefficients of two independent formulations, based on high quality, but different equations of state, give values of these coefficients that are generally close except near the edges of the range where data are available.

Further progress will require new dielectric constant data in the liquid above the boiling point and in the supercritical regime. Although these are challenging regimes because of the substantial conductivity of water in the denser states, and the impurity effects due to corrosion, progress may be possible if use is made of the new flow methods that are beginning to dominate high-temperature aqueous physical chemistry.

We are not optimistic that the data situation in the supercooled liquid can be easily remedied. The dielectric constant measurements in that range require very small samples, or the use of emulsifiers, in order to extend the lifetime of the metastable state. The newest equations of state have already been pushed to the limit as far as representing the available data, but the higher derivatives of multiparameter equations of state will always have reduced reliability near the edge of the experimental range.

Note added in proof. After completion of the manuscript, the following paper was brought to our attention: W. J. Ellison, K. Lamkaouchi, and J.-M. Moreau, J. Mol. Liquids **68**, 171 (1996). This paper reviews and correlates the dielectric data and their frequency dependence for liquid water between the freezing point and the boiling point.

10. Acknowledgments

We are greatly indebted to Dr. R. F. Kayser, Chief of the Physical and Chemical Properties Division at NIST, for his staunch support of the project throughout its long duration. We have had several consultations with Professor E. U. Franck. Professor M. Neumann advised on high-temperature extrapolations. Dr. S. Penoncello was involved in early stages of the project. We thank J. S. Gallagher for producing Table 20, and for providing Fig. 22, and Dr. R. D. Mountain for the comparison of computer simulation results with the new formulation, Fig. 23. Dr. A. H. Harvey has served as a thorough and critical reviewer and has carefully checked many of the numerical results. Dr. A. Anderko reviewed the manuscript and recommended developing auxiliary equations for the dielectric constant of saturated water and steam. Dr. D. A. Archer provided useful criticism.

11. Appendix

Values of the dielectric constant of water and steam at selected integer values of temperature, in Kelvin (ITS-90) and of pressure, in MPa, are presented in Table 19. Values in ranges where no data exist are indicated in italics. Entries in bold-face are in supercooled water. Liquid-vapor and fluid-solid phase boundaries are indicated by horizontal bars. In Table 20, dielectric constant values are tabulated with density and temperature as entries. This is the preferred representation for the supercritical regime, and also facilitates comparison with computer simulation results.

TABLE 19. Dielectric constant of water and steam as a function of temperature and pressure.

	p/MPa										
T/K	0.1	1	2	5	10	20	30	40	50	60	70
260	**93.41**										
265	**91.26**										
270	**89.18**	——	——	——	——	——	——	——	91.25	91.64	92.04
275	87.16	87.20	87.24	87.36	87.57	87.97	88.38	88.77	89.16	89.55	89.93
280	85.19	85.23	85.27	85.39	85.59	85.98	86.37	86.76	87.14	87.51	87.89
285	83.27	83.30	83.34	83.46	83.65	84.04	84.42	84.80	85.17	85.53	85.89
290	81.39	81.42	81.46	81.57	81.76	82.14	82.51	82.88	83.24	83.60	83.96
295	79.55	79.58	79.62	79.73	79.92	80.29	80.65	81.01	81.37	81.72	82.06
300	77.75	77.78	77.82	77.93	78.11	78.48	78.83	79.19	79.54	79.88	80.22
305	75.99	76.02	76.06	76.17	76.35	76.71	77.06	77.41	77.75	78.09	78.42
310	74.27	74.30	74.33	74.44	74.62	74.98	75.32	75.67	76.01	76.34	76.67
315	72.58	72.61	72.65	72.76	72.93	73.28	73.63	73.97	74.30	74.63	74.96
320	70.93	70.97	71.00	71.11	71.28	71.63	71.97	72.31	72.64	72.96	73.28
325	69.32	69.36	69.39	69.50	69.67	70.02	70.35	70.69	71.01	71.34	71.65
330	67.75	67.78	67.82	67.92	68.09	68.44	68.77	69.10	69.43	69.75	70.06
335	66.21	66.24	66.27	66.38	66.55	66.89	67.23	67.55	67.88	68.19	68.51
340	64.70	64.73	64.77	64.87	65.04	65.38	65.72	66.04	66.36	66.68	66.99
345	63.23	63.26	63.30	63.40	63.57	63.91	64.24	64.56	64.88	65.20	65.51
350	61.79	61.82	61.85	61.96	62.13	62.47	62.80	63.12	63.44	63.75	64.06
355	60.38	60.41	60.45	60.55	60.72	61.06	61.39	61.71	62.03	62.34	62.65
360	59.00	59.03	59.07	59.17	59.34	59.68	60.01	60.33	60.65	60.96	61.27
365	57.66	57.69	57.72	57.83	58.00	58.34	58.67	58.99	59.30	59.61	59.92
370	56.34	56.37	56.41	56.51	56.68	57.02	57.35	57.67	57.99	58.30	58.60
375	*1.006*	55.09	55.12	55.22	55.40	55.74	56.07	56.39	56.70	57.01	57.32
380	*1.006*	53.83	53.86	53.97	54.14	54.48	54.81	55.13	55.45	55.76	56.06
390	*1.005*	51.39	51.43	51.53	51.71	52.05	52.38	52.71	53.03	53.34	53.64
400	*1.005*	49.06	49.10	49.21	49.39	49.73	50.07	50.39	50.71	51.02	51.33
410	*1.005*	46.84	46.87	46.98	47.16	47.51	47.85	48.18	48.50	48.82	49.12
420	*1.005*	44.70	44.74	44.85	45.04	45.39	45.74	46.07	46.39	46.71	47.02
430	*1.004*	42.66	42.70	42.81	43.00	43.36	43.71	44.05	44.38	44.70	45.01
440	*1.004*	40.70	40.74	40.85	41.05	41.42	41.77	42.12	42.45	42.77	43.09
450	*1.004*	38.81	38.85	38.97	39.17	39.55	39.92	40.27	40.61	40.93	41.25
460	*1.004*	1.041	37.04	37.17	37.37	37.76	38.14	38.50	38.84	39.17	39.50
470	*1.004*	*1.039*	35.30	35.43	35.64	36.04	36.43	36.80	37.15	37.49	37.82
480	*1.004*	*1.038*	33.61	33.75	33.97	34.39	34.79	35.17	35.53	35.87	36.21
490	*1.003*	*1.036*	1.078	32.13	32.36	32.79	33.21	33.60	33.97	34.32	34.66
500	*1.003*	*1.034*	*1.074*	30.55	30.79	31.25	31.68	32.09	32.47	32.84	33.18
525	*1.003*	*1.031*	*1.066*	26.79	27.07	27.61	28.09	28.54	28.96	29.35	29.73
550	*1.003*	*1.028*	*1.059*	1.177	23.53	24.18	24.75	25.26	25.73	26.17	26.58
575	*1.002*	*1.026*	*1.054*	*1.154*	20.00	20.87	21.58	22.19	22.74	23.23	23.68
600	*1.002*	*1.024*	*1.049*	*1.137*	1.365	17.50	18.48	19.25	19.90	20.48	20.99
625	*1.002*	*1.022*	*1.045*	*1.124*	*1.306*	13.62	15.28	16.35	17.18	17.87	18.47
650	*1.002*	*1.020*	*1.041*	*1.112*	*1.267*	2.066	11.58	13.37	14.50	15.36	16.08
675	*1.002*	*1.019*	*1.038*	*1.103*	*1.238*	1.744	5.359	10.05	11.78	12.91	13.79
700	*1.002*	*1.017*	*1.036*	*1.095*	*1.214*	1.603	2.666	6.260	8.963	10.50	11.59
725	*1.002*	*1.016*	*1.033*	*1.088*	*1.195*	1.514	2.158	3.772	6.298	8.184	9.494
750	*1.002*	*1.015*	*1.031*	*1.082*	*1.179*	1.452	1.921	2.831	4.424	6.183	7.600
775	*1.001*	*1.014*	*1.029*	*1.076*	*1.166*	1.404	1.775	2.396	3.405	4.726	6.031
800	*1.001*	*1.013*	*1.027*	*1.071*	*1.154*	1.365	1.674	2.142	2.844	3.791	4.854
825	*1.001*	*1.013*	*1.026*	*1.067*	*1.143*	1.334	1.598	1.973	2.501	3.201	4.029
850	*1.001*	*1.012*	*1.024*	*1.063*	*1.134*	1.307	1.538	1.850	2.269	2.810	3.459
875	*1.001*	*1.011*	*1.023*	*1.059*	*1.126*	1.284	1.489	1.757	2.102	2.536	3.056
900	*1.001*	*1.011*	*1.022*	*1.056*	*1.118*	*1.265*	*1.449*	*1.682*	*1.975*	*2.335*	*2.761*
950	*1.001*	*1.010*	*1.020*	*1.050*	*1.105*	*1.232*	*1.385*	*1.570*	*1.793*	*2.057*	*2.363*
1000	*1.001*	*1.009*	*1.018*	*1.046*	*1.095*	*1.206*	*1.336*	*1.489*	*1.668*	*1.874*	*2.108*
1050	*1.001*	*1.008*	*1.016*	*1.041*	*1.086*	*1.184*	*1.298*	*1.428*	*1.576*	*1.744*	*1.931*
1100	*1.001*	*1.007*	*1.015*	*1.038*	*1.078*	*1.167*	*1.266*	*1.379*	*1.505*	*1.646*	*1.801*
1150	*1.001*	*1.007*	*1.014*	*1.035*	*1.072*	*1.151*	*1.240*	*1.339*	*1.449*	*1.569*	*1.701*
1200	*1.001*	*1.006*	*1.013*	*1.032*	*1.066*	*1.139*	*1.219*	*1.307*	*1.403*	*1.508*	*1.622*

TABLE 19. Dielectric constant of water and steam as a function of temperature and pressure—Continued

	p/MPa										
T/K	80	100	150	200	250	300	350	1400	1450	1500	1000
260		——	*99.66*	*101.5*	*103.3*	*105.0*	*106.6*	*108.2*	*109.8*		
265	——	95.41	*97.31*	*99.11*	*100.8*	*102.5*	*104.1*	*105.7*	107.2	——	
270	*92.43*	*93.19*	*95.04*	*96.80*	*98.48*	*100.1*	*101.7*	*103.2*	*104.7*	*106.2*	
275	90.31	91.05	92.85	94.55	96.19	97.77	99.30	100.8	102.3	103.7	
280	88.25	88.98	90.72	92.38	93.97	95.51	97.00	98.45	99.87	101.3	
285	86.25	86.96	88.65	90.27	91.82	93.32	94.77	96.18	97.56	98.91	
290	84.30	84.99	86.65	88.22	89.74	91.19	92.61	93.98	95.32	96.64	
295	82.41	83.08	84.70	86.24	87.71	89.14	90.51	91.85	93.16	94.44	
300	80.56	81.22	82.80	84.31	85.75	87.14	88.48	89.79	91.06	92.31	——
305	78.75	79.40	80.96	82.43	83.85	85.20	86.52	87.79	89.04	90.25	101.3
310	76.99	77.63	79.16	80.61	82.00	83.33	84.61	85.86	87.08	88.26	99.06
315	75.28	75.90	77.41	78.84	80.20	81.50	82.77	83.99	85.18	86.34	96.87
320	73.60	74.22	75.71	77.11	78.45	79.74	80.97	82.17	83.34	84.48	94.76
325	71.97	72.58	74.05	75.43	76.75	78.02	79.23	80.41	81.56	82.67	92.73
330	70.37	70.98	72.43	73.80	75.10	76.34	77.54	78.70	79.83	80.92	90.78
335	68.81	69.42	70.85	72.20	73.49	74.72	75.90	77.04	78.15	79.23	*88.89*
340	67.29	67.89	69.31	70.65	71.92	73.14	74.30	75.43	76.52	77.58	*87.07*
345	65.81	66.40	67.82	69.14	70.40	71.60	72.75	73.86	74.94	75.98	*85.31*
350	64.36	64.95	66.35	67.67	68.91	70.10	71.24	72.34	73.40	74.43	*83.61*
355	62.95	63.53	64.93	66.23	67.47	68.64	69.77	70.85	71.90	72.92	*81.96*
360	61.57	62.15	63.53	64.83	66.05	67.22	68.33	69.41	70.44	71.45	*80.36*
365	60.22	60.80	62.18	63.46	64.68	65.83	66.94	68.00	69.03	70.02	*78.81*
370	58.90	59.48	60.85	62.13	63.34	64.48	65.58	66.63	67.65	68.63	*77.31*
375	57.61	58.19	59.56	60.83	62.03	63.17	64.25	65.29	66.30	67.27	*75.85*
380	56.36	56.94	58.30	59.57	60.76	61.88	62.96	63.99	64.99	65.95	*74.43*
390	53.94	54.51	55.87	57.12	58.30	59.41	60.47	61.49	62.47	63.41	*71.71*
400	51.62	52.20	53.55	54.80	55.96	57.06	58.11	59.11	60.07	61.00	*69.12*
410	49.42	50.00	51.34	52.58	53.74	54.83	55.86	56.85	57.79	58.71	*66.68*
420	47.32	47.90	49.24	50.48	51.62	52.70	53.72	54.69	55.63	56.53	*64.35*
430	45.31	45.89	47.24	48.47	49.61	50.67	51.68	52.65	53.57	54.45	*62.13*
440	43.39	43.98	45.33	46.55	47.69	48.74	49.74	50.69	51.60	52.48	*60.03*
450	41.56	42.15	43.51	44.73	45.86	46.91	47.90	48.84	49.74	50.60	*58.02*
460	39.81	40.40	41.77	42.99	44.11	45.16	46.14	47.07	47.96	48.81	*56.11*
470	38.13	38.74	40.11	41.33	42.45	43.49	44.46	45.38	46.26	47.10	*54.28*
480	36.53	37.14	38.52	39.75	40.87	41.90	42.86	43.78	44.64	45.47	*52.55*
490	34.99	35.61	37.01	38.24	39.35	40.38	41.34	42.24	43.10	43.92	*50.89*
500	33.52	34.15	35.56	36.79	37.91	38.93	39.89	40.78	41.63	42.44	*49.30*
525	30.08	30.75	32.20	33.46	34.57	35.59	36.53	37.41	38.24	39.03	*45.64*
550	26.96	27.67	29.18	30.46	31.59	32.60	33.53	34.40	35.22	35.99	*42.38*
575	24.10	24.86	26.46	27.77	28.91	29.92	30.85	31.71	32.51	33.26	*39.45*
600	21.46	22.29	23.98	25.34	26.49	27.51	28.44	29.28	30.07	30.82	*36.82*
625	19.00	19.92	21.72	23.13	24.31	25.34	26.26	27.10	27.88	28.61	*34.45*
650	16.69	17.72	19.65	21.12	22.32	23.36	24.29	25.13	25.90	26.62	*32.31*
675	14.51	15.67	17.76	19.28	20.52	21.57	22.50	23.33	24.10	24.81	*30.36*
700	12.44	13.75	16.01	17.60	18.87	19.93	20.87	21.70	22.46	23.17	*28.60*
725	10.49	11.97	14.40	16.06	17.36	18.44	19.38	20.21	20.97	21.67	*26.98*
750	8.702	10.34	12.93	14.65	15.97	17.07	18.01	18.85	19.60	20.30	*25.51*
775	7.145	8.857	11.58	13.35	14.70	15.81	16.76	17.60	18.35	19.04	*24.15*
800	5.872	7.562	10.35	12.17	13.54	14.66	15.61	16.45	17.20	17.88	*22.91*
825	4.894	6.468	9.246	11.09	12.47	13.60	14.55	15.39	16.14	16.82	*21.76*
850	4.169	5.571	8.263	10.10	11.49	12.62	13.58	14.41	15.16	15.83	*20.70*
875	3.637	4.852	7.399	9.215	10.60	11.73	12.68	13.51	14.25	14.92	*19.71*
900	*3.241*	*4.284*	*6.647*	*8.416*	*9.787*	*10.91*	*11.85*	*12.68*	*13.41*	*14.08*	*18.80*
950	*2.707*	*3.477*	*5.441*	*7.066*	*8.374*	*9.460*	*10.39*	*11.20*	*11.92*	*12.57*	*17.15*
1000	*2.369*	*2.956*	*4.557*	*6.003*	*7.218*	*8.250*	*9.143*	*9.930*	*10.63*	*11.27*	*15.72*
1050	*2.138*	*2.601*	*3.908*	*5.172*	*6.280*	*7.244*	*8.091*	*8.845*	*9.524*	*10.14*	*14.45*
1100	*1.970*	*2.347*	*3.427*	*4.523*	*5.520*	*6.409*	*7.203*	*7.918*	*8.567*	*9.160*	*13.34*
1150	*1.843*	*2.158*	*3.063*	*4.012*	*4.905*	*5.717*	*6.454*	*7.127*	*7.742*	*8.309*	*12.35*
1200	*1.744*	*2.011*	*2.781*	*3.606*	*4.403*	*5.143*	*5.823*	*6.451*	*7.031*	*7.569*	*11.47*

TABLE 20. Dielectric constant of water and steam as a function of temperature and density.

	ρ/kg m^{-3}									
T/K	50	100	150	200	250	300	350	400	450	500
580	1.379									
600	1.367									
620	1.355	1.822								
640	1.344	1.795	2.371							10.21
660	1.334	1.770	2.325	3.012	3.834	4.790	5.878	7.090	8.417	9.850
680	1.325	1.746	2.282	2.943	3.734	4.653	5.698	6.863	8.138	9.516
700	1.316	1.724	2.242	2.880	3.642	4.527	5.533	6.653	7.881	9.208
750	1.296	1.675	2.154	2.741	3.439	4.250	5.170	6.195	7.319	8.534
800	1.278	1.634	2.079	2.622	3.268	4.017	4.866	5.811	6.848	7.971
850	1.263	1.597	2.014	2.521	3.122	3.818	4.606	5.484	6.448	7.491
900	*1.250*	*1.565*	*1.957*	*2.433*	*2.995*	*3.646*	*4.382*	*5.203*	*6.103*	*7.079*
950	*1.238*	*1.537*	*1.907*	*2.355*	*2.884*	*3.495*	*4.187*	*4.957*	*5.802*	*6.719*
1000	*1.227*	*1.512*	*1.863*	*2.287*	*2.786*	*3.362*	*4.014*	*4.740*	*5.537*	*6.402*
1050	*1.218*	*1.489*	*1.823*	*2.225*	*2.698*	*3.244*	*3.861*	*4.548*	*5.302*	*6.121*
1100	*1.209*	*1.469*	*1.787*	*2.170*	*2.620*	*3.138*	*3.724*	*4.376*	*5.092*	*5.869*
1150	*1.201*	*1.450*	*1.755*	*2.120*	*2.549*	*3.042*	*3.600*	*4.221*	*4.903*	*5.643*
1200	*1.194*	*1.433*	*1.725*	*2.075*	*2.484*	*2.956*	*3.488*	*4.081*	*4.731*	*5.438*
Saturation										
T/K→	577.95	616.99	634.68	642.96	646.25	647.07	647.05	646.11	643.27	637.55
ϵ	1.381	1.826	2.384	3.074	3.907	4.885	6.003	7.260	8.670	10.26

	ρ/kg m^{-3}									
T/K	550	600	650	700	750	800	850	900	950	1000
300										78.03
320										71.80
340										66.34
360										61.53
380										57.29
400									49.92	53.53
420									46.71	50.19
440									43.87	47.21
460								38.24	41.33	44.54
480								36.11	39.07	42.15
500							31.44	34.19	37.04	40.00
520							29.84	32.47	35.20	38.05
540						25.94	28.39	30.93	33.55	36.29
560					22.45	24.74	27.09	29.52	32.05	34.69
580				19.32	21.45	23.65	25.91	28.25	30.68	*33.23*
600			16.52	18.50	20.54	22.65	24.83	27.08	29.43	*31.89*
620		14.02	15.85	17.75	19.72	21.75	23.85	26.02	28.28	*30.67*
640	11.81	13.48	15.24	17.07	18.96	20.92	22.94	25.04	27.23	*29.54*
660	11.38	12.99	14.68	16.44	18.27	20.16	22.11	24.14	26.26	*28.49*
680	10.99	12.54	14.17	15.87	17.63	19.46	21.35	23.31	*25.37*	*27.53*
700	10.63	12.12	13.70	15.34	17.04	18.81	20.64	22.54	*24.53*	*26.64*
750	9.835	11.21	12.66	14.17	15.75	17.38	19.08	20.85	*22.70*	*24.66*
800	9.173	10.45	11.79	13.19	14.66	16.18	17.76	*19.42*	*21.15*	*22.99*
850	*8.610*	*9.797*	*11.05*	*12.36*	*13.73*	*15.15*	*16.64*	*18.19*	*19.83*	*21.56*
900	*8.125*	*9.237*	*10.41*	*11.64*	*12.93*	*14.27*	*15.67*	*17.14*	*18.68*	*20.32*
950	*7.702*	*8.748*	*9.853*	*11.01*	*12.23*	*13.50*	*14.82*	*16.21*	*17.68*	*19.24*
1000	*7.330*	*8.318*	*9.363*	*10.46*	*11.61*	*12.81*	*14.07*	*15.39*	*16.79*	*18.28*
1050	*7.000*	*7.937*	*8.928*	*9.971*	*11.06*	*12.21*	*13.41*	*14.67*	*16.00*	*17.42*
1100	*6.705*	*7.596*	*8.539*	*9.532*	*10.57*	*11.67*	*12.81*	*14.02*	*15.29*	*16.66*
1150	*6.439*	*7.289*	*8.188*	*9.137*	*10.13*	*11.18*	*12.28*	*13.43*	*14.66*	*15.97*
1200	*6.199*	*7.011*	*7.871*	*8.779*	*9.734*	*10.74*	*11.79*	*12.90*	*14.08*	*15.34*
Saturation										
T/K→	628.82	616.34	599.78	578.91	553.30	522.40	485.36	440.64	384.39	
ϵ	12.06	14.12	16.53	19.36	22.80	27.11	32.73	40.56	52.72	

12. References

[1] P. Debye and E. Hückel, Phys. Z. **24**, 185 (1923).
[2] M. Born, Z. Phys. **1**, 45 (1920).
[3] D. P. Fernández, Y. V. Mulev, A. R. H. Goodwin, and J. M. H. Levelt Sengers, J. Phys. Chem. Ref. Data **24**, 33 (1995).
[4] A. S. Quist and W. L. Marshall, J. Phys. Chem. **9**, 3165 (1965).
[5] H. C. Helgeson and D. H. Kirkham, Am. J. Sci. **274**, 1089 (1974).
[6] H. I. Oshry, Ph.D. dissertation, University of Pittsburgh (1949).
[7] B. B. Owen, R. C. Miller, C. E. Milner, and H. L. Cogan, J. Phys. Chem. Ref. Data **65**, 2065 (1961).
[8] K. Heger, Ph.D. dissertation, University of Karlsruhe (1969).
[9] J. H. Keenan, F. G. Keyes, P. G. Hill, and J. G. Moore, *Steam Tables* (Wiley, New York, 1969).
[10] D. J. Bradley and K. S. Pitzer, J. Phys. Chem. **83**, 1599 (1979).
[11] M. Uematsu and E. U. Franck, J. Phys. Chem. Ref. Data **9**, 1291 (1980).
[12] K. Heger, M. Uematsu, and E. U. Franck, Ber. Bunsenges. Phys. Chem. **84**, 758 (1980).
[13] D. G. Archer and P. Wang, J. Phys. Chem. Ref. Data **19**, 371 (1990).
[14] P. G. Hill, J. Phys. Chem. Ref. Data **19**, 1233 (1990).
[15] J. W. Johnson and D. Norton, Am. J. Sci. **291**, 541 (1991).
[16] D. P. Fernández, A. R. H. Goodwin, and J. M. H. Levelt Sengers, Int. J. Thermophys. **16**, 929 (1995).
[17] Yu. V. Mulev, S. N. Smirnov, and M. R. Muchailov, Teploenergetica (in press, 1996).
[18] H. Preston-Thomas, Metrologia **27**, 3 (1990).
[19] W. Wagner and A. Pruss, private communication (1995); J. Phys. Chem. Ref. Data (submitted).
[20] Release on the IAPWS Formulation 1995 for the Thermodynamic Properties of Ordinary Water Substance for General and Scientific Use, Fredericia, Denmark, September 1996, to be obtained from the Executive Secretary of IAPWS, Dr. R. B. Dooley, Electric Power Research Institute, 3412 Hillview Avenue, Palo Alto, CA 94304-1395.
[21] R. J. Speedy and C. A. Angell, J. Chem. Phys. **65**, 851 (1976).
[22] I. M. Hodge and C. A. Angell, J. Chem. Phys. **68**, 1363 (1978).
[23] J. B. Hasted and M. Shahidi, Nature **262**, 777 (1976).
[24] D. Bertolini, M. Cassettari, and G. Salvetti, J. Chem. Phys. **76**, 3285 (1982).
[25] G. Stell and J. S. Høye, Phys. Rev. Lett. **33**, 1268 (1974).
[26] D. Bedeaux and P. Mazur, Physica **67**, 23 (1973).
[27] T. Doiron and H. Meyer, Phys. Rev. **B 17**, 2141 (1979).
[28] B. J. Thijsse, T. Doiron, and J. M. H. Levelt Sengers, Chem. Phys. Lett. **72**, 546 (1980).
[29] M. H. W. Chan, Phys. Rev. B **21**, 1187 (1980).
[30] M. W. Pestak and M. H. W. Chan, Phys. Rev. Lett. **46**, 943 (1981).
[31] H. A. Lorentz, *Theory of Electrons* (Leipzig, 1909).
[32] C. J. F. Böttcher, *Theory of Electric Polarization*, 2nd ed., revised by O. C. Van Belle, P. Bordewijk, and A. Rip (Elsevier, Amsterdam, 1973).
[33] P. Debye, Phys. Z. **13**, 97 (1912).
[34] R. P. Bell, Trans. Faraday Soc. **27**, 797 (1931).
[35] L. Onsager, J. Am. Chem. Soc. **58**, 1486 (1936).
[36] J. G. Kirkwood, J. Chem. Phys. **7**, 911 (1939).
[37] F. E. Harris and B. J. Alder, J. Chem. Phys. **21**, 1031 (1953).
[38] H. Fröhlich, Physica **22**, 898 (1956).
[39] R. H. Cole, J. Chem. Phys. **27**, 33 (1957).
[40] N. E. Hill, Trans. Faraday Soc. **59**, 344 (1963).
[41] J. B. Hasted, *Aqueous Dielectrics* (Chapman and Hall, London, 1973).
[42] H. Fröhlich, *Theory of Dielectrics* (Oxford University, Oxford, 1958).
[43] J. B. Hasted, in Water, *A Comprehensive Treatise*, Vol. 1, Chap. 7, edited by F. Franks (Plenum, New York, 1972).
[44] O. A. Nabokov and Yu. A. Lyubimov, J. Struct. Chem. **27**, 731 (1986).
[45] G. Oster and J. G. Kirkwood, J. Chem. Phys. **11**, 175 (1943).
[46] E. U. Franck, S. Rosenzweig, and M. Christoforakos, Ber. Bunsenges. Phys. Chem. **94**, 199 (1990).
[47] G. N. Patey, D. Levesque, and J. J. Weis, Mol. Phys. **38**, 219 (1979).
[48] R. Deul, Ph.D. dissertation, University of Karlsruhe (1984).
[49] R. Deul and E. U. Franck, Ber. Bunsenges. Phys. Chem. **95**, 847 (1991).
[50] S. Goldman, C. Joslin, and E. A. Wasserman, J. Phys. Chem. **98**, 6231 (1994).
[51] H. J. C. Berendsen, J. R. Grigera, and T. P. Straatsma, J. Phys. Chem. **91**, 6269 (1987).
[52] E. A. Wasserman, B. J. Wood, and J. Brodholt, Ber. Bunsenges. Phys. Chem. **98**, 906 (1994).
[53] G. P. Johari, J. Chem. Phys. **80**, 4413 (1984).
[54] M. Neumann, J. Chem. Phys. **82**, 5663 (1985).
[55] M. Sprik, J. Chem. Phys. **95**, 6762 (1991).
[56] Y. Guissani and B. Guillot, J. Chem. Phys. **98**, 8221 (1993).
[57] M. Neumann, Proceedings of the 12th ICPWS, Orlando, FL, 1994, edited by H. J. White, Jr., J. V. Sengers, D. Neumann, and J. C. Bellows (Begell House, New York, 1995).
[58] R. D. Mountain and A. Wallqvist, NISTIR 5778 (1996).
[59] P. Schiebener, J. Straub, J. M. H. Levelt Sengers, and J. S. Gallagher, J. Phys. Chem. Ref. Data **19**, 677 (1990).
[60] W. L. Lees, Ph.D. dissertation, Harvard University (1949).
[61] C. E. Milner, Ph.D. dissertation, Yale University (1955).
[62] H. L. Cogan, Ph.D. dissertation, Yale University (1958).
[63] E. W. Rusche, Ph.D. dissertation, New Mexico University (1966).
[64] R. L. Kay, G. A. Vidulich, and K. S. Pribadi, J. Phys. Chem. **73**, 445 (1969).
[65] Yu. M. Lukashov, Ph.D. dissertation, Moscow Power Institute (1981).
[66] G. C. Åkerlöf, J. Am. Chem. Soc. **54**, 4125 (1932).
[67] P. Albright, J. Am. Chem. Soc. **50**, 2098 (1937).
[68] P. S. Albright and L. J. Gosting, J. Am. Chem. Soc. **68**, 1061 (1946).
[69] F. H. Drake, G. W. Pierce, and M. T. Dow, Phys. Rev. **35**, 613 (1930).
[70] L. A. Dunn and R. H. Stokes, Trans. Faraday Soc. **65**, 2906 (1969).
[71] J. K. Fogo, S. W. Benson, and C. S. Copeland, J. Chem. Phys. **22**, 209 (1954).
[72] T. E. Gier and H. S. Young, as reported by A.W. Lawson and A.J. Hughes in High Pressure Physics and Chemistry, Vol. I, edited by R. S. Bradley (Academic, New York, 1963).
[73] B. P. Golubev, Ph.D. (Doctor) dissertation, Moscow Power Institute (1978).
[74] E. H. Grant, T. J. Buchanan, and H. F. Cook, J. Chem. Phys. **26**, 156 (1956).
[75] F. E. Harris, E. W. Haycock, and B. J. Alder, J. Chem. Phys. **21**, 1943 (1953); J. Phys. Chem. **57**, 978 (1953).
[76] U. Kaatze and V. Uhlendorf, Z. Phys. Chem. (Neue Folge) **126**, 151 (1981).
[77] Yu. M. Lukashov, B. P. Golubev, and F. B. Ripol-Saragosi, Teploenergetika **22-6**, 79 (1975).
[78] C. G. Malmberg and A. A. Maryott, J. Res. Natl. Bur. Stand. **56**, 1 (1956).
[79] M. R. Muchailov, Ph.D. (Candidate) dissertation, Moscow Power Institute (1988).
[80] B. K. P. Scaife, Proc. Phys. Soc. London **B68**, 790 (1955).
[81] E. Schadow and R. Steiner, Z. Phys. Chem. (Neue Folge) 66, 105 (1969).
[82] K. R. Srinivasan, Ph.D. dissertation, Carnegie-Mellon University (1973).
[83] K. R. Srinivasan and R. L. Kay, J. Chem. Phys. **60**, 3645 (1974).
[84] E. P. Svistunov, B. P. Golubev, and S. N. Smirnov, Teploenergetika **21-6**, 69 (1974).
[85] T. Tyssul Jones and R. M. Davis, Philos. Mag. **28**, 307 (1939).
[86] G. A. Vidulich and R. L. Kay, J. Phys. Chem. **66**, 383 (1962).
[87] G. A. Vidulich, D. F. Evans, and R. L. Kay, J. Phys. Chem. **71**, 656 (1967).
[88] J. Wyman and E. N. Ingalls, J. Am. Chem. Soc. **60**, 1182 (1938).
[89] J. Wyman, Phys. Rev. **35**, 623 (1930).
[90] E. R. Cohen and B. N. Taylor, J. Phys. Chem. Ref. Data **17**, 1195 (1988).
[91] Report of Investigation, NIST Standard Reference Material 8535 (Vienna Standard Mean Ocean Water), NIST Standard Reference Materials Program, Gaithersburg, MD (1992).
[92] C. G. Gray and K. E. Gubbins, *Theory of Molecular Fluids*, Vol. 1 (Clarendon, Oxford, 1984).
[93] W. Wagner, Fortschr.-Ber. VDI-Z., Vol. 3 (#39) VDI-Verlag, Düsseldorf (1974), p. 39.
[94] B. N. Taylor and C. E. Kuyatt, NIST Technical Note 1297 (1994).
[95] J. M. H. Levelt Sengers, C. M. Everhart, G. Morrison, and K. S. Pitzer, Chem. Eng. Commun. **47**, 315 (1986).

[96] E. A. Guggenheim, *Thermodynamics* (North-Holland, Amsterdam, Netherlands, 1967).
[97] K. S. Pitzer, *Activity Coefficients in Electrolyte Solutions*, Chap. 3 (CRC, Boca Raton, FL, 1991).
[98] P. S. Z. Rogers and K. S. Pitzer, J. Phys. Chem. Ref. Data **11**, 15 (1982).
[99] R. P. Breyer and B. R. Staples, J. Soln. Chem. **15**, 749 (1986).
[100] L. Haar, J. S. Gallagher, and G. S. Kell, NBS/NRC Steam Tables (Hemisphere, Washington, DC, 1984).
[101] A. Saul and W. Wagner, J. Phys. Chem. Ref. Data **18**, 1537 (1989).